Selection and characterization of D-enantiomeric peptides
for the investigation of options for therapy and diagnosis of Alzheimer's disease

Dissertation

zur Erlangung des akademischen Grades
Doktorin der Naturwissenschaften (Dr. rer. nat.) an der
Fakultät für Biologie, Chemie und Geowissenschaften der
Universität Bayreuth

vorgelegt von

Marwa Malhis

aus Aleppo

Coburg 2020

This doctoral thesis was prepared at the Institute for Bioanalysis at Coburg University of Applied Sciences in cooperation with the Faculty of Biology, Chemistry and Geosciences at the University of Bayreuth from April 2016 until July 2019 and was supervised by Prof. Dr. Aileen Susanne Funke and Prof. Dr. Andreas Römpp.

This is a full reprint of the thesis submitted to obtain the academic degree of Doctor of Natural Sciences (Dr. rer. nat.) and approved by the Faculty of Biology, Chemistry and Geosciences of the University of Bayreuth.

Date of submission: 15.04.2020

Date of defence: 07.12.2020

Acting dean: Prof. Dr. Matthias Breuning

Doctoral committee:

Prof. Dr. Aileen Funke (reviewer)
Prof. Dr. Klaus Ersfeld (reviewer)
Prof. Dr. Andreas Römpp (chairman)
Prof. Dr. Birte Höcker

Acknowledgements

I would like to express my deepest appreciation to my supervisor, Prof. Dr. Susanne Aileen Funke for her guidance and continuous support throughout this work. I have learned a lot from her and I feel so honored and grateful to have had the opportunity to work together. I am also very thankful to Prof. Dr. Andreas Römpp, who co-supervised this project, for his feedback and his great scientific advices on my work.

I would also like to extend my special thanks to Dr. Max Holzer from the Paul Flechsig Institute for Brain Research for his wonderful scientific ideas and for welcoming me to Leipzig.

I gratefully acknowledge the national conference of the women's representative foundation in Bavaria (LaKoF) who made my Ph.D. work possible. I am sincerely honored to have been selected as a recipient of the LaKoF scholarship from the beginning of my Ph.D. studies until its completion.

I am also thankful to all members of the institute for bioanalysis during my time there, who provided such an open atmosphere for research. My special appreciation goes to Antje Vondran for her scientific support during my Ph.D. studies and her continuous words of encouragement. In particular, I want to thank my dear friend Katharina Trunzer, who gave a great deal of emotional support and fun moments during our everyday work.

Thanks also to my bachelor students, Martial LeBras Nono and Lucy Pia Wunderlich, who contributed to the outlook of my dissertation.

I would like to express my ultimate gratitude to my parents, my sisters and my brother for their love and encouragement. I have been blessed with a loving, supportive family who have always believed in me and taught me that I could do anything I set my mind to. I wouldn't be the person I am today without them and their support. Last but definitely not least, I thank my best friend and my beloved husband Mazen, who has shared this entire journey with me and has been there every step of the way. He has seen me through the ups and downs of the entire process and without his love and kindness, I have no balance in my life. I also dedicate this Ph.D. thesis to my two lovely daughters, Hoor and Sidra, who are the joy of my life and a powerful source of inspiration and energy. I love you more than anything and I appreciate all your patience during mommy's Ph.D. studies.

Table of contents

List of figures

List of tables

Abbreviations

aa	amino acids
Aß	amyloid beta peptide
AD	Alzheimer's disease
AS	ammonium sulfate
BSA	bovine serum albumin
$C_2H_2NaO_2$	Sodium acetate
$CaCl_2$	Calcium chloride
CNS	Central nervous system
CSF	Cerebrospinal fluid biomarker
Da	Dalton
DNA	deoxyribonucleic acid
DTT	dithiothreitol
E. coli	*Escherichia coli*
EDTA	Ethylenediaminetetraacetate
ELISA	Enzyme-linked immunosorbent assay
FAM	5(6)-Carboxyfluorescein
h	hour
H_2O_2	hydrogen peroxide
HCL	Hydrochloric acid
HEPES	4-(2-hydroxyethyl)-1-piperazineethanesulfonic
HPR	Horseradish peroxidase
IPTG	Isopropyl β-D-thiogalactopyranoside
PHFs	paired helical filament
PHF6	a hexapeptide motif comprising a sequence VQIVYK
PHF6*	a hexapeptide motif comprising a sequence VQIINK
kDa	Kilodalton
LB-Medium	Luria-Bertani-medium
mA	Milliampere

Min	Minutes
MT	Microtubules
MW	Molecular weight
NaCl	Sodium chloride
NaHCO$_3$	Sodium hydrogen carbonate
NaPi	Sodium phosphate buffer
nm	Nanometre
NFT	Neurofibrillary tangles
No.	Number
OD$_{600}$	Optical density at 600 nm
PAGE	Polyacrylamide-gel electrophoresis
PBS	Phosphate buffered saline
PEG	Polyethylene glycol
PHF	Paired helical filaments
PI	Isoelectric point
rpm	Rotations per minute
RT	Room temperature
S	Seconds
SDS	Sodium Dodecyl Sulphate
ssDNA	Single strand DNA
TBS	Tris Buffered Saline
TBST	Tris Buffered Saline with Tween-20
TEMED	Tetramethyl ethylenediamine
THT	Thioflavin T
Tris	Tris(hydroxymethyl)aminomethane
WB	Western blott
V	Volume
v/v	Volume by volume
Xgal	X-Gal, 5-Bromo-4-chloro-3-indolyl-β-D

Zusammenfassung

Die Alzheimer-Demenz (AD), lateinisch Morbus Alzheimer, ist eine neurodegenerative Erkrankung, die durch die fortschreitende Abnahme kognitiver Funktionen gekennzeichnet ist und mit Verhaltensstörungen und neuropsychologischen Symptomen assoziiert. Bis heute ist die Behandlung von AD nur symptomatisch. Trotz der bisherigen Forschungsanstrengungen ist kein kausales Medikament zugelassen, welches den Krankheitsverlauf aufgehalten oder rückgängig machen kann.

Die Hauptmerkmale der AD sind die Entstehung von amyloiden Plaques und das Auftreten von neurofibrilliären Bündeln. Neurofibrilliäre Bündel bestehen hauptsächlich aus aggregierten Tau-Proteinen. Tau-Protein-Aggregation führt zu einem Verlust der Tau-Funktion (etwa der Stabilisierung der Mikrotubuli) sowie zu Neurotoxizität und Zelldegeneration. Die Bildung amyloider Tau-Aggregate wird innerhalb von Tau durch zwei aus sechs Aminosäuren bestehenden Fragmente angetrieben: i) VQIINK (PHF6*), zu Beginn von Repeat 2 gelegen, und ii) VQIVYK (PHF6), zu Beginn von Repeat 3 gelegen. Es wurde kürzlich beschrieben, dass das PHF6*-Segment die pathologische Tau-Aggregation stärker antreibt als das PHF6-Fragment.

Peptide, die die Tau-Aggregation inhibieren, sind mögliche Kandidaten für zukünftige Therapien bei Alzheimer. Zur Selektion affiner Peptide für spezielle Bindepartner ist die molekularbiologische Methode des Phagendisplays eine einfache und schnelle Möglichkeit.

Ziel dieser Arbeit war es, D-enantiomere Peptide zu entwickeln, die die pathologische Aggregation des Tau-Proteins hemmen können. D-Peptide können L-Peptiden für Anwendungen *in vivo* überlegen sein, da sie proteaseresistent sind und in der Regel das Immunsystem nicht aktivieren.

Ein weiteres Ziel dieser Arbeit war es herauszufinden, welches der beiden Tau Fragmente, PHF6 oder PHF6*, das bedeutsamere therapeutische Target für die Entwicklung von Tau-Aggregations-inhibierenden Peptiden ist.

Mittels Phagendisplay und Spiegelbild-Phagendisplay konnten D-Peptide entwickelt werden, die die Formation von Tau-Fibrillen inhibierten. Zwei Selektionen wurden durchgeführt: die erste Selektion wurde gegen Tau-Monomer mittels Phagendisplay

durchgeführt; die zweite Selektion wurde gegen D-Enantiomere PHF6*-Fibrillen mittels Spiegelbild-Phagendisplay durchgeführt. PHF6*-fibrillen wurden in der zweiten Selektion adressiert, da eine aktuelle Studie zeigte, dass die PHF6*-Sequenz die Aggregation des Tau-Proteins stärker antreibt als die PHF6-Sequenz.

Das besonders vielversprechende Peptid MMD3 wurde sowohl in der Selektion gegen Tau-Monomer als auch in der Selektion gegen D-Enantiomere PHF6*-Fibrillen identifiziert. Es konnte per Thioflavin-Assay bestätigt werden, dass MMD3 und seine retro-inverse Version MMD3rev sowohl die Aggregation von PHF6* als auch die Fibrillenbildung des Volllänge-Tau-Proteins inhibierten.

In einem ersten Ansatz zur Untersuchung, welches der beiden Hexapeptide innerhalb von Tau, PHF6 oder PHF6*, das effektivere Ziel zur Aggregations-Inhibition ist, wurde die inhibitorische Wirkung von MMD3 und MMD3rev (gerichtet gegen PHF6*) mit den bereits beschriebenen Peptiden, die gegen PHF6 bzw. PHF6* gerichtet sind, verglichen. Dieses erste vorläufige Ergebnis zeigte, dass gegen PHF6 bzw. gegen PHF6*-gerichtete Peptide ähnlich wirksam in ihren aggregationsinhibierenden Eigenschaften sind. Allerdings steht hier eine weitere Charakterisierung mit verschiedenen biochemischen und biophysikalischen Methoden noch aus.

Die in dieser Arbeit identifizierten D-Peptide MMD3 und MMD3rev sind vielversprechende Kandidaten für einen neuen medikamentösen Ansatz der Behandlung der Alzheimer-Demenz und werden aktuell bei einem Kooperationspartner vom Deutschen Zentrum für Neurodegenerative Erkrankungen (DZNE) weiter charakterisiert.

Summary

Morbus Alzheimer (AD) is a neurodegenerative disease, characterized by steady loss of cognitive functions, behavioral changes and neuropsychological symptoms. Today, AD can be treated only symptomatically. There is no drug available, which stops or reverses the pathological changes in AD. Alzheimer's disease is characterized by two pathological hallmarks, amyloid plaques and neurofibrillary tangles (NFTs). NFTs are composed of aggregated tau protein. The accumulation of tau into NFTs reduces normal tau function and causes neuronal dysfunction. The formation of tau aggregates is triggered by two hexapeptide sequences within tau: VQIINK (PHF6*), which is located at the beginning of the second repeat (R2) and VQIVYK (PHF6), which is located at the beginning of the third repeat (R3). PHF6* segment has recently been described as a more potent driver of tau aggregation than PHF6.

Peptides that inhibit the pathological aggregation of tau are potentially useful candidates for future therapies in AD. The use of the molecular biology screening technique, phage display, allows fast and simple selection of peptides that bind to a desired target protein.

The aim of this study was to develop specific D-enantiomeric peptides that inhibit the pathological aggregation of tau. D-enantiomeric peptides were chosen as they are protease stable and considerably less immunogenic than L-peptides.

Another objective of this project was to investigate which of the both sequences within tau, PHF6 or PHF6*, is the more effective target for the development of tau aggregation inhibiting peptides.

Employing phage display and mirror image phage display, we selected specific peptides to inhibit tau fibril formation. Two selections were performed; the first selection was conducted using monomers of L-enantiomeric full-length tau as a target for phage display. In addition, we performed a second selection using fibrils of the D-enantiomeric hexapeptide VQIINK (PHF6*) as a target for mirror image phage display. PHF6* segment was targeted in our second selection since PHF6* was recently reported as a more powerful driver for tau aggregation as PHF6.

The most interesting obtained peptide, designated MMD3, was found both in the selection against tau monomer and in the selection against D-PHF6* fibrils. MMD3 and its retro-inverso form, designated MMD3rev, clearly inhibited PHF6* aggregation as well as full-length tau aggregation in Thioflavin T (THT) assays.

In addition, we performed preliminary experiments to investigate which of the both sequences, PHF6 or PHF6*, is the more effective target for inhibitors of tau fibril formation. We compared the tau aggregation inhibiting effects of MMD3 and MMD3rev with other peptides, which were previously described in the literature and target either PHF6 or PHF6*, respectively. From our early preliminary data, it seems likely that PHF6 and PHF6* aggregation inhibitors are comparably effective in inhibiting the aggregation of full-length tau. However, further characterization using different biochemical and biophysical methods is still required.

Our selected peptides MMD3 and MMD3rev present promising candidates for therapeutic and diagnostic applications in AD research. Currently, MMD3 and MMD3rev are further characterized in the German Center for Neurodegenerative Diseases (DZNE).

1 Introduction

1.1 Alzheimer's disease

Alzheimer's disease (AD) was first described as a presenile dementia more than 100 years ago by the German psychiatrist Alois Alzheimer. AD is defined as a slowly progressing, irreversible neurodegenerative disease, associated with a progressive decline of cognitive functions (Alzheimer, 1907).

In 2017, there were nearly 50 million individuals with dementia around the world, and 4.6 million new cases are predicted to appear every year, implying 81.1 million cases by 2040 (Prince et al., 2013, World Health Organisation 2017). AD is the principle cause of dementia and accounts for 70 % of all cases (Anand et al., 2012; Galimberti and Scarpini, 2012). A person's risk of developing AD is about 10 -12 % (Bird, 1993). AD predominantly affects people over 65 and the risk reaches nearly 50% after age 85 (Weuve et al., 2014; Zhao et al., 2014). Regardless of age, women are more likely to develop Alzheimer's disease (Farrer et al., 1997).

To date, AD can be treated only symptomatically. As a result, AD symptoms ultimately necessitate nursing care. Indeed, more than 40 % of all places in German nursing homes are occupied by patients suffering from dementia (Bickel, 1996).

1.2 Neuropathology of Alzheimer's disease

Alzheimer's brains can be differentiated from healthy brains by a large loss in brain weight and volume associated with a shrinkage and loss of neuronal functions (Figure 1a) (Gomez-Isla et al., 1996). In addition, AD brains have a significant atrophy of the hippocampus and the cortex, which is elevated sixfold comparing with normal elderly people (Fox et al., 2000; Fotuhi et al., 2009).

AD is defined by two major neuropathological hallmarks, the extracellular deposition of amyloid plaques built by β-amyloid (Aβ) and the intracellular accumulation of neurofibrillary tangles (NFT) consisting of abnormally phosphorylated tau proteins (see Figure 1b) (McKhann et al., 1984).

These two protein aggregates share some biochemical characteristics. Both Aβ and tau form fibrils, which represent the main constituent of amyloid plaques (Aβ fibrils) and neurofibrillary tangles (tau fibrils). Both proteins undergo several post-translational modifications, such as phosphorylation, truncation and/or pyroglutamate in the brain of AD patients (Götz et al., 2001, Lasagna-Reeves CA et al 2010).
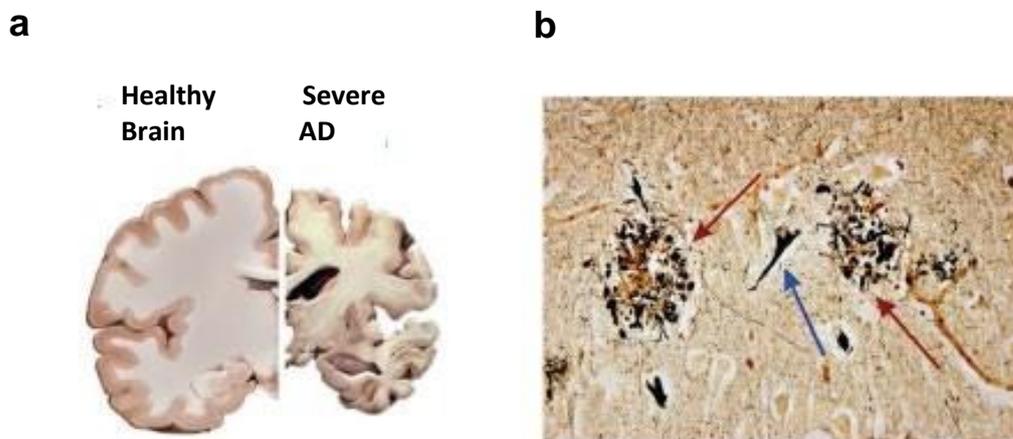
Figure 1: Neuropathology of Alzheimer's disease. (a) Brain of a healthy individual compared to the brain of a patient with severe Alzheimer disease. The mass and volume of the brain are significantly decreased in AD (National Institute of Aging 2015). (b) Photomicrograph of the temporal cortex of a patient with Alzheimer's disease (modified Bielschowski stain; original magnification, 400x). Two amyloid plaques (red arrows) with a neurofibrillary tangle (blue arrow) between them are shown (modified according to Perl, 2010; Dammers, 2015).

1.3 The microtubule-associated protein tau

Tau protein was first discovered in 1975 and was one of the first microtubule-associated proteins (MAPs) to be identified (Weingarten et al., 1975). This started a research stream focused on the biological role of tau in microtubule-stabilization. Under pathological conditions, tau protein detaches the microtubules and forms aberrant filaments. The loss of microtubule-stabilizing function of tau leads to axonal transport defects and synaptic dysfunction (Fig. 2) (Weingarten et al., 1975; Cleveland et al., 1977; Binder et al., 1985)
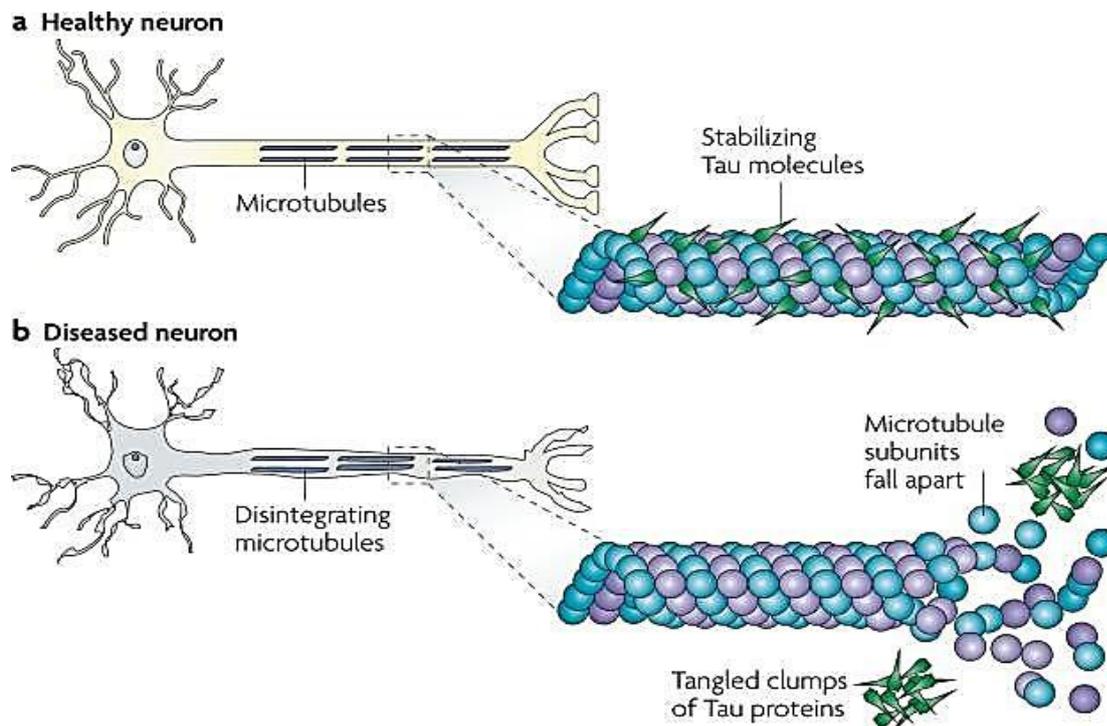
Figure 2: Tau in healthy neurons and in tauopathies. (a) Tau directly binds to a microtubule (MT) within cells and stabilizes it, which dynamically regulates the structure and function of the MT. **(b)** Under pathological conditions; tau protein detaches the MT and assembles into filamentous structures that eventually form neurofibrillary tangles (NFTs). The loss of tau function results in MT instability and reduced axonal transport, which is a common feature in several neurodegenerative diseases, known as tauopathies, including Alzheimer's disease (according to Brunden et al., 2009).

1.3.1 Tau structure and characteristics

Human tau is encoded by the MAPT gene on chromosome 17q21 (Neve et al., 1986). This protein is found mainly in the axons of the CNV (Central Nervous System) and comprises a family of six isomers produced by alternative splicing. Tau isomers range from 352 to 441 amino acids with apparent molecular weights between 45 and 65 kDa when run on sodium dodecyl sulfate-polyacrylamide gel electrophoresis (SDS-PAGE). They differ by the presence or absence of regions encoded by exons 2, 3 and 10 (Goedert et al. 1989).
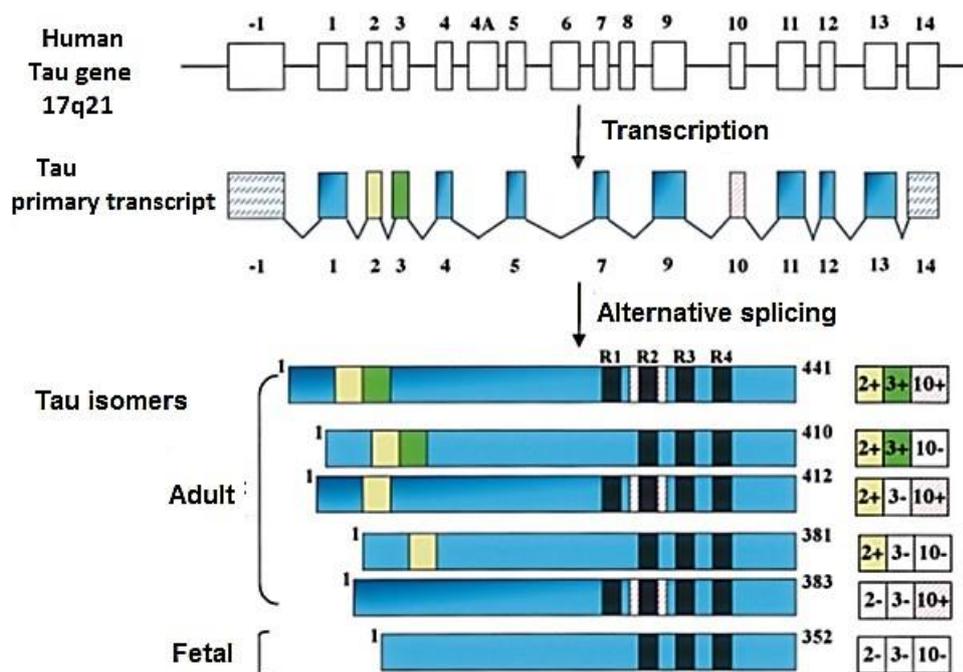
Figure 3: Schematic representation of the human tau gene, the human tau primary transcript and the six human tau isoforms. Chromosome 17 contains the human tau gene, which is located at position 17q21. There are six different tau isoforms, they differ by the presence or absence of one or two 29 amino acids inserts encoded by exon 2 (yellow box) and 3 (green box) in the amino-terminal section, together with either three (R1, R3 and R4) or four (R1–R4) repeat-regions (black boxes) in the carboxy-terminal section. The fourth microtubule-binding domain is encoded by exon 10 (slashed box) (lower panel). The adult tau isoforms are the longest 441-amino acid component (2+3+10+), the 410-amino acid component (2+3+10-), the 412-amino acid component de(2+3-10+), the 381-amino acid component (2+3-10-) and the 383-amino acid component (2-3-10+). The shortest 352-amino acid isoform (2-3-10-) is found only in the fetal brain, and hence is referred as fetal tau isoform (according to Buee et al., 2000).

Tau proteins stabilize microtubules and promote their assembly by binding to the MT through a repetitive region in their Carboxy-terminal fragment, and hence the C-terminal section is named the "binding domain". The repetitive regions in the binding domain are the repeat domains (R1-R4) (Lee et al., 1989). In contrast, the amino-terminal section does not bind to microtubules, projecting away from the microtubule surface. It is thus named the "projection domain". The projection domain binds to other cytoskeletal elements and plasma proteins (Hirokawa et al., 1988)

The overall amino acid composition of tau gives it the hydrophilic character. Due to its high solubility, normal tau protein does not form a folded structure. Indeed, evidences obtained from a variety of biophysical methods (e.g. NMR) reveals that the entire tau molecule is "natively unfolded" (Schweers et al., 1994).
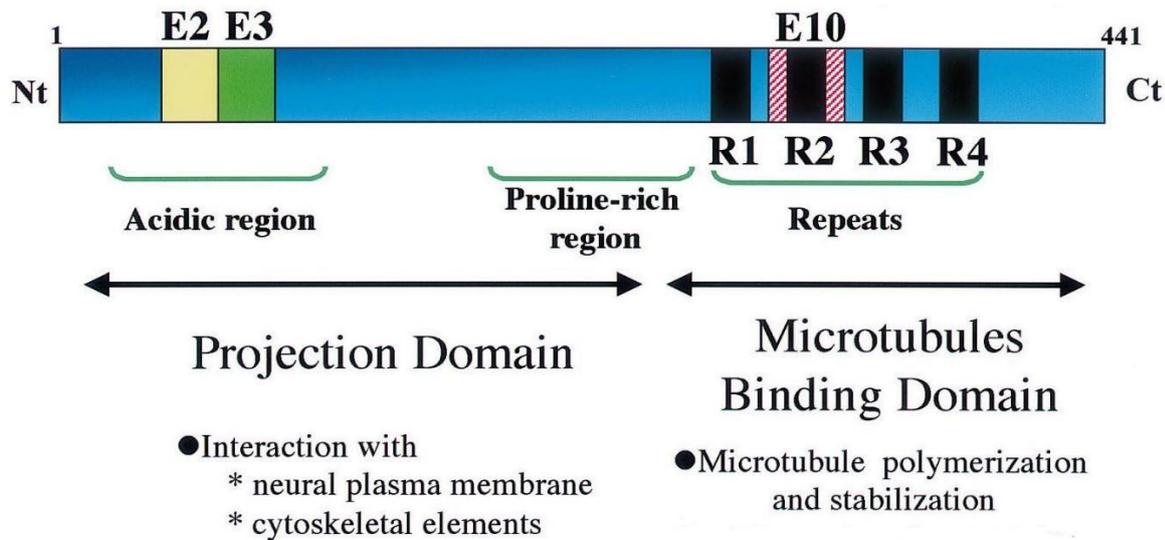
Figure 4: Schematic representation of the functional domains of the longest tau isoform (2+3+10+). The projection domain, which includes an acidic region and a proline-rich region, interacts with cytoskeletal elements. The C-terminal part, named the microtubule binding domain, binds to the MTs to stabilize them (according to Buee et al., 2000 with modifications).

1.3.2 Tauopathies and the aggregation of tau protein

The most apparent pathological event in several neurodegenerative diseases is the aggregation of tau isoforms into intraneuronal filaments. Under pathological conditions, monomeric tau self-assemblies and forms the small oligomeric tau species, which continue to accumulate and form filaments. In AD, these filamentous inclusions are named paired helical filaments (PHFs), PHFs subsequently form neurofibrillary tangles (NFTs) in neurons (Figure 5).

Recent research findings suggest that large insoluble tau aggregates, such as filaments and tangles, do not appear to be the toxic species in neurodegenerative diseases. However, tau oligomers, pre-filament tau aggregates consisting of two or more tau molecules in a multimeric structure, are considered to be the key toxic form of tau in tauopathies. Furthermore, oligomeric tau species can be found in a hyperphosphorylated and an unphosphorylated form, and these oligomeric structures can be both soluble and insoluble. As the oligomers exist in such a variety of states, it becomes more challenging to understand their potential role in tauopathies (Cowan et al., 2012; Guzmán-Martinez et al., 2013). However, Lasagna-Reeves et al. 2010 and

Lasagna-Reeves et al. 2011 have demonstrated that tau oligomers are toxic *in vitro* and *in vivo* and reported that *in vitro* they cause much more cellular damage than tau monomers or fibrils.

It was previously thought that the aggregation of tau in AD is due to the abnormal phosphorylation of tau proteins. However, normal tau protein is also phosphorylated in the brain and does not assemble into filaments. Furthermore, non-phosphorylated recombinant tau proteins aggregate into filaments under physiological conditions *in vitro* when polyanions (like heparin) are present. This suggests that several factors in addition to phosphorylation may cause the formation of pathological tau aggregates. In tauopathies, other mechanisms (e.g. ubiquitination, oxidation, glycation) may also play a role in the aggregation of tau proteins into PHFs (Buee et al., 2000).
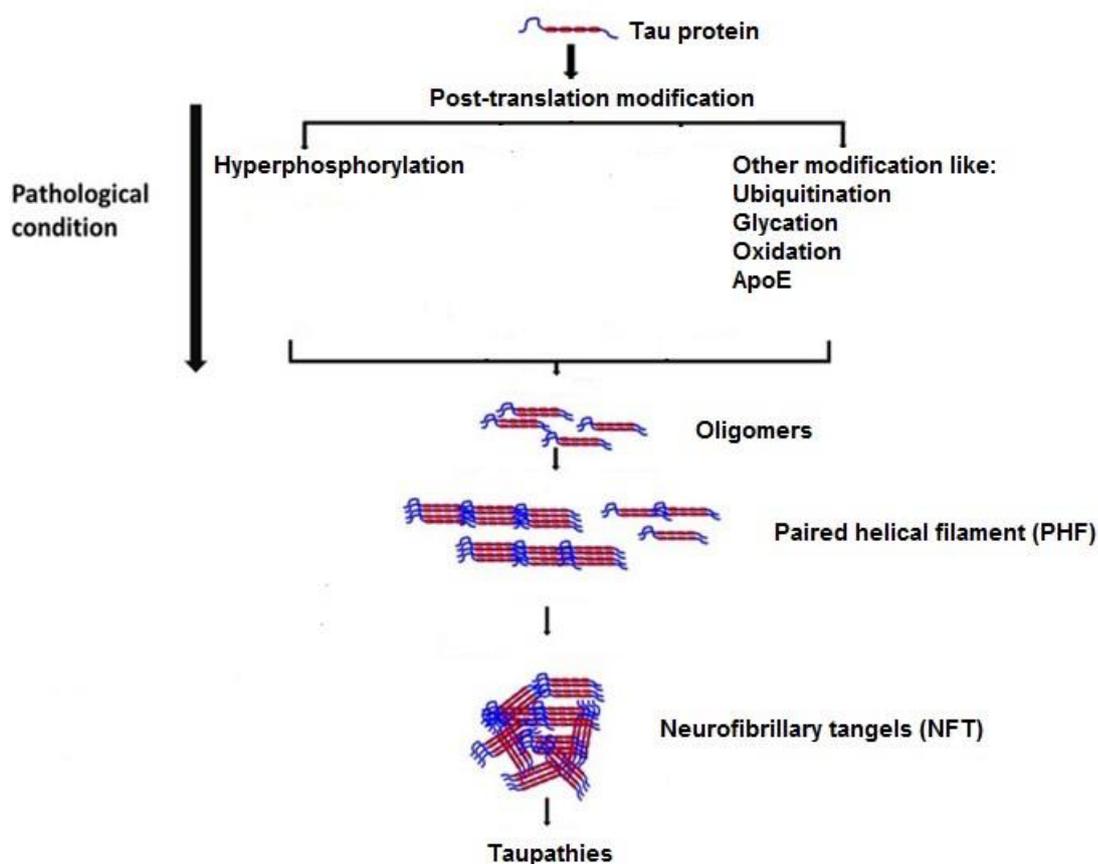
Figure 5: Schematic representation of the changes in tau leading to pathological aggregation. Under pathological conditions, the aggregation is initiated and tau-protein monomers self-assembly and form oligomers. The small oligomeric tau species are toxic. Tau oligomers continue to accumulate and form filaments (PHF), which eventually form the neurofibrillary tangles (NFT) characteristic of the disease (according to Guzmán-Martinez et al., 2013 with modifications).

1.3.3 The dominant role of PHF6 (VQIVYK) and PHF6* (VQIINK) in tau aggregation

The insoluble aggregates of tau protein are involved in tau-related diseases, termed tauopathies, in which tau appears in an aggregated, chemically modified state (phosphorylation, oxidation, and glycation). Experimental aggregation studies, as well as computer simulations, have shown that tau aggregation is also strongly driven by two hexapeptide fragments, namely PHF6 (VQIVYK) and PHF6* (VQIINK). *In vitro* studies have revealed that short tau peptides containing PHF6 or PHF6* can aggregate and form fibrils (Pickhardt et al., 2004).

The PHF6 segment is located at the start of the third repeat (R3) and is present in all tau isoforms. In contrast, the PHF6* segment is located at the start of the second repeat (R2) and is present only in four-repeat (4R) tau isoforms (Figure 6) as it is encoded by an alternatively spliced exon 10 sequence (Eschmann et al., 2015).
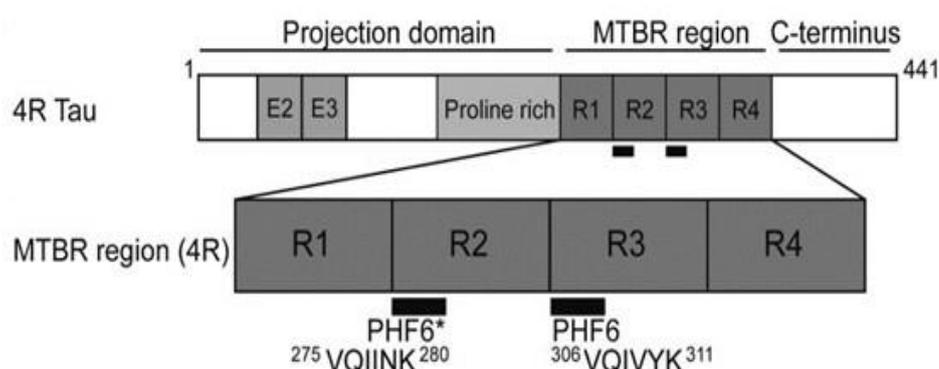
Figure 6: Diagram of the MTBR showing the location and sequence of the two hexapeptide units (PHF6* and PHF6). The full-length four-repeat (4R) tau consists of 441 amino acids, the longest isoform in the human central nervous system. This isoform has a projection domain as well as four repeats in the microtubule binding repeat region (MTBR). The PHF6 segment is located at the beginning of the third repeat (R3) and the PHF6* segment is located at the beginning of the second repeat (R2) (Eschmann et al., 2015).

Until recently, it was thought that PHF6, 306-VQIVYK-311, is the most potent driver for tau assembly into paired helical filaments (PHF), and that mutations in this six-residue segment could decrease or increase the aggregation of tau. Furthermore, the PHF6 hexapeptide can self-aggregate *in vitro* even in the absence of any polyanionic cofactor

like heparin and forms fibrils similar to full-length tau fibrils. *In silico* studies on the PHF6 self-aggregation fragment found a zipper-like arrangement of the amino acid residues owing to hydrophobic stabilization (von Bergen et al. 2000; Goux et al. 2004; Ganguly et al., 2015). However, in 2018, Seidler et al. suggested that the VQIINK segment (PHF6*) is the more powerful driver of tau aggregation (Seidler et al., 2018).

1.4   Diagnosis of Alzheimer's disease

1.4.1   Current diagnostic methods

The diagnosis of Alzheimer's disease (AD) is so challenging and the definitive diagnosis requires post-mortem examination of brain tissue. The current diagnosis of AD is based mainly on patient interview, disease history, clinical neuropsychological examination, and identification of typical symptoms of AD. As AD is associated with a large loss in brain weight and volume, a brain scan, using either computed tomography (CT) or magnetic resonance imaging (MRI), is recommended in the standard evaluation of AD. Both CT and MRI scans can reveal the loss of brain mass associated with AD. Other brain scans, such as Positron emission tomography (PET) can also be performed. While CT scans and MRIs can only reveal changes in later stages of the disease and are unable to detect problems at the cellular level, PET scans are able to detect early pathological cellular changes (McKhann et al., 1984; DeCarli et al., 1990).

Although Aß and tau are both considered key biomarkers in AD and correlate with disease progression, latest development in radiological imaging have allowed the detection of AD pathological biomarkers using PET. Over the past decade, the development of non-invasive diagnostic neuroimaging markers for AD lead to increase the diagnostic accuracy in AD. Most notably, molecular imaging of brain amyloid by PET imaging using radiotracers that label fibrillar forms of amyloid-β. Patients are injected with a radiolabelled tracer agent and undergo a specialized PET scan, which detects the aggregation of amyloid-β peptides into plaques in the living brain. At the present time, ^{18}F-labeled amyloid radiotracers (^{18}F-florbetapir, ^{18}F-florbetaben, and ^{18}F-flutemetamol) have been approved for use in clinical settings in US and in Europe. In

practice, using of amyloid PET imaging is still limited because of its high cost for most patients (McKhann et al., 2011; Laccarino et al., 2017; Weller et al., 2018).

Moreover, AD biomarkers can be detected in the cerebrospinal fluid biomarker (CSF) of AD patients. Aβ42, total tau (t-tau) and phosphorylated tau (p-tau) have been the focus of biomarkers research due to the direct correlation with pathological hallmarks (Tapiola et al., 2009). Many studies have demonstrated an increase of approximately 300% in the concentration of t-tau in AD patients compared to normal elderly individuals. In several studies, elevated p-tau levels have also been detected in the CSF of AD patients in comparison to controls, with sensitivity and specificity of between 80 and 90% (Biagioni et al., 2011). However, there is high inter- and intra-laboratory variation so the classical cut-off of pathological levels varies between laboratories performing the same method. Another limitation of this method, that CSF-levels of AD biomarkers are altered in diabetic and prediabetic patients (Lu et al., 2018; Bogdanovic et al., 2018)

1.4.2 Diagnostic methods under investigation

Despite the hypothesis that Aß accumulation is the primary cause of AD, studies have shown that the pathological changes in tau correlate more closely with cognitive changes and disease progression. Therefore, detecting pathological changes in tau provides attractive targets for novel diagnostic strategies (Wu et al., 2017). PET-tau is under intense development and several tau tracers have been developed and tested in human PET studies. Currently available tau tracers fall into 4 groups: the nonselective tracer 18F-FDDNP, quinoline derivatives, pyrido-indole derivatives, and phenyl/pyridinylbutadienyl-benzothiazoles/benzothiazoliums derivative (PBB3). These promising tau-specific PET tracers are now available for clinical evaluation and present a major breakthrough in AD research (Saint-Aubert et al., 2017).

Detection of plasma biomarkers in blood plasma could enable a minimally invasive test. Recent studies on plasma levels of Aß as a marker for AD demonstrated that brain amyloid positivity could be accurately evaluated using one blood sample. Studies have reported increased t-tau levels in the plasma of AD patients. However, several improvements in technologies to use plasma level of t-tau as a blood biomarker for

dementia are also being developed. This may facilitate the detection of tau oligomers or other tau species, which play a key role in tau aggregation (Biagioni et al., 2011, Bateman et al., 2019).

1.5 Therapeutic strategies of Alzheimer's disease

1.5.1 Current medication therapies

Despite all scientific efforts, there is still no curative treatment for AD. Currently, there are four medications available for the treatment of AD. Three cholinesterase inhibitors (CIs) donepezil, rivastigmine, and galantamine. These drugs inhibit the enzymatic breakdown of acetylcholine, a neurotransmitter that is responsible for cognitive function in the brain, and increase its concentration. The fourth drug is memantine. Memantine is an N-methyl-d-aspartate receptor antagonist that blocks the effect of glutamate, a neurotransmitter in the brain, by preventing its binding to the target receptors. This protects neurons from excitotoxicity and prevents neuronal cell death, which may reduce behavioral and psychological symptoms of AD. However, all established treatments are only symptomatic, they slow down the disease progression and can delay the symptom, but they do not significantly improve cognitive function or cure the disease (Wenk et al., 1995; Rogers et al., 1998; Parsons et al. 1999; Reisberg et al., 2006).

1.5.2 Current research and possible future treatment

Therapies under study are compounds that target the pathological biomarkers of AD: extracellular amyloid β (Aβ) plaques and intracellular neurofibrillary tangles (NFTs) (McKhann et al., 1984).

Although it is still controversial if Aβ is the causative protein leading to AD, AD therapy research has been predominantly focused on "Amyloid hypothesis" and several Alzheimer's therapeutics have been developed by targeting amyloid beta peptide. Aß-related therapeutic strategies involve, decreasing the production of Aß or enhancing its clearance. However, the literature provides major arguments for and against the amyloid hypothesis. It seems likely, that Aβ is key initiator of AD and amyloid plaques are necessary, but not sufficient, to cause AD. So far, all Aβ-targeting drugs developed

to treat AD have not succeeded and the recent research suggests that the main driver of AD is tau, not Aβ (Kametani et al., 2018).

It has been also considered controversy whether tau hypothesis is the primary causative of AD or plays more a secondary role. However, candidate drugs targeting tau currently seem to be the most promising strategy for AD drugs development (Frost et al., 2015). Here, an overview of the principal strategies targeting tau in AD, as described in the literature, is provided.

Modulating tau phosphorylation

Due to the correlation between tau phosphorylation and AD pathology, tau-protein kinase inhibitors constitute potentially useful treatments. In fact, tau hyperphosphorylation *in vivo* seems likely due to multiple protein kinases. Precisely which kinase is the most effective target to minimize pathological tau phosphorylation remains an open question (Wang et al., 2007; Zhang et al., 2013). Many protein kinases, such as GSK-3β, MARK, and CDK5, have been considered as attractive AD therapeutic targets. However, therapeutic agents that modulate tau phosphorylation, such as Tideglusib and Lithium (available GSK-3β inhibitor), have not demonstrated clinical benefit to date (Anand and Sabbagh, 2015; Lovestone et al., 2015; Medina, 2018).

Microtubule stabilizers

Another tau-targeting therapeutic strategy in neurodegenerative diseases is stimulating microtubule stabilization. As is known that detachment of tau from microtubules causes loss of tau MT-stabilizing function, resulting in the suggestion that MT-stabilizing molecules could be used as therapeutic agents. Among such MTstabilizing molecules, which has reached an advanced clinical phase, is davunetide (also known as NAP). Davunetide is an eight-amino acid peptide that has shown promising effects in tau transgenic mice, but later clinical trials in AD patients ended in failure (Matsuoka et al., 2008; Boxer et al., 2014).

Anti-tau immunotherapy

Anti-tau immunotherapy for several neurodegenerative disorders represents a potential strategy for the clearance of pathological proteins in these diseases. Anti-tau

active immunotherapy strategies utilize specific antibodies that bind to pathological tau, leading to a clear up of tau pathological species and a potential improvement in neuronal function (Huang and Mucke, 2012). Studies have reported a reduction in filamentous tau inclusions in transgenic mice by active immunization targeting phosphorylated tau (Asuni et al., 2007). The clearance mechanism of intracellular proteins, such as tau, by immunization is still unknown, but it may involve lysosomal proteolysis and autophagy of tau-antibody complexes (Sigurdsson, 2009). To achieve a successful immunotherapy approach, it is important to identify the correct epitopes and conformations that differentiate between physiological and pathological tau. In summary, a number of anti-tau immunotherapy are already in clinical trials such as ABBV-8E12, BIIB092, AADvac-1 and ACI-35 (Medina, 2018).

Tau aggregation inhibitors

As tau aggregation correlates with clinical Alzheimer disease progression, the inhibition of tau aggregation could protect the damaged neurons. Several tau aggregation inhibiting substances have been described in the literature. Methylene blue, which inhibits tau–tau interactions and reduces soluble tau through other mechanisms, has shown promising results in terms of delaying disease progression in a phase II clinical trial carried out of the course of one year. Clinical phase III trials with an optimized formulation of methylene blue (LMTX) are in progress to investigate the potential of LMTX in slowing the progression of the disease in AD patients (Gura, 2008; Huang and Mucke, 2012; Jadhav et al., 2019). Several chemical compounds that inhibit tau fibril formation have been identified, including phenothiazines (Wischik et al., 1996) anthraquinones (Pickhardt et al., 2005), polyphenols (Taniguchi et al., 2005), quinoxalines (Crowe et al., 2007) and phenylthiazolyl-hydrazides (Pickhardt et al., 2007). However, excluding the phenothiazine methylene blue, none of these molecules has been tested *in vivo*, and most of the compounds described above have biochemical characteristics that likely render them unsuitable as CNS-targeted therapeutics (Crowe et al., 2018).

1.6 D-peptides for therapy and diagnosis of Alzheimer's disease

The use of small D-peptides for diagnosis and therapy of AD by may represent a reasonable alternative to chemical pharmaceuticals. Peptides are specified as (linear) molecules consisting of two or more (<100) amino acids. D-enantiomeric peptides are extremely protease resistant, which extends their period of biological activity and renders them prime candidates for the development of therapeutic drugs. D-peptides are considerably less immunogenic than L-peptides and their suitability for *in vivo* applications has been confirmed. In addition, studies showed systemic absorption of therapeutic D-peptides after oral administration (Milton et al., 1992; Pappenheimer et al., 1994; Pappenheimer et al., 1997; Chalifour et al., 2003; Funke et 2010). Therefore, small peptides that bind to Aβ or tau and influence aggregation are of particular interest.

Several small peptides that prevent aggregation of Aβ have already been described and some of them have been shown to be effective in AD animal models. In addition, Aβ binding peptides have been developed for use in *in vivo* imaging methods for possibly early diagnosis of AD. Using mirror image page display method, the group of Willbold in Germany identified D-Peptide D3 (rprtrlhthrnr). D3 disassembles Aβ aggregates and reduces the amyloid plaque burden in APP/PS1 double transgenic mice. It has been demonstrated that D3 peptide, when injected or infused into animal, did not cause an inflammatory response and was able to bind to Aβ1–42 in the brains of transgenic mice. Furthermore, it has been shown that D3 is taken up by neurons. Oral treatment with D3 led to an improvement in pathology and behavior in APP/PS1 double transgenic mice, indicating that the peptide is capable to cross the blood brain barrier using transcytosis. Recently, D-enantiomeric peptide RD2, derived from D3 by rational design, was successfully tested in a phase I clinical study (van Groen et al., 2008; van Groen et al., 2009; Funke et al., 2010; Leithold et al., 2016; Klein et al. 2016; Kutzsche et al., 2017; van Groen et al., 2017; Elfgen et al. 2019; Willbold and Kutzsche; 2019).

As it previously mentioned, the majority of existing AD therapeutic research has focused on Aβ. However, to date little research has been directed towards the development of tau-targeted peptides.

In 2011, the Eisenberg group developed a D-amino acid inhibitor of tau fibril formation using computer-aided structure-based design. The peptide TLKIVW was designed to

interact favorably with the 306-VQIVYK-311 segment on tau (PHF6). It has been demonstrated that VQIVYK plays a crucial role in tau fibrillization and is commonly used as a model for tau fibrillization. The designed peptide, TLKIVW, inhibits the aggregation of PHF6 as well as of the tau constructs K12 and K19 (Sievers et al., 2011).

In 2016, a study by our group showed a modulation of the tau aggregation mechanism by 12 amino acid D-enantiomeric peptides (Dammers et al., 2016). Mirror phage display selections were conducted using fibrils of the D-enantiomeric PHF6 as a target. The study showed that PHF6 binding D-enantiomeric peptides APT, KNT, LPS, TD28, and TD28rev, selected by mirror image phage display, inhibit PHF6 and full-length tau fibrillization. Furthermore, the selected peptides were able to penetrate tau expressing N2a cells.

In a very recent study in 2018 by the Eisenberg group, the authors hypothesized that PHF6* is a more powerful driver for tau aggregation than PHF6, and that inhibitors based on the structure of PHF6 fragment only partially inhibit the fibrillization of full-length tau. Using PHF6* segment as a template, they designed structure-based inhibitors that inhibit seeding by tau fibrils in a concentration-dependent manner. The most promising designed peptide, named as W.MINK, showed its ability to inhibit the aggregation of full-length tau in THT assays. In addition, W.MINK was able to block the seeding of intracellular tau, induced by exogenous tau40 fibres, in HEK293 biosensor cells (Seidler et al., 2018).

1.7 Phage display as a tool for drug discovery

Phage display technology constitutes an important approach for discovering novel target-specific ligands for proteins. Antibodies and peptides are expressed on a phage surface and used for target screening. In 1985, phage display was discovered by George P. Smith after he demonstrated the display of fusion proteins on the virion surface (Smith, 1985). Phage display has been widely used in many therapeutic and diagnostic approaches as a result of its economical, rapid, and effective properties (Qiang et al., 2017).

A bacteriophage (phage) is a virus that infects bacteria. There are three types of bacteriophage; filamentous, lambda and T7 phage. The filamentous phage family includes three strains M13, f1 and fd (Salivar et al., 1964; Smith, 1985). The M13 phage is commonly used for phage display (Huang et al., 2012). Foreign DNA fragments can be inserted into a phage gene to encode a fusion protein, leading to physical linkage between the DNA sequence and the peptide sequence. Ph.D. peptide library series (New England BioLabs, Inc., USA) is the most widely used peptide library, in which the displayed peptides (12-mer) are fused to the minor coat proteins (pIII) (Parmley and Smith, 1988; Qiang et al., 2017).

A typical phage display peptide library contains a large number of phage particles (a population of $> 10^{12}$ phage clones), whereby each displays a different peptide. Therefore, biopanning, a procedure to select specific binders, is essential to enrich the desired binding molecules. The target molecule is immobilized on a solid support such as microtiter plate wells (Watters et al., 1997). Phages from the library are added to the immobilized target. Nonbinding clones are washed away and clones bound to the target are eluted by different strategies. The eluted bound phages are amplified in *E.coli* and used for the next round of biopanning to re-select bound phages (see Figure 7). Several rounds of biopanning are necessary in a screening procedure until the phage pool is enriched with specific binding phages. For determining the binding activity of obtained monoclonal phages, tests are used, for example an enzyme-linked immunosorbent assay (ELISA). The sequence of the binding peptides is identified by sequencing of the phage DNA encoding the peptide (Cwirla et al., 1990; Scott and Smith, 1990).
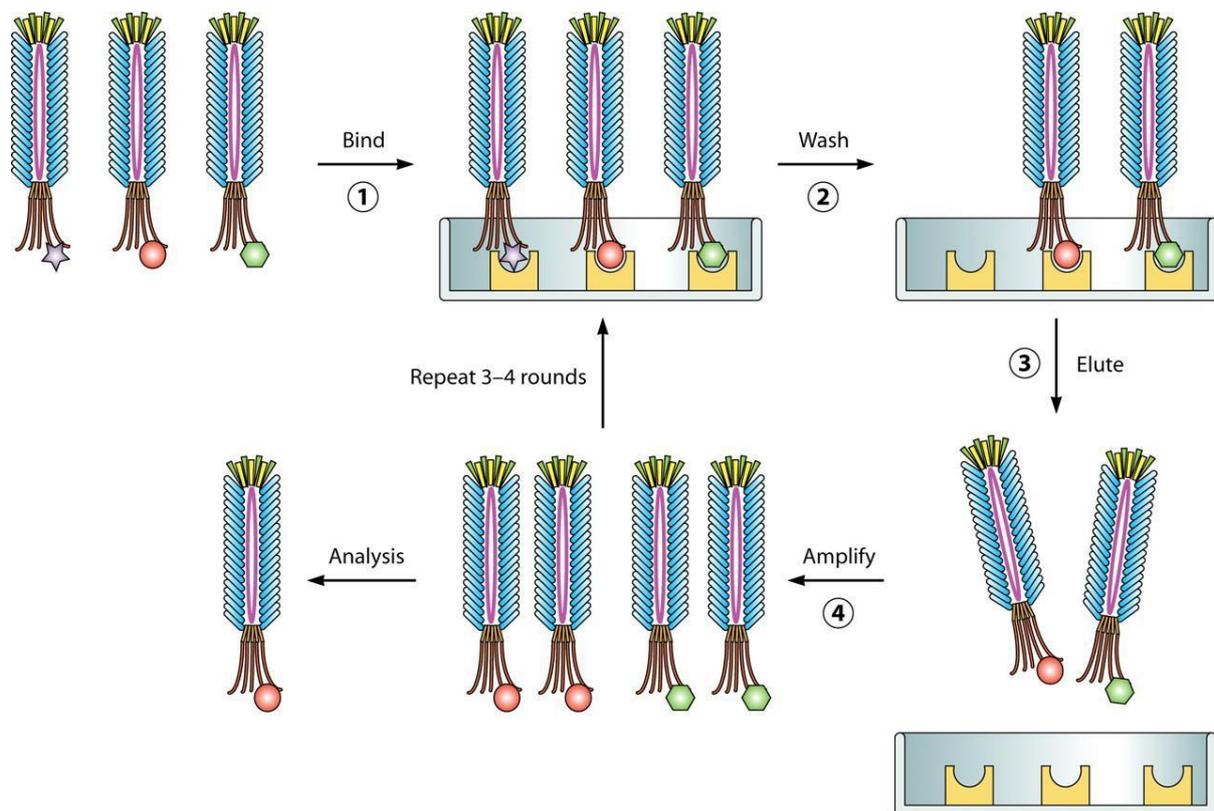
Figure 7: The principle of the phage display system for the selection of peptides binding to an immobilized target. A phage library is incubated on a target-coated surface, followed by extensive washing to remove non-specific phages. Subsequently, bound phages are eluted and amplified in *E.coli*. The amplified phages are used for the next round of biopanning to reselect bound phages. After several selection rounds (3-4), individual bound phage clones are isolated. ssDNA of the phages clones are extracted and after sequencing, the peptides sequences are identified (Huang et al., 2012).

Phage display and its application is the subject of many patents, and therapeutic products developed by this technology are available on the market (Bazan et al., 2012). However, despite the success of many phage display selections and the discovery of strong binders for several targets, confused results can be obtained. Phages with no actual affinity to the target may be selected, instead of specific ligands (Vodnik et al., 2011). The obtained peptides that bind to other components of the screening system and do not exhibit specific affinity to targets are named target-unrelated peptides (TUPs) (Menendez and Scott, 2005). However, several freely accessible tools compare each sequence with their database and assist in the reporting and excluding of possible target-unrelated peptides (Vodnik et al., 2011; Qiang et al., 2017).

1.7.1 Mirror image phage display

The main disadvantages of peptides selected from biologically encoded libraries are their short half-life *in vivo* as a result of fast degradation by enzymes, and their ability to trigger an immune response. Thus, Schumacher and co-workers developed an elegant approach in 1996, termed the mirror image phage display, which allows the peptides identification in the D-conformation (Dintzis et al., 1993; Schumacher et al., 1996).

In a common phage display approach, an L-peptide library is expressed on the surface of the phages and bind to the L-enantiomeric form of the immobilized target protein. By employing mirror image phage display, the biopanning is performed against the mirror image of the original protein target, which is composed of the same amino acid sequence but in unnatural D-enantiomeric form (see Figure 8). A cause of the symmetry, the synthesized D-enantiomeric form of the selected peptides will bind to the L-enantiomeric form of the target protein. The D-enantiomeric peptides have many advantages over L-peptides. Mainly, they have a long serum and salvia half-live due to their resistance to proteases. Furthermore, while L-peptides should be injected to avoid digestion, D-peptides can be absorbed into the systemic circulation following oral administration (Milton et al., 1992; Pappenheimer et al., 1994; Chalifour et al., 2003; Sadowski et al., 2004). However, mirror image phage display can be performed against target proteins which fold spontaneously and do not require molecular chaperones for functional folding. Because it is not clear if the natural chaperones can fold the D-form of the protein or D-form of the chaperon is required (Weinstock et al., 2014).

A number of mirror image phage display approaches used for the selection of D-peptides seemed to be interesting and promising for the diagnosis and therapy of Alzheimer's disease. D-enantiomeric peptide D3 was selected, in a mirror image phage display, against monomeric and small oligomeric D-Aß peptide as a target. D3 showed promising results in Alzheimer's transgenic mice after oral treatment (van Groen et al., 2008). In addition, a study by our group (Dammers et al., 2016) identified PHF6 binding D-enantiomeric peptides, using mirror image phage display, that inhibit PHF6 and full-length tau fibrillization *in vitro*. Moreover, the selected peptides were able to penetrate tau expressing N2a cells.
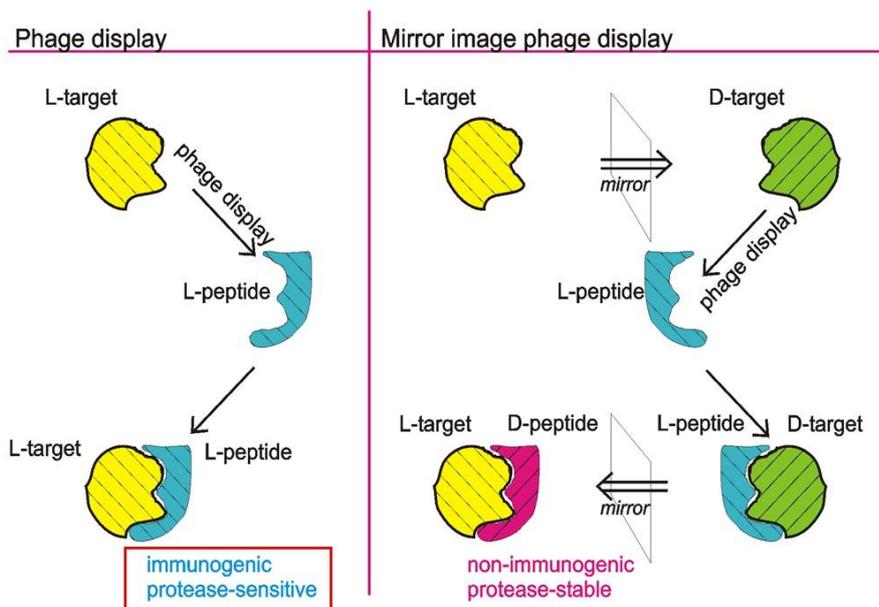
Figure 8: The principle of phage display and mirror image phage display. In phage display, the L-enantiomeric form of the protein-target is used and the L-peptides that bind to the target are selected. The selected L-peptides have the disadvantages that they are immunogenic and protease-sensitive. In mirror image phage display, the D-enantiomeric form of any protein-target is synthesized and used for the selection. The L-peptides that bind to the D-enantiomeric target, are selected. The D-enantiomeric form of the selected L-peptides are synthesized. These synthesized D-peptide will bind to the L-enantiomeric form of the target. The D-peptides have many advantages comparing with L-peptides. Mainly, they are non-immunogenic and resistant to proteases (according to Funke and Willbold, 2009 with modifications).

2   Objective of the thesis

To date no curative drug for AD has been developed, and those therapies that are currently available can only delay the progression of the disease. Therefore, there is a need for novel diagnostic and therapeutic approaches for AD and the recent research suggests that targeting tau pathology represents a promising lead in this regard.

In this project, the main aim was to develop novel therapeutic D-enantiomeric peptides that target tau protein using both phage display and mirror image phage display. D-enantiomeric peptides were chosen as they are stable against protease and considerably less immunogenic than L-peptides (Schumacher et al., 1996; Chalifour et al., 2003; Sadowski et al., 2004). Another aim of this study was to investigate which of the both fragments within tau, PHF6 or PHF6*, is likely the more effective target for the development of tau aggregation inhibiting peptides.

First, large quantities of tau protein were needed for this project. Thus, it was necessary to establish a method for expression and purification of full-length tau protein.

Next, the first phage display selection was performed against the L-enantiomeric full-length tau monomer. The selected L-peptides were synthesized as D-peptides. In addition, using mirror image phage display, the second selection was performed against the fibrils of the D-enantiomeric hexapeptide 275-VQIINK-280 (PHF6*), representing residues 275–280 of the tau protein.

The selected peptides from both selections were characterized by Thioflavin T (THT) assays in order to determine whether they can modulate pathological tau aggregation *in vitro.*

The ability of the selected peptides to bind to tau monomers, tau fibrils, PHF6 fibrils and PHF6* fibrils was tested using ELISA (Enzyme-Linked Immunosorbent Assay). To enable the use of this method, FAM-labeled versions of the peptides were synthesized.

Also, we performed early preliminary experiments to investigate the hypothesis that PHF6* is the superior target for inhibitors of pathological tau aggregation. The tau aggregation inhibiting effects of the most promising peptides resulting from this project, MMD3 and MMD3rev, were compared with another peptide, designated APT, which

was selected against PHF6 fibrils earlier by our group. As controls, we further tested the performance of two peptides previously described in the literature, TLKIVW and W.MINK, which target PHF6 and PHF6*, respectively.

3 Material and Methods

3.1 Material

Unless otherwise stated, all chemicals and reagents were purchased from Bio-Rad Laboratories GmbH (München), Carl Roth GmbH + Co. KG (Karlsruhe), GE Healthcare (Freiburg), Merck Chemicals GmbH (Darmstadt), New England BioLabs GmbH (NEB; Frankfurt a. M.), Sigma-Aldrich Chemie GmbH (Taufkirchen), Thermo Fisher Scientific/Life Technologies GmbH (Darmstadt) and VWR International GmbH (Ismaning).

3.1.1 Antibodies

The antibodies listed below were aliquoted upon arrival and frozen at -20 °C.

Table 1: List of the used antibodies.

description	target	appilcation	Catalog number	manufacturer
Anti-Tau [TAU-5] (primary antibody)	Human protein tau	WB	AHB0042	Invitrogen
Anti-M13 monoclonal, HRP conjugate (primary antibody)	Bacteriophage M13	ELISA	27-942101	GE Healthcare
anti-FITC-HRP, sheep (primary antibody)	Fluorescein isothiocyanate (FITC)	ELISA	640005	AbD Serotec, Puchheim
Goat-anti-Mouse IgG-h+l, AP conjugate (secondary antibody)	Mouse species	WB	A90616AP	Bethyl Lab., Inc., Montgomery

3.1.2 Bacterial strains

Escherichia coli	Genotype	application	manufacturer
E. coli BL21 (DE3)	F– ompT gal dcm lon hsdSB(rB-mB-) λ(DE3 [lacI lacUV5-T7 gene 1 ind1 sam7 nin5])	gene expression	Life Technologies, Darmstadt
E. coli ER2738	F´ proA+ B+ lacIq Δ(lacZ)M15 zzf::Tn10(TetR)/fhuA2 glnV Δ(lac-proAB) thi-1 Δ(hsdS-mcrB)5	phage display	New England BioLabs, Ph.D. Phage Display Libraries Kit, Frankfurt a. M.

3.1.3 Plasmids and primers

plasmid	insert	vector	manufacturer
pET28a(+)_tau 441aa	Full length human tau protein 2N4R	pET28a(+)	Genentech (San Francisco)

primer	sequence	manufacturer
-96 gIII sequencing primer	5´- GTATGGGATTTGCTAAACAAC–3´	Sigma-Aldrich

3.1.4 Peptides

All peptides used in this thesis are listed in Table 1 and Table 2. All peptides were purchased from JPT Peptide Technologies GmbH (Berlin). The company provided HPLC-purified lyophilisates with a stated purity of > 95 %. The peptides were stored at -20°C.

Table 2: List of synthetic peptides

name	amino acid sequence	chirality
PHF6	VQIVYK	L
PHF6*	VQIINK	L
PHF6*	vqiink	D
Sievers	tlkivw	D
APT	aptllrlhslga	D
W.MINK	DVWMINKKRK	L

Table 3: List of synthetic peptides selected during this thesis

name	amino acid sequence	chirality	target of the selection
MM1	GSWNTFRAQPTI	L	Tau monomer
MM2	LTPHKHHKHLHA	L	Tau monomer
MM3	DPLKARHTSVWY	L	Tau monomer/ PHF6* fibrils
MM4	HMSYGNGTRDTP	L	Tau monomer
MM5	GSPLSNPTRMWL	L	Tau monomer
MM6	DTLVKQNKLMAA	L	Tau monomer
MM7	HLSSPYWIGSMR	L	Tau monomer
MM8	HLTATELANSYH	L	Tau monomer
MMD2	ltphkhhkhlha	D	Tau monomer
MMD2rev	ahlhkhhkhptl	D	Tau monomer
MMD3	dplkarhtsvwy	D	Tau monomer/ PHF6* fibrils
MMD3rev	ywvsthraklpd	D	Tau monomer/ PHF6* fibrils

MMD2-Lys(FAM)-NH2	LTPHKHHKHLHA-Lys(FAM)NH2	D	Tau monomer
MMD3-Lys(FAM)-NH2	DPLKARHTSVWY-Lys(FAM)-NH2	D	Tau monomer/ PHF6* fibrils
MMP1	GRDMPMSALMRH	L	PHF6* fibrils
MMP2	WPHDTKRYLFPA	L	PHF6* fibrils
MMP3	YVPANNYHLHSP	L	PHF6* fibrils
MMP4	HPAPHRYHSNLH	L	PHF6* fibrils
MMP5	TRTATLADNSWL	L	PHF6* fibrils
MMP6	HSDLWRRSFELM	L	PHF6* fibrils
MMPD2	wphdtkrylfpa	D	PHF6* fibrils
MMPD6	hsdlwrrsfelm	D	PHF6* fibrils

3.1.5 Buffers, media and kits

All used buffers, solutions and media are listed in Table 4; they were prepared in distilled, deionized water. All kits used are listed in Table 5.

Table 4: List of buffers and media.

description	composition
Blocking buffer (ELISA)	0,1% (w/v) bovine serum albumin in 0.1 M NaHCO3 buffer, pH 8.6
Blocking buffer (phage display)	5 mg/mL bovine serum albumin in 0.1 M NaHCO3, pH 8.6 sterile filtered
Blocking buffer (WB)	1x TBS 0,05% Tween-20 5% milk

Buffer A	20 mM HEPES pH 6.8
Buffer B	20 mM HEPES 1 M NaCl pH 6.8
Calcium chloride (CaCl2) buffer	50 mM, pH 9,0
Coomassie brilliant blue staining solution	0,25% coomassie blue R250 50% methanol 10% acetic acid

destaining solution	9% methanol 9% acetic acid 9% glycerine
Heparin stock solution	1 mM heparin in ddH2O
IPTG stock solution	500 mM in H2O, sterile filtered
IPTG/Xgal	5 g/l IPTG 4 g/l Xgal in Dimethylformamid
IPTG/Xgal/LB plates	1 ml from IPTG/Xgal stock solution for 1 l LB-agar
Kanamycin	50 mg/ml in H2O, sterile filtered; used concentration: 50 µg/ml
LB-Agar	1,5% (w/v) Agar-Agar in LB medium
LB medium	1% (w/v) Trypton 0,5% (w/v) Hefeextrakt 0,5% (w/v) NaCl dissolved in ddH2O and autoclaved

Lysis buffer	20 mM HEPES 1 mM EDTA 2 mM Proteaseinhibitor 2 mM 2-Mercaptoethanol pH 6.8
0.5 M Napi-buffer (sodium phosphate)	0.5 M Na2HPO4 pH 9 0.5 M H2NaPO4 pH 4 Mix the solutions to final pH 7
1x PBS	1,37 M NaCl 27 mM KCl 14 mM KH2PO4 100 mM Na2HPO4 in ddH2O, pH 7.5
PBST	1x PBS 0,01% (v/v) Tween-20
PefaBlock stock solution	200 mM in sterile ddH2O
PEG/NaCl	20% (w/v) polyethylene glycol–8000 2.5 M NaCl, autovlaved
10x SDS running buffer	25 mM Tris 192 mM glycerine 0,1% (w/v) SDS pH 8,3
4x SDS sample buffer	40% (v/v) glycerine 250 mM Tris-HCl, pH 6.8 8% (w/v) SDS 0,015% (w/v) Bromophenol blue 20% (v/v) β-Mercaptoethanol
1x TBS (WB)	20 mM Tris-HCl, pH 7.5 150 mM NaCl
1x TBS (phage display)	50 mM Tris-HCl, pH 7.5 150 mM NaCl

Tetracyclin	20 mg/ml in 1:1 EtOH:H2O; used concentration: 20 µg/ml
Thioflavin T stock solution	1 mM thioflavin T in ddH2O
Top-Agar	7 g/l Agar-Agar in LB-medium autoclaved
1x Transfer buffer	25 mM Tris 192 mM Glycine pH 8.3
Washing buffer (ELISA)	1x PBS 1% (v/v) Tween-20
Washing buffer (WB)	1x TBS 0,05% (v/v) Tween-20

Table 5: List of used kits.

description	manufacturer
Ph.D.-12 Phage Display Peptide Library Kit	New England BioLabs, Frankfurt a.M.
Pierce™ 660nm Protein Assay Kit	Thermo Fisher Scientific, Darmstadt
TMB Peroxidase EIA Substrate Kit	Bio-Rad Laboratories, München
AP Conjugate Substrate Kit	Bio-Rad Laboratories, München

3.2   Microbiological methods

3.2.1   Calcium chloride method for preparation of chemical competent cells

Chemical competent cells were prepared by inoculation of 100 ml LB medium with one colony *E. coli* BL21 (DE3). The culture was incubated overnight at 37°C and by rotation

of 120 rpm. The next day, 200 ml LB medium were inoculated with 20 ml of overnight cell culture and incubated at 37 °C with 140 rpm shaking until $OD_{600} \geq 0.6$ was reached. The cells were harvested by centrifugation for 20 min at 4000x g and 4°C. The supernatant was discarded, the pellet was resuspended in 20 mL ice-cold 50 mM CaCl2 buffer and incubated on ice for 30 min. The cells were separated by centrifugation for 10 min at 4 °C and 4000x g. Finally, the pellet was resuspended in 10 mL ice-cold CaCl2 50 mM solution and incubated for 15 min on ice. Bacterial glycerol stocks were prepared by adding sterile glycerol to a final concentration of 25 % and the cell suspension was portioned into 200 µL aliquots. The chemical competent cells were stored at -80 °C.

3.2.2 Heat shock transformation of DNA into chemically competent cells

The plasmid pET28a(+)_tau441aa was transformed into the chemically competent cells *E. coli* BL21 (DE3) via heat shock. The cells were thawed on ice, 1 µg of the plasmid DNA was added and they were incubated on ice for 15 min. The cells were heated up to 42 °C for 90 seconds and then cooled on ice for 2 min. The transformed cells were filled up to a total volume of 1 mL with LB media and incubated for 1 hour (h) at 37 °C and 130 rpm. The cells were plated out onto agar plates including kanamycin at a concentration of 50 µg/ml in two steps of 200 and 800 µL, respectively.

The plates were incubated overnight at 37 °C.

3.3 Molecular biological methods

3.3.1 Expression of recombinant human tau protein

One transformed colony was picked from the kanamycin agar plate, inoculated into 50 ml LB containing 50 µg/ml kanamycin. This culture was allowed to grow overnight under shaking (130 rpm) at 37°C. The following morning, 1 L main culture LB media containing 50 µg/mL Kanamycin, 0.5 % glucose and 10 mM MgCl2 was inoculated with 10 ml overnight culture and divided into 2 different 2 L shaking flasks filled with 500 mL volume. The culture was incubated at 37 °C and 150 rpm until an extinction at 600 nm wavelength $OD_{600} \geq 0.6$ was reached. Subsequently, tau expression was induced by adding IPTG to a final concentration of 1 mM. After induction for 3 h at 37°C and 150

rpm, cells were pelleted by centrifugation at 4000x g for 20 min at 4 °C. The resulting pellet was then resuspended in 14 ml of lysis buffer and immediately stored at -20°C until further use.

To check for successful tau expression, 1 ml of uninduced and induced samples were aliquoted and centrifuged for 1 min at 14000 rpm. The resulting pellets were suspended in 4x SDS sample buffer (200 µl for one unit of OD_{600}). The samples were boiled at 95 °C for 5 min and analyzed using SDS-PAGE.

3.3.2 Extraction of recombinant tau protein

The frozen resuspended cell pellet was thawed on ice, the cell lysate was pipetted into a fresh falcon tube and boiled for 10 min. Through this boiling treatment, most of the proteins are denatured apart from tau, which remains in solution preserving its physiological function. After cooling the boiled cell lysate on ice for 10 min, the denatured proteins were removed by centrifugation at 4°C, 5000x g for 1 h. The supernatant containing tau protein was taken for further purification. 20 µl were taken from the supernatant and prepared for SDS-PAGE analysis.

3.4 Protein chemical methods

The purification of the tau protein was performed according to two protocols; the first was a modified version of that described by Margittai et al., 2004 and the second was a modified version of that described by KrishnaKumar et al., 2017. In the first protocol (Margittai et al., 2004), various purification methods were used such as ammonium sulfate precipitation, anion exchange chromatography and cation exchange chromatography. The high purified tau protein obtained from this method was used for the phage display selection. In the purification method reported by KrishnaKumar et al., 2017, they established a simplified protocol for efficient extraction in which tau lysate was purified by cation exchange chromatography. The purified tau protein obtained from this method was used for the thioflavin T aggregation assays.

3.4.1 Ammonium sulfate precipitation

Ammonium sulfate precipitation was carried out on ice to avoid protein degradation. Ammonium sulfate was added to the protein solution until a saturated solution of 50% concentration was obtained. The solution was allowed to precipitate overnight at 4°C. The precipitated proteins were collected by centrifugation. The pellet was dissolved in distilled water including 5 mM DTT and stored at 4 °C.

3.4.2 Cation exchange chromatography

The prepacked column HiTrap SP FF (GE Healthcare, Freiburg) was used. The column is packed with SP Sepharose Fast Flow, which is a negatively charged matrix, so the positively charged protein tau can bind to the column and a cation exchange can be performed. The column was equilibrated with buffer A according to the instructions supplied with the column. The sample, which contained the tau protein, was loaded into the column with flow rate 1 ml/min. After two washing steps with five-column volume (CV), tau protein was eluted by increasing the salt concentration, 0.1 M – 0.7 M NaCl in buffer A, using stepwise gradient elution. Fractions of 4 ml were collected. 20 µl samples from each fraction were taken for SDS-PAGE analysis.

3.4.3 Anion exchange chromatography

The positively charged Q sepharose Fast Flow (GE Healthcare, Freiburg) was used as a matrix. 2 ml of the slurry was prepared according to the manufacturer's instructions and transferred to a fritted column. After washing the slurry with an HEPES buffer, the fractions containing tau were loaded onto the column and the run was started with a flow rate of 1 ml/min. The flow through containing the tau protein was then collected.

3.4.4 Ultrafiltration

The samples containing recombinant tau protein were concentrated via ultrafiltration. Amicon® Ultra-15 centrifugal filter unit (Merck KGaA, Darmstadt) with a mass weight cut-off (MWCO) of 10 kDa was equilibrated with buffer A by centrifugation at 4000 x g, 8 °C for 10 min. The samples were filled into the column and centrifuged at 4000 x g, 8 °C until the desired volume was reached.

3.4.5 SDS-Polyacrylamide-gel electrophoresis (SDS-PAGE)

Protein samples were separated on standard 12% SDS-PAGE after mixing with 4x SDS sample buffer and heating at 95 °C for 5 min. The separating gel solution and the stacking gel solution were prepared according to Table 6 and Table 7 and poured into the gel cassette. A pre-stained protein ladder „Precision Plus ProteinTM Standard Dual Color" (Bio-Rad, München) was used

Table 6: Ingredients of 12 % SDS separating gel.

Ingredients	Volume
Acrylamid (30 %)	4 ml
1,5 M Tris/HCl buffer pH 8,8 (Bio-Rad)	2,5 ml
H2O	3,4 ml
10 % (w/v) SDS solution	0,1 ml
ammonium persulfate (APS) 10 % (w/v)	50 µl
TEMED	5 µl

Table 7: Ingredients of 5 % SDS stacking gel.

Ingredients	Volume
Acrylamid (30 %)	0.85 ml
1,5 M Tris/HCl buffer pH 6,8 (Bio-Rad)	1.25 ml
H2O	2,85 ml
10 % (w/v) SDS solution	50 µl
ammonium persulfate (APS) 10 % (w/v)	25 µl
TEMED	5 µl

3.4.6 Coomassie Brilliant Blue staining

The gel containing the SDS-Page separated proteins was stained with Coomassie Brilliant Blue G 250 staining solution for 20 min. To remove excess dye from the gel surface, the gel was incubated in destaining solution overnight. Finally, the gel was analysed with „GelDocTM XR+ Imaging System" (Bio-Rad, München).

3.4.7 Western Blot

Proteins bands were transferred from SDS-PAGE to nitrocellulose membrane 0.2 µM. The membrane was pre-wetted with transfer buffer for 10 min prior to use. The transfer was performed in a Wet-Blotting apparatus (Bio-Rad, München) for 1 h at 400 mA at 4°C. After transfer, the membrane was incubated in the blocking buffer at 4°C overnight. After three washing steps with TBST for 8 min each, the membrane was incubated with the primary antibodies anti-tau (TAU-5) in a dilution of 1:1000 in blocking buffer for 1h at RT with mild agitation. This was followed with three washing steps with TBST. The membrane was then incubated with alkaline phosphatase conjugated secondary antibodies (diluted in blocking buffer 1:5000) for 1h at RT and then washed three times with TBST. Antibodies detection was performed using APSubstrate „AP Conjugate Substrate Kit "(Bio-Rad) according to manufacturer's instruction and bands were visualised using „GelDocTM XR+ Imaging System"(BioRad, München)

3.4.8 Determination of protein concentration

The protein concentration of tau was determined using Pierce 660 nm Protein Assay kit. The kit was used according to the manufacturer's instructions. BSA was used as a standard in range of 100 µg/ml to 2 mg/ml. The assay was performed in a 96 well microtiter plate. 10   µL of each BSA standard, unknown sample and the blank sample were pipetted into the wells. 150 µL of the working reagent were added to each well. The plate was incubated under shaking for 5 min at RT. The absorbance was read at 660 nm. A standard curve based on the absorbance values of the BSA standard was generated and the concentration could be determined.

3.5 Phage display for selection of novel binding peptides

The first phage display selection was done against the L-enantiomeric full-length tau monomer and the second selection was performed by employing mirror image phage display against fibrils of D-enantiomeric PHF6*.

3.5.1 Preparation of D-PHF6* fibrils for mirror image phage display selection

PHF6* stock solution was prepared by dissolving the lyophilized acetylated Denantiomeric PHF6* in hexafluoro-2-propanol (HFIP) to a molarity of 1.5 mM. PHF6* fibrillizes spontaneously under incubation at room temperature. The fibrillization was started by incubating 100 µM PHF6* in 50 mM NaPi buffer pH 7.0 with 10 µM ThT at RT for 30 h. NaPi and 10 µM ThT without addition of peptide was used as a negative control. The fibril formation of PHF6* was monitored by ThioflavinT (ThT) assay. For ThT fluorescence measurement, 70 µL of the sample were pipetted into a black 96well half area µclear flat-bottom plate, three replicates per sample. The fluorescence measurement was performed in photometer POLARstar optima (BMG-Labtechnologies, Ortenberg, Germany), excitation/emission wavelengths were set at 450/482 nm. The mean and the standard deviations of results were calculated using Microsoft Excel 2013 (Microsoft Corp.)

3.5.2 The first panning round of the selections

First, 150 µl of either the fibrillized D-enantiomeric PHF6* peptide, prepared as described above, or full length tau monomer in concentration of 100 µg/ml (diluted in 0.1 M NaHCO3; pH 8.5) were immobilized on polystyrene 96-well microtiter plates (Greiner Bio-One International GmbH, Frinckenhausen). The plate was covered with gas permeable sealing film and incubated at 4°C overnight with 300 rpm agitation. The next day, the coating solution was poured off, and the well was blocked with 300 µl blocking buffer for 1 h at 4°C and 300 rpm agitation. The blocking solution was discarded and the well was washed six times with TBST (TBS + 0.1% [v/v] Tween-20). 10 µl of Ph.D.-12[TM] Phage Display Library (equivalent to 1 x 10^{11} phage) were diluted with TBST to 100 µl and pipetted into a coated well. The plate was incubated for 1h at RT and 300 rpm. After discarding the unbound phages, the plate was washed 10 times with TBST. The bound phages were eluted by decreasing the pH with 200 µl of the elution buffer (0.2 M Glycine-HCl (pH 2.2) +1 mg/ml BSA). After 20 min incubation at RT with the elution buffer, the bound phages were pipetted into a microcentrifuge tube and neutralized with 15 µl of 1 M Tris-HCl, pH 9.1.

3.5.3 Determination of the output titer

To determine the phage titer following elution, 10 ml LB medium were inoculated with one colony of *E.coli* ER2738 and incubated at 37°C, 130 rpm. When OD_{600} of 0.5 was reached, 10 µl of the eluated phages were taken to prepare 10 to 10^4- fold serial dilution of phage in LB. 100 µl of *E. coli* ER2738 culture were pipetted into microcentrifuge tubes, one for each phage dilution. The infection was then conducted by adding 5 µl of each phage dilution to each *E.coli* culture tube. The tubes were vortexed quickly, and incubated at RT for 5 minutes. Subsequently, the infected cells were transferred to sterile tubes containing melted Top Agar 45°C, briefly vortexed and immediately poured onto pre-warmed LB/IPTG/Xgal plates. The plates were allowed to cool for 5 minutes, inverted, and incubated overnight at 37°C. The next day, the plaques on the plates were counted and the output titer in plaque forming units (pfu) per ml was calculated.

3.5.4 Amplification of the eluate

For phage amplification, 20 ml of LB-medium containing tetracycline 20 µg/ml were inoculated with one colony of *E.coli* ER2738 and incubated at 37°C and 130 rpm shaking. The culture was grown until OD_{600} reached the early-log phase (0.01–0.05). The rest of the eluated phages were amplified by adding the eluate to the 20 ml *E.coli* ER2738 culture and were incubated with shaking for 4.5 hours at 37°C. The culture was transferred to a centrifuge tube and centrifuged for 10 minutes at 5000 x g at 4°C. The pellet was discarded and the supernatant was transferred to a fresh tube and recentrifuged. The upper 80% of the supernatant was transferred to a fresh tube and 1/6 volume of 20% PEG/2.5 M NaCl was added to it. The phages were precipitated at 4°C overnight. The next morning, phage precipitation was spun at 5000 x g for 50 minutes at 4°C, the supernatant was discarded and the pellet was suspended in 1 ml of TBS. The suspension was transferred to a microcentrifuge tube and spun at 14000 rpm for 5 minutes at 4°C.

The resulting pellet was discarded and the supernatant was pipetted into a fresh microcentrifuge tube and reprecipitated by adding 1/6 volume of 20% PEG/2.5 M NaCl following by incubation on ice for 60 min. The bacteriophages were pelleted by centrifugation at 4°C, 14000 rpm for 10 min. The phage pellet was suspended in 200

µl of TBS, recentrifuged at 4°C, 14000 rpm for 1 min at the supernatant was pipetted in a new tube and stored at 4°C. This was the amplified eluate.

3.5.5 Determination of the input titer

The amplified eluate was titered, as described in Section 3.5.3 and a serial dilution of the amplified eluate 10-10^{11} was prepared. The dilutions from 10^8 to 10^{11} were plated on LB/IPTG/Xgal plates, the plates were incubated at 37°C overnight. After counting the plaques on the plates, the input titer in plaque forming units (pfu) per ml was calculated.

3.5.6 Biopanning rounds from 2 to 4

The following panning rounds 2-4 were performed as described in Sections 3.5.1-3.5.4. For each following panning round the amplified eluate from the previous panning round was taken instead of the phage library. After determining the input titer of each round, the volume of the amplified eluate which should be taken to the next round was calculated to be equivalent to the number of phages used in the first round (1x10^{11} phages). Starting from the second panning round, the Tween concentration in the washing steps was raised to 0.5% (v/v).

3.5.7 Enrichment ELISA

To evaluate the success of the selection and to examine the binding properties of the selected phages in each panning round to the target, enrichment ELISA was performed. 4 wells were coated with the target protein diluted in coating buffer NaHCO3 at a concentration of 100 µg/ml. As a negative control, a coating buffer without the target protein was added to 4 wells.

The plate was covered with gas permeable sealing film and incubated at 4°C, 300 rpm overnight. Next morning, after discarding the coating solution, the wells were completely filled with the blocking buffer and incubated at 4°C, 300 rpm for 2h. In a

separate plate, to exclude the plastic binding phages, 80 µl of the amplified eluate of each panning round were pipetted into two wells of the 96-well plate, mixed with 80 µl of the blocking buffer and incubated on a shaker at RT for 20 minutes. After discarding the blocking buffer from the first plate, the plate was washed 6 times with TBST (Tween 0.1% or 0.5%, the same concentration used in the panning round wash steps). The diluted phage eluates were transferred to the corresponding wells followed by incubation at RT, 300 rpm for 1h. After washing the plates for six times, 200 µl of HRP-conjugated anti-M13 antibody (diluted in blocking buffer 1:5000) were added to the adequate wells and incubated at RT, 300 rpm for 1h. Subsequently, the plate was washed six times and 100 µl of TMB substrate solution were added to each well and incubated for 15 minutes at RT with gentle agitation. 100 µl of 20% H_2SO_4 were then added to stop the enzymatic reaction. When TMB substrate reacts with peroxidase, a soluble blue reaction product is obtained and by adding the stop solution the color changes from blue to yellow. The absorption was measured at 450 nm with the plate reader Multiscan Go (Thermo Fisher Scientific, Darmstadt).

3.5.8 Plaque amplification for ELISA

10 µl of the amplified eluate from the third and fourth panning round were used to prepare a serial dilution $10\text{-}10^9$. Dilutions from $10^6\text{-}10^9$ were plated on LB/IPTG/Xgal plates as described in Section 3.5.3.

In the next day, for each phage clone to be characterized ,15 ml of LB medium were inoculated with a single colony of ER2738 and incubated at 37°C until OD_{600} 0.01–0.05. Randomly selected blue plaques from the LB/IPTG/Xgal plates were picked using a pipette tip, transferred to the *E.coli* culture and incubated for 37°C with shaking for 4.5 hours. The subsequent steps were performed as described in Section 3.5.4 and the suspension of each phage clone was stored at 4°C until performing single phage ELISA.

3.5.9 Single phage ELISA

Single phage ELISA was performed to test the binding properties of a selected phage clone to the target protein. Single phage ELISA was carried out as described in Section

3.5.7; here instead of the amplified phage eluates from each panning round, the purified individual phage clone solutions were applied to the coated plate (Figure 9). The rest of the positive phage clones solutions were mixed with an equal volume of sterile glycerol and stored at -20°C.
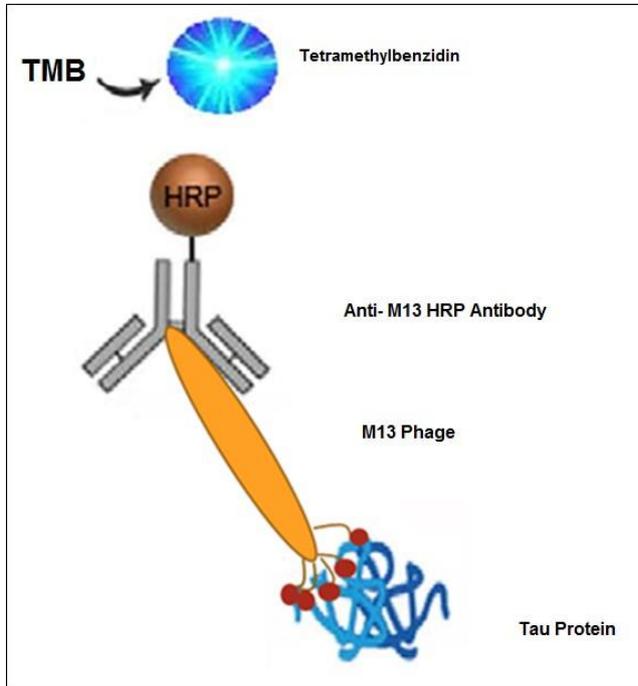
Figure 9: Schematic representation of single phage ELISA, which was performed to confirm whether a selected phage clone binds to the tau protein. The plate was coated with tau protein. After blocking, each individual phage clone solution was added to the respective wells and incubated. After washing away, the unbound phages, the bound phages were detected using antiM13 HRP-conjugated antibodies. The unbound antibodies were washed away and a TMB substrate, which reacts with HRP to give a blue color, was added. The enzymatic reaction was stopped with 20% H_2SO_4 and the absorption was measured at 450 nm.

3.5.10 Extraction of phage DNA

ssDNA of the positive phages that showed a high binding signal to the target in single phage ELISA was isolated using QIAprep spin M13 Kit (QIAGEN, Hilden). For each phage clone, 10 ml LB+Tet were inoculated with one colony of *E. coli* ER2738 and incubated at 37°C, 130 rpm until OD_{600} 0.01-0.05. Subsequently, 3 ml of the culture were infected with 5 µl of phage clone suspension and incubated at 37°C, 130 rpm for 4.5 h. The isolation of the DNA was conducted according to the instructions of the manufacturer „QIAprep® M13 Handbook"(QIAGEN). The DNA was elated in 70 µl water.

The concentration of the ssDNA was measured using Nanodrop Multiscan Go (Thermo Fisher Scientific, Darmstadt).

3.5.11 Sequencing and analysing of phage DNA

The isolated ssDNA samples were sequenced by GATC Biotech AG (Köln), 5 µl of ssDNA in concentration ≥ 20 µg/ml were mixed with 5 µl -96 gIII sequencing primer (Sigma-Aldrich) in concentration of 10 pmol and sent for sequencing.

The obtained DNA sequences were translated into amino acid sequences using (http://insilico.ehu.es/translate/).

During rounds of biopanning phages may bind to contaminants in the target sample, plastic plates, capturing reagents (streptavidin, biotin) or blocking agent such as BSA. In addition, a faster propagation rate of some phage clones can lead to recover such clones, regardless of their binding affinity. The obtained peptides that bind to nontarget molecules in the selection system and do not have specific affinity to the target protein are known as target-unrelated peptides (TUPs) (Menendez and Scott, 2005). Target-unrelated peptides lead to false positive results. Hence, it is required to determine whether the positive clones selected using the phage display library are TUP sequences. Therefore, a useful website named SAROTUP, an abbreviation for "Scanner And Reporter Of Target-Unrelated Peptides" that assists in the reporting and excluding of possible target-unrelated peptides, has been established.

All identified peptides resulting from the selections were compared to already known peptides in the SAROTUP database to exclude possible target-unrelated peptides obtained via phage display (http://immunet.cn/sarotup/). The hydrophobicity, net charge, and molecular weight were determined using the PepCalc (https://pepcalc.com/) and Peptide 2.0 Inc (https://www.peptide2.com/).

3.5.12 Single phage ELISA with the same quantity of each phage

After excluding the plastic binders and other target-unrelated phages, another type of single phage ELISA was performed by adding the same amount of each phage clone to the coated plate.

10 µl from each phage clone suspension were taken and titered as described in Section 3.5.3. The next day, the plaques on the plates were counted and the plaque forming units (pfu) per ml was calculated. The ELISA was performed as previously described

in Section 3.5.9 with the only modification being that the volume of each phage clone suspension that was added to the coated plate, was calculated to contain 3×10^{10} phages.

3.5.13   Synthesis of the peptides

All peptides were produced commercially using reversed phase high performance liquid chromatography with purity of > 95% (JPT Biotech, Berlin, Germany). In the case of FAM-labelled peptides, an additional lysine residue was attached to the respective peptide C-terminally. The D- or L-enantiomeric PHF6* and PHF6 peptides were obtained N-terminally acetylated. Charge distribution has an important effect on the propensity of peptides to form fibrils. By blocking the peptides, which leads to absence of N- and C-terminal charges, they will closely mimic the fibrillization of hexapeptides fragments (PHF6 and PHF6*) within tau. However, unacetylated PHF6* and PHF6 do not fibrillize *in vitro*.

3.6   *In vitro* characterization of peptides' abilities to inhibit the aggregation of tau, PHF6* or PHF6 using thioflavin assays

3.6.1   Fibrillization of full-length tau protein

Recombinant full-length tau protein does not aggregate alone *in vitro* in physiological conditions (Friedhoff et al., 1998). Therefore, heparin was used as an inducing cofactor since heparin-induced tau aggregation represents a good model for pathological aggregation of tau. The kinetic of aggregation was measured using THT fluorescence. Thioflavin-T (ThT) is a benzothiazole dye which binds to formed ß-sheet structures, and the measurement of relative fluorescence intensity leads to quantify the amount of bound dye.

24 µM of tau protein was incubated with 6 µm heparin in HEPES and 10 µM of THT was supplemented to solution. Negative controls were tested by incubation of the recombinant protein without heparin in the presence of THT and by incubation of HEPES buffer with THT. The mixtures were pipetted into a black 96-well half area

μclear flat-bottom plate (Greiner Bio-One International GmbH, Frinckenhausen), the plate was covered with sealing film and incubated at 37°C for 72 h. Fibril formation was quantified by measuring the relative fluorescence intensity at 450/482 nm at a POLARstar optima microtiter plate reader (BMG-Labtechnologies, Ortenberg, Germany), three replicates per run. The mean and the standard deviations of the results were calculated using Microsoft Excel 2013 (Microsoft Corp.).

3.6.2 Full-length tau protein fibrillization inhibition assays

Purified recombinant tau protein at a concentration of 24 μM was incubated with 6 μM heparin and 10 μM ThT in an HEPES buffer. The peptides were added in different molar ratios 1:10, 1:5 or 1:1 (tau:peptide). As a positive control, tau was incubated with heparin and THT. As negative controls, the fluorescence of tau alone with THT was measured as well as the fluorescence of the buffer HEPES in the presence of THT. The samples were pipetted into a black 96-well μclear flat-bottom plate, the plate was covered with sealing film and incubated at 37°C for 72 h. The relative fluorescence intensity was measured at 450/482 nm at a POLARstar optima microtiter plate reader. The relative fluorescence of the samples with peptides were normalized to the positive controls, which were each set to equal 100%. The mean of three absorption values was calculated using Microsoft Excel 2013 (Microsoft Corp.), as well as the standard deviation.

3.6.3 PHF6* and PHF6 fibrillization inhibition assays

The fibrillization conditions of the hexapeptide segments PHF6 and PHF6* were established as previously described in Section 3.5.1, the only difference was using of 50 μM of PHF6 solution. Also, 100 μM PHF6* or 50 μM PHF6 was incubated with the respective peptide at a concentration of 1:10 (PHF6 or PHF6*: peptide) in Napi buffer. THT was added to the sample at a concentration of 10 μM. As a positive control, PHF6 or PHF6* was incubated without peptides in Napi buffer with 10 μM THT. As a negative control, Napi buffer was incubated with THT. The samples were pipetted into a 96-well black μclear flat-bottom plate, the plate was covered with sealing film and incubated at RT for 30 h. The relative fluorescence intensity was measured at 450/482 nm on a

POLARstar optima microtiter plate reader. The mean of three absorption values was calculated using Microsoft Excel 2013 (Microsoft Corp.), as well as the standard deviation.

3.7 Characterization of the binding properties of the selected peptides to tau monomers, tau fibrils, PHF6* fibrils and PHF6 fibrils by ELISA

The plate was coated with tau monomers as well as tau fibrils at a concentration of 10 µg/ml in NaHCO3 pH 8.3, or with PHF6* fibrils as well as PHF6 fibrils at a concentration of 50 µg/ml in NaHCO3. As a negative control, NaHCO3 buffer was incubated in the wells in place of the target protein solution. The plate was covered with sealing film and incubated at RT with 300 rpm agitation for 1 h. After 3 times of washing with PBST 1% Tween-20, the wells were blocked with 1% BSA in PBS for 1h at RT and 300 rpm followed by 3 times washing with PBST. The FAM-labeled peptides were added in increasing concentrations 1µg/ml, 5 µg/ml, 10 µg/ml and 20 µg/ml, in the case of tau monomers and tau fibrils; and 10 µg/ml, 20 µg/ml and 50 µg/ml in the case of PHF6 fibrils and PHF6* fibrils, then incubated for 1h at RT with 300 rpm agitation. The plate was washed 3 times with PBST and a horseradish peroxidase-conjugated sheep anti-FITC secondary antibody was used to detect bound peptides. Subsequently, the TMB substrate solution was transferred to the relevant wells. Finally, the reaction was stopped with 20% H2SO4 and the plate was read at 450 nm. The mean of three absorption values was calculated using Microsoft Excel 2013 (Microsoft Corp.), as well as the standard deviation.

4 Results

4.1 Expression and purification of recombinant tau protein

Purified full-length tau protein was continuously required throughout this project, firstly to perform the phage display selection against the tau monomer and subsequently to characterize the selected peptides in aggregation assays and to test the binding properties of the peptides in ELISA experiments.

The sequence of the full–length tau gene 2N4R was synthetically cloned into the pET28a(+) vector system by Genentech. After the transformation of pET28a(+)-441aa plasmid into *E.coli* BL21 (DE3), protein expression was performed according to Margittai et al. (Margittai et al., 2004). Tau protein production was induced with 1 mM IPTG and incubated for 3 hours. On SDS-PAGE, the intensity of the tau band in the sample post-induction was higher than in the sample pre-induction, indicating that tau expression responds to IPTG induction (Figure 10 A). The longest isoform of the human protein tau has a molecular weight of 45.8 kDa but migrates at 60 kDa on SDSPAGE.

Tau purification was conducted according to Margittai et al. (2004) with some minor modifications; after boiling the cell lysate and precipitating the proteins with ammonium sulfate, the suspended cell lysate was purified using a cation exchange column. Tau is highly positively charged at neutral pH, with a theoretical PI of 8.24. Therefore, a cation exchange chromatography column can separate the tau protein from other contaminating proteins. The tau protein bound to the negatively charged matrix and was eluted with an increasing salt gradient (Figure 10 B). Subsequently, eluted fractions containing tau protein were pooled and passed through an anion exchange chromatography column. Here, the target molecule tau passed unbound through the positive charged column, while the impurities bound to the column. As shown in figure 10 C, only a purified tau band was observed on the polyacrylamide gel without any additional bands. Most of the tau protein obtained from this method was used for the phage display selection against tau monomer.

The tau protein was also purified according to the protocol reported by KrishnaKumar et al., 2017, they established a simplified protocol for efficiently extracting tau protein

in a one-step purification process through direct boiling. Here, the cell pellet was suspended in lysis buffer after 3 hours of induction and directly boiled in a water bath for about 10 min. The boiled lysate was purified using one chromatography method, cation exchange chromatography. The bound tau was eluted with an increasing salt gradient (0.1M-0.7M) and analyzed by SDS-PAGE. The eluted fraction containing 0.3 M NaCl was taken for further use. In this fraction, a thick tau band and some light bands below the tau band were observed on the gel (Figure 11). The tau protein obtained from this method was used for the thioflavin T aggregation assays.

The total obtained amount of tau protein from both protocols was about 3 mg from one litre culture.
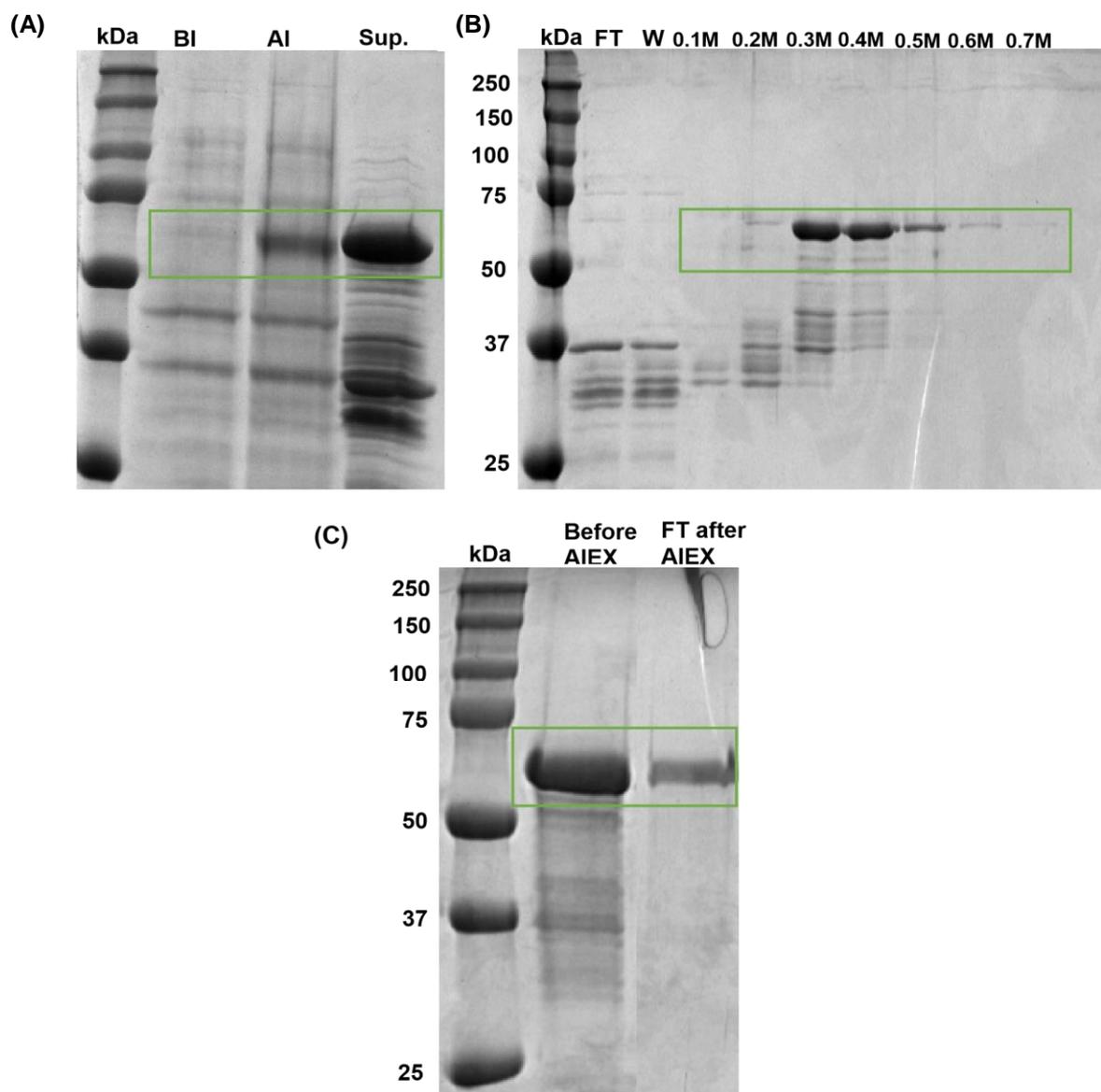
Figure 10: Example of the expression and purification procedure of full-length tau according to Margittai et al., 2004. (A) The human protein tau was expressed in *E. coli* BL21

(DE3) cells. The cells were grown until OD600 ≥ 0.6 was reached, a sample was saved (**BI**= before induction), after inducing the cells with a final concentration of 1 mM IPTG for 3 hours (**AI**= after induction), the cells were pelleted by centrifugation. The supernatant was discarded and the cells pellet was suspended in lysis buffer and boiled. The lysate was centrifuged again and the supernatant containing tau proteins was saved (**Sup.** = supernatant). **(B)** After precipitating the proteins with ammonium sulfate, the suspended cell lysate was loaded into a cation exchange column. After collecting the flow through (**FT**=flow through), the column was washed with HEPES buffer (**W**= solution collected after washing step) and tau protein was eluted with an increasing salt gradient (0.1M -0.7M NaCl) (**0.1M-0.7M**=eluted fractions with NaCl concentration from 0.1-0.7M). **(C)** Fractions containing tau protein were collected (**Before AIEX**= eluted fractions containing tau before loading into anion exchange column) and the flow through which contains purified tau was collected (**FT after AIEX**= flow through after loading into anion exchange column). Samples were taken after each step and prepared for SDS-gel, 10 µl were loaded into SDS-gel as well as 5 µl from the molecular weight marker, **kDa** (Precision Plus ProteinTM Standard Dual, Bio-Rad).
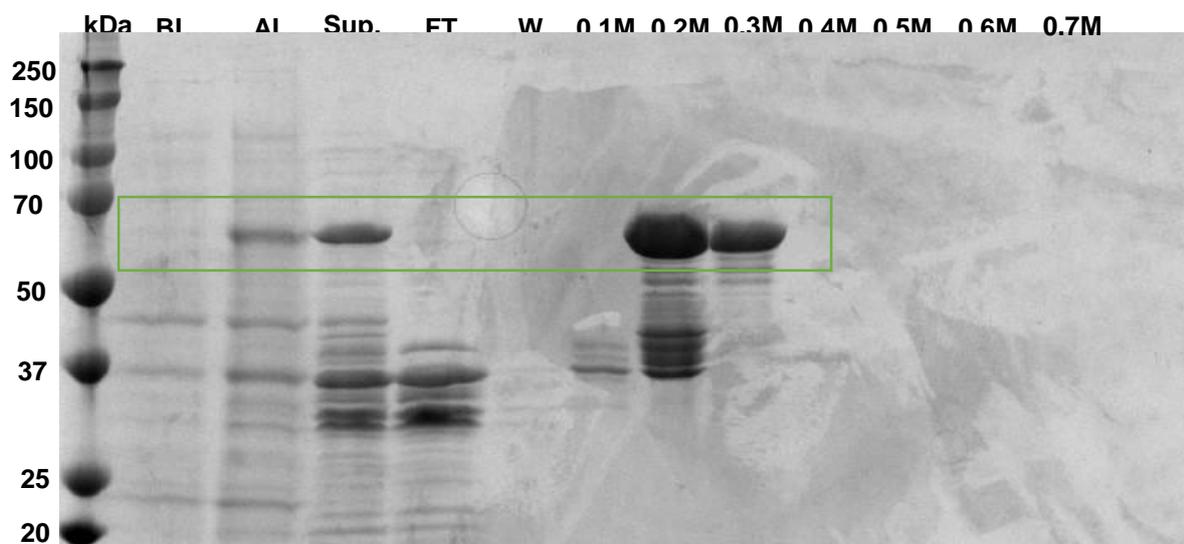
Figure 11: Example of the expression and purification procedure of full-length tau according **to KrishnaKumar et al., 2017**. The human protein tau was expressed in *E. coli* BL21 (DE3) cells. The cells were grown until OD600 ≥ 0.6 was reached, a sample was saved (**BI**= before induction), after inducing the cells with a final concentration of 1 mM IPTG for 3 hours (**AI**= after induction), the cells were pelleted by centrifugation. The supernatant was discarded and the cells pellet was suspended in lysis buffer and boiled. The lysate was centrifuged again and the supernatant containing tau proteins was saved (**Sup.** = supernatant). The supernatant was loaded into a cation exchange column. After collecting the flow through (**FT**=flow through), the column was washed with an HEPES buffer (**W**= solution collected after washing step) and tau protein was eluted with an increasing salt gradient (0.1M -0.7M NaCl) (**0.1M-0.7M**=eluted fractions with NaCl concentration from 0.1-0.7M). Samples were taken after each step and

prepared for SDS-gel, 10 µl were loaded into SDS-gel as well as 5 µl from the molecular weight marker, **kDa** (Precision Plus ProteinTM Standard Dual, Bio-Rad).

Western blot analysis of the purified tau protein

Western blot was performed to determine the nature of additional bands under the band of tau protein after performing the purification according to KrishnaKumar et al., 2017. Samples were taken from the eluted fractions containing 0.2 and 0.3 M NaCl. After separating the proteins using SDS-PAGE, the protein bands were transferred into a membrane and the bands were visualized after immunodetection. We expected the bands below the main band of tau protein to be degradation products, which potentially present additional bands. Using a tau specific antibody, we were able to confirm that these bands were degradation products, which would migrate ahead of the band of interest a cause to their lower molecular weight.

The signal demonstrated that the protein running at a size of around 60 kDa is the recombinant protein tau, which has a theoretical molecular weight of 45.8 kDa. However, the Western Blot showed that all fragments react with the tau specific antibody anti-TAU 5, indicating that all fragments belong to the recombinant protein tau. In a 0.3 M fraction, a light band above tau protein by 250 kDa could be seen. This band was interpreted as tau dimers or trimers (see Figure 12).
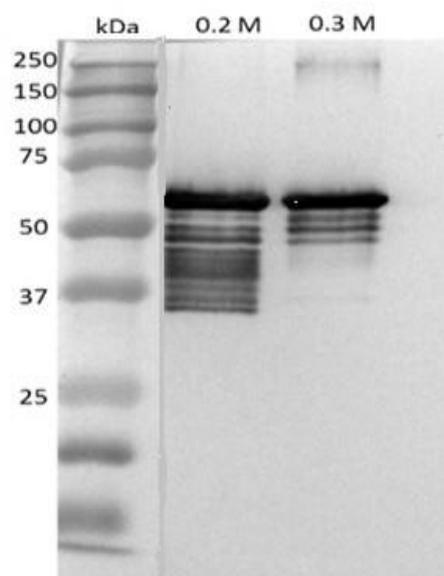
Figure 12: Western blot analysis of purified recombinant tau protein. After cation exchange chromatography, samples from the eluted fractions consisting of 0.2 M NaCl and 0.3 M NaCl were taken and prepared for SDS-PAGE. After separating proteins by electrophoresis, the separated proteins were transferred from the gel onto a nitrocellulose membrane. Subsequently, the membrane was blocked. After blocking, primary antibodies anti Tau 5 were added to the

49

membrane and incubated. After washing, the secondary antibodies (goat-anti-mouse AP conjugate) were added onto the membrane. Antibodies were detected using AP substrate „AP Conjugate Substrate Kit "and bands were visualised using „GelDocTM XR+ Imaging System".**kDa**: molecular weight marker, **0.2 M**: eluted fraction containing 0.2 M NaCl, **0.3 M**: eluted fraction containing 0.3 M NaCl

4.2 Phage display selection against full-length tau monomer

The principal aim of this Ph.D. project was to select D-enantiomeric peptides that bind to the tau protein and inhibit its pathological aggregation. Usually, to generate D-enantiomeric binding peptides to a specific target, mirror image phage display selection against the D-enantiomeric form of the target is performed. Since it was difficult to obtain D-enantiomeric full-length tau protein (length 441amino acids) for mirror image phage display from manufacturers of peptides, the L-enantiomeric full-length tau monomer was used as a target for the selection. The obtained L-enantiomeric peptides were then synthesized as D-enantiomeric peptides.

To obtain tau specific binding partners, 1x 10^{11} phages from Ph.D.-12 Phage Display Peptide Library were added to a tau coated plate, the unbound phages were washed away and the bound phages were eluted by decreasing the pH. The eluted phages were amplified in *E.coli* ER2738 and taken for another panning round. Four panning rounds were performed, after each panning round the input titer and the output titer were calculated. The number of plaque forming units (pfu) was counted and phages were prepared to the next panning round by diluting to a concentration of 1x 10^{11} phages.

4.2.1 Enrichment ELISA after four panning rounds

An enrichment ELISA was carried out to evaluate in which panning round the entire phage pool had the highest affinity to the tau. The wells were coated with tau protein and the amplified phage pools from all panning rounds were added to coated wells. The bound phages were detected with anti-M13 HRP conjugated antibodies. The obtained signal intensity was proportional to the amount of bound HPR conjugated antibody and thus proportional to the amount of binding phages in the respective eluate. As negative controls, wells were filled with coating buffer and coating buffer containing 1% BSA.

The absorbance signal of wells containing tau, representing the binding, was significantly higher than that of negative control wells. This indicated the success of the selection (Figure 13).

As expected, the increase in the ELISA signal following the second round of biopanning is likely due to the presence of a greater abundance of target-binding phages in the third and fourth round pool. The enrichment ELISA can be estimated after rounds of selection by calculating the ratio of specific binding signal versus non-specific binding signal. Each ratio value is obtained using the absorbance of the target wells to the negative control wells. The binding ratio in this selection was more than 2 for all panning rounds (Table 8). A ratio threshold of 2 or greater indicates the likely presence of specific binding phages (Miersch et al., 2015).

To isolate single phage clones, the eluate of the later rounds of selection (i.e. rounds 3 and 4, which showed higher binding signal to the target), was infected into *E.coli* ER2738 and plated on IPTG/Xgal LB plates. The binding properties of the individual phage clones to the target were tested using single phage ELISA.
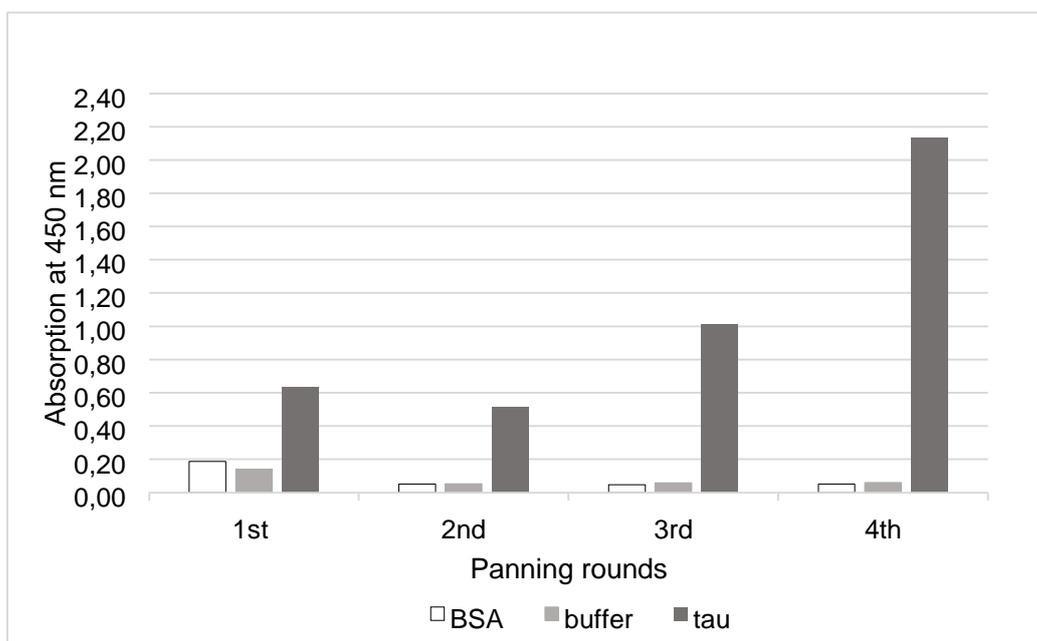
Figure 13: Enrichment ELISA showed the enrichment of tau specific phages during the affinity selection process. Wells were coated with 100 µg/ml tau protein, wells containing only buffer or buffer with 1% BSA were used as negative controls. After blocking, amplified phages from round one to four were added to the respective wells and incubated for 1h. The unbound phages were washed away and the bound phages were detected using anti-M13

HRP monoclonal antibody. After washing the unbound antibodies, the enzymatic transformation of the TMB substrate was measured at 450 nm.

Table 8: Binding ratio of tau monomer to the negative control (buffer) by enrichment ELISA.

Round of panning	1	2	3	4
Enrichment ELISA (A450 nm ratio) tau monomer: buffer	4.8	10	20.2	35.5

4.2.2 Single phage ELISA

Individual phage clones from the third and fourth panning rounds were picked from LB/IPTG/Xgal plates, amplified in *E.coli* ER2738 and, after several steps of precipitation and centrifugation, individual phage stocks were produced. The resulting phage stocks were added to tau coated wells to determine whether a selected phage clone binds to the target, without using a target-specific antibody. The detection was performed using anti-M13 HRP conjugated antibodies.

Single phage ELISA data was analyzed by comparing the absorbance of the wells coated with tau protein to the absorbance of the negative control wells. As shown in Figure 14, some phage clones showed a significantly higher absorption value in comparison to the negative controls, indicating binding to tau protein. These clones included clone numbers, e. g. 2, 3, 5 and 7. Other clones exhibited slightly stronger binding to their antigen compared to negative controls, e.g. clones 22, 26 and 27. Phages such 9, 21 and 31 exhibited a relatively high binding to the negative control wells, potentially indicating a plastic binder phage.

The DNA of the positive clones, with the potentially highest binding to tau protein, was sequenced to determine the identity of the peptide expressed on the phage surface.

The binding properties of 96 clones from the third and fourth panning round were characterized. Figure 14 represents an example of the binding properties of 32 phage clones.
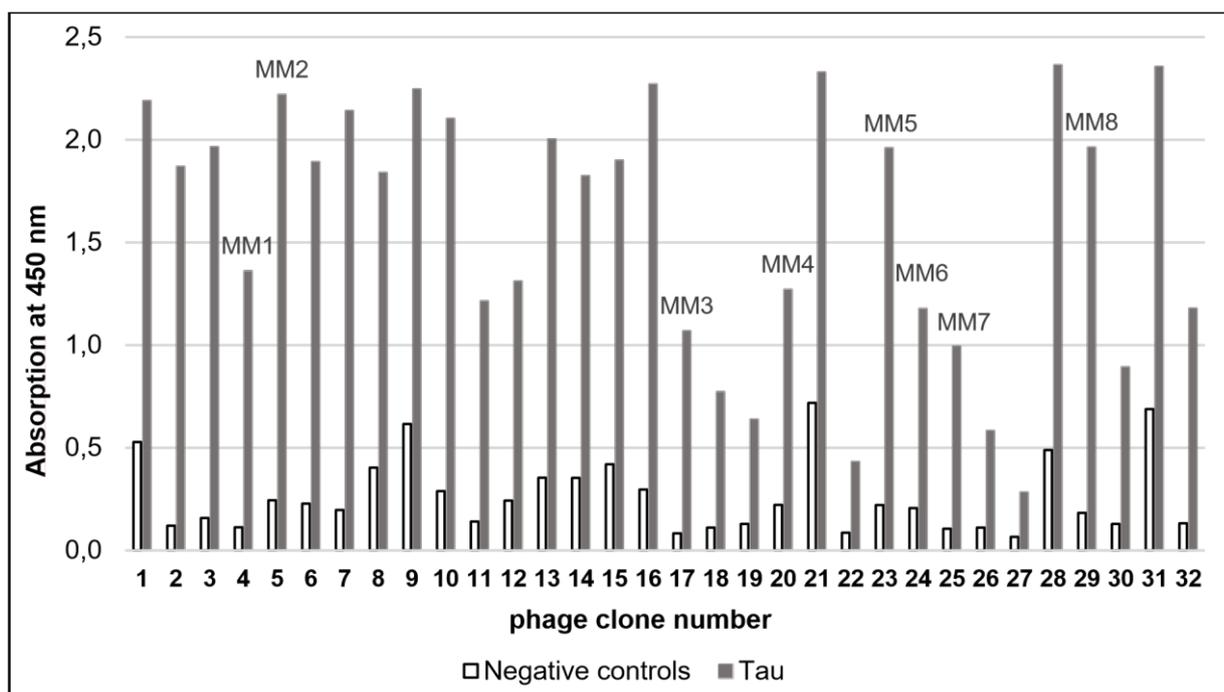
Figure 14: Identification of binding properties of individual randomly-selected phage clones to tau protein with single clone ELISA. Tau protein in concentration of 100 µg/ml was immobilized on the plate. As negative controls, wells were filled with the coating buffer. After blocking, individual phage stocks were added to the respective wells and incubated for 1h. After 6 times of washing, phages were detected with anti-M13 HRP monoclonal antibody. After washing the unbound antibodies, the enzymatic transformation of the TMB substrate was measured at 450 nm. The figure represents an example of 32 phage clones, approximately 96 phage clones were tested. Later, the synthesized peptides from the phage clones 4, 5, 17, 20, 23, 24, 25 and 29 were named as MM1, MM2, MM3, MM4, MM5, MM6, MM7 and MM8 respectively.

4.2.3 DNA extraction for identification of peptides sequences

The peptide sequences expressed by the promising phages were identified by DNA sequencing of the corresponding genome. Some phage clones did not contain an insert, which was designed to add a peptide spacer between the peptide sequence and the DNA of the phage.

All peptide sequenced after the selection are listed in Table 9. Different characteristics of the identified peptides, such as the charge, hydrophobicity and molecular weight, were analyzed using web tools like PepCalc (https://pepcalc.com/) and Peptide 2.0 Inc (https://www.peptide2.com/) listed in Table 9.

Interestingly, we did not find any dominating amino acid sequences in 28 sequences. Some sequences were selected twice, three-fold or four-fold. The peptide sequences

were compared to those sequences listed in the SAROTUP database ("Scanner And Reporter Of Target-Unrelated Peptides", a website which can detect target-unrelated peptides resulting from biopanning: http://immunet.cn/sarotup/), and the PepBank database (database of peptides from public data sources: http://pepbank.mgh.harvard.edu/). However, no hits were found.

From the identified 28 sequences, a phage clone (No. 9, KVWPSPSMMFST) was predicted in SAROTUP as a plastic binder. Phage clones that according to SAROTUP had a relatively high probability of being rapidly growing phages were also excluded (i.e. YSLRLTSVTAPT, TLGTFTHNKPPH, and NHTEASSPLNRA).

Some phage clones were recognized to be rapidly growing phages with low probability. The faster growing rate of some phage clones renders such clones predominant and more likely to be isolated despite they are unlikely to specifically bind to the target. To exclude faster propagation of certain phage clones, the remaining peptide sequences were additional screened for their binding to tau monomer by ELISA using the same concentration of phages from each individual phage stock.

Table 9: selected peptides from the phage display selection against the tau monomer. The peptides' sequences were determined after DNA sequencing of the promising phage clones. The frequency of each sequence was listed in the table. Peptides' characteristics like charge, hydrophobicity and molecular weight in Dalton were also analyzed using the websites Peptide 2.0 Inc and PepCalc and listed below. Each sequence was allocated a number in the list.

No.	sequence	frequency	charge	hydrophobicity	MW (Da)	name
1	HLSSPYWIGSMR	4/28	+1	41%	1433. 64	MM7
2	HNTGGKMDLPKW	1/28	+1.1	33%	1383.58	_
3	TSAVWSKTVSLS	1/28	+1	41%	1265.41	_
4	DPLKARHTSVWY	1/28	+1	41%	1472.65	MM3
5	YSLRLTSVTAPT	3/28	+1	41%	1308.48	_
6	NHTEASSPLNRA	1/28	+0.1	33%	1296.35	_
7	SSMALDQYTQGS	1/28	-1	25%	1287.36	_
8	DTLVKQNKLMAA	1/28	+1	50%	1331.58	MM6
9	KVWPSPSMMFST	1/28	+1	58%	1397.66	_
10	HLTATELANSYH	1/28	-0.8	33%	1356.44	MM8
11	LTPHKHHKHLHA	1/28	+2.5	33 %	1455.67	MM2

12	HMSYGNGTRDTP	2/28	+0.1	16%	1335.41	MM4
13	SYPHSTSKDLKP	1/28	+1.1	25%	1359.48	_
14	TLGTFTHNKPPH	1/28	+1.2	33%	1349.49	_
15	SPHLHTSSPWER	1/28	+0.2	33%	1433.53	_
16	GSPLSNPTRMWL	1/28	+1	50%	1358.57	MM5
17	TSHHLHNTTTRG	1/28	+1.3	8%	1361.42	_
18	NLPYPPTLLYAS	1/28	0	58%	1348.54	_
19	DIYAHPKSASHR	1/28	+1.2	33%	1381.5	_
20	YLNTAWGNIMPV	1/28	0	58%	1378.6	_
21	NHTEASSPLNRA	1/28	+0.1	33%	1296.35	_
21	HSLRSSHHPTPG	1/28	+1.6	25%	1312.40	_
22	GSWNTFRAQPTI	1/28	+1	41%	1377.5	MM1

4.2.4 Single phage ELISA using the same concentration of each phage clone

After using SAROTUP to exclude known target-unrelated peptides, 18 peptides remained. Before determining which peptides should be synthesized and further characterized, false positive results had to be distinguished from true positive clones. The binding properties of the remaining phage clones to tau monomer were tested again by ELISA using the same concentration of each phage clone. After amplifying each phage clone stock in *E.coli* and titering the obtained phage solution, the plaques on LB/IPTG/Xgal plates were counted and the pfu/ml was calculated. The same phage concentration: 3×10^{10} pfu/ml from each phage solution was added to the tau-coated plate and the bound phages were detected using anti-M13 HRP monoclonal antibody. After measuring the plate, the absorption values of the tau-coated wells in the cases of phage clones number 1, 4, 8, 10, 11, 12, 16 and 22 were relatively high in comparison to the negative controls wells (buffer and buffer containing 1% BSA). This indicated a binding of these phage clones to the tau protein. Phage clone No.22 resulted in the highest absorption signal (Figure 15)

Eight peptides (No.1 HLSSPYWIGSMR, No.4 DPLKARHTSVWY, No.8 DTLVKQNKLMAA, No.10 HLTATELANSYH, No.11 LTPHKHHKHLHA, No.12 HMSYGNGTRDTP, No.16 GSPLSNPTRMWL and No. 22 GSWNTFRAQPTI) were

selected to be synthesized as L-enantiomer peptides to further characterize them and test their potential to inhibit tau aggregation.
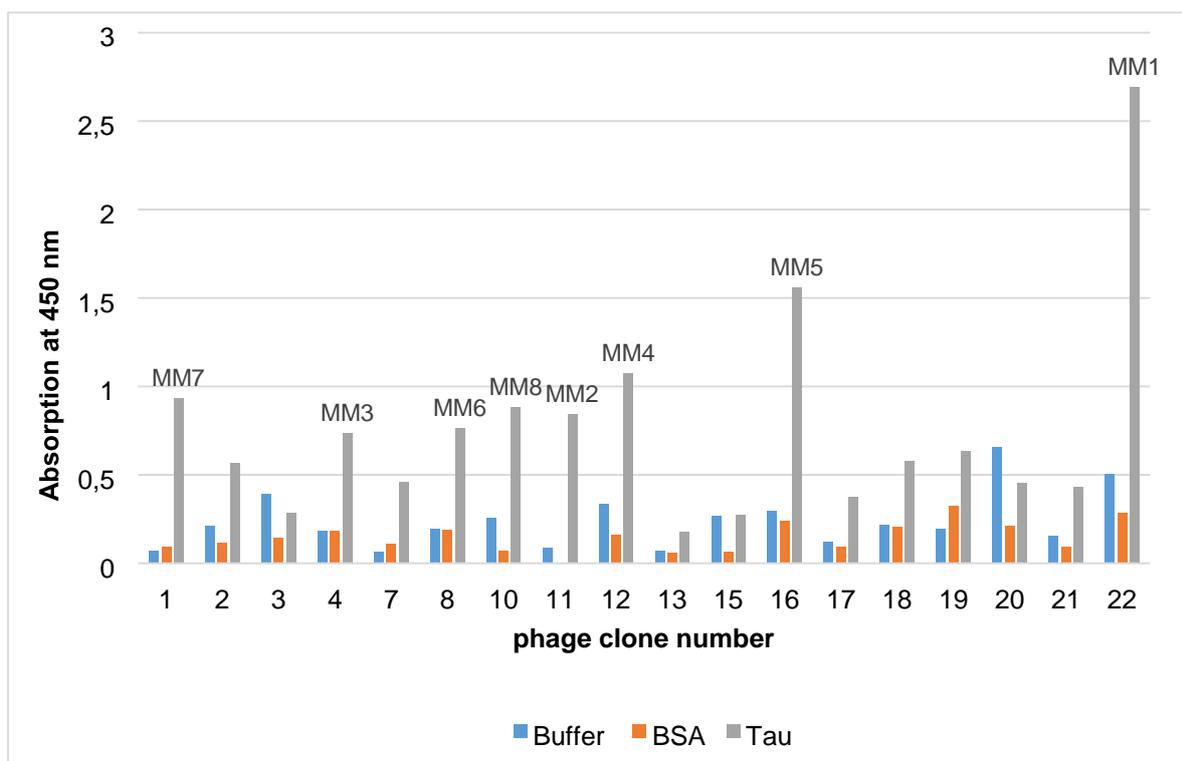
Figure 15: **After sequencing, identification of the binding properties of predicted positive phage clones to the tau protein by single clone ELISA using the same concentration of each phage clone.** 100 µg/ml of tau protein was immobilized on the plate. For negative controls, coating buffer and coating buffer containing 1% BSA were used. After blocking, individual phage stock in concentration of 3×10^{10} were added to the respective wells and incubated for 1h. After 6 times of washing, phages were detected with anti-M13 HRP monoclonal antibody. After washing the unbound antibodies, the enzymatic transformation of the TMB substrate was measured at 450 nm. The synthesized peptides from the phage clones 22, 11, 4, 12, 16, 8, 1 and 10 were named as MM1, MM2, MM3, MM4, MM5, MM6, MM7 and MM8 respectively.

4.3   *In vitro* characterization of peptides abilities to inhibit the aggregation of full-length tau using thioflavin assays

4.3.1   Aggregation of tau protein

Before beginning to test the ability of the selected peptides to inhibit the aggregation of full-length tau, it was necessary to establish the fibrillization conditions of the tau protein.

To induce the aggregation of tau, the polyaninon heparin was added to tau. Thioflavin T, a fluorescence dye which binds to protein fibrils, was added to the solution. The fluorescence changes were monitored after transferring the solutions to a black plate and the relative fluorescence was measured every hour for 72h. As negative controls, tau was incubated in HEPES buffer with ThT, without the addition of heparin, as well as HEPES buffer was incubated with THT. By starting with the measurement 0 h, it was possible to detect a very low fluorescence signal as there were no fibrils in solution and most dyes did not bind to the intermediates formed. A considerable increase in the fluorescence signal of THT was observed in the first 12 hours and it continued to increase until 36 h. This increase in fluorescence occurred as the dye (THT) was able to bind to the tau fibrils formed in this phase. After 36 hours of incubation, a plateau of the signal was reached, due to the saturation of the fibrils present. Both negative controls were constant at a low relative fluorescence intensity (see Figure 16).
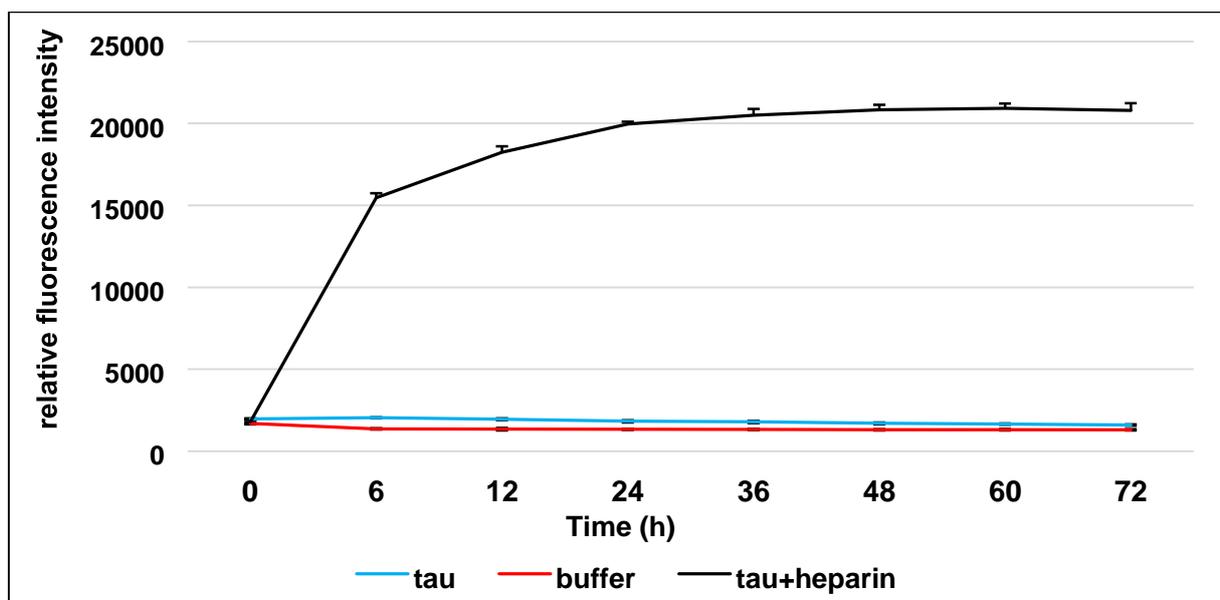
Figure 16: An increase in THT fluorescence intensity indicates tau protein aggregation in the presence of heparin, whereas tau protein does not aggregate in the absence of heparin. 24 µM recombinant full-length tau protein, 6 µM heparin and 10 µM ThT were incubated in HEPES buffer (black line). As a negative control, 24 µM tau was incubated in HEPES with 10 µM ThT, without addition of heparin (blue line) as well as HEPES buffer was incubated with 10 µM ThT (red line). All solutions were pipetted into a black 96-well µclear flatbottom plate and incubated at 37°C for 72 h in photometer POLARstar optima. The relative fluorescence intensity was read out at excitation and emission maxima of 450 and 482 nm, respectively, at a POLARstar Optima microtiter plate reader (mean +/- standard deviations of results, three replicates per run).

4.3.2 The potential of the selected L-enantiomer peptides to inhibit the aggregation of full-length tau

To test the ability of the L-synthesized peptides to inhibit the aggregation of tau *in vitro*, thioflavin assays were performed. The peptides were added to the aggregation mixture at a molar ratio of 1:5 and/or 1:10 (tau:peptide), respectively. As a positive control, tau was incubated with heparin without the addition of peptides, negative controls were tau alone with THT and buffer including THT. The relative fluorescence of the positive control was set to be 100% after 72 h of incubation and the relative fluorescence of the samples was normalized to the positive control. As shown in Figure 17, MM2 and MM3 significantly reduced tau aggregation, especially in a ratio of 1:10. MM2 reduced the fibril formation of tau to approximately one half in a molar ratio of 1:5 and in molar ratio of 1:10 MM2 accomplished almost complete inhibition of tau fibril formation. In the case of MM3, both molar ratios 1:5 and 1:10 were almost equally efficient in significantly inhibition of tau fibril formation. MM4 and MM5 exhibited no significant effect on tau fibril formation, while peptides MM1, MM6, MM7 and MM8 appeared to even increase fibrillization of tau.

A
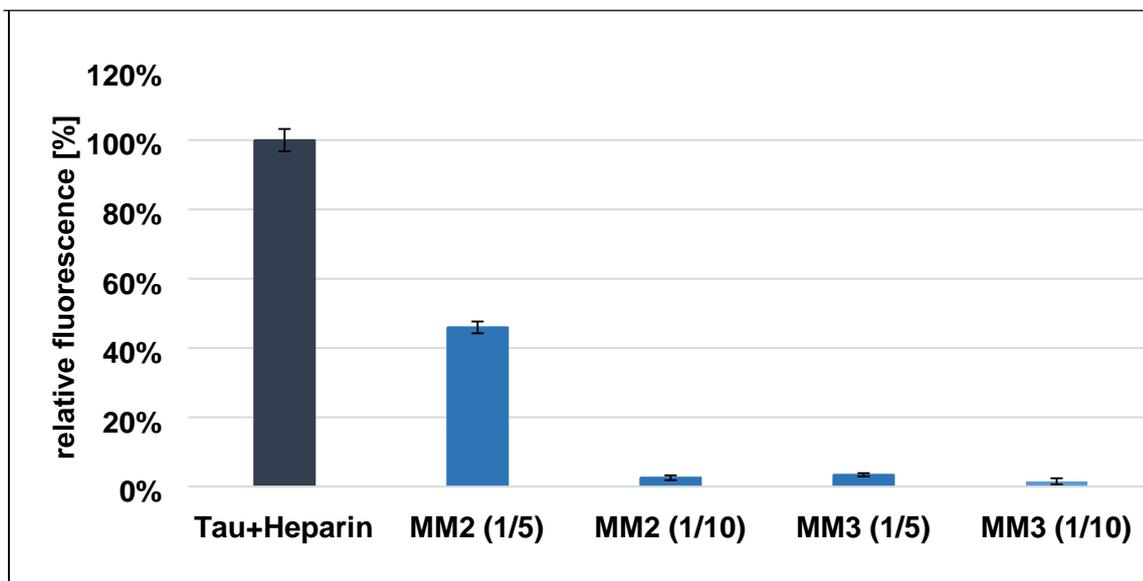
B
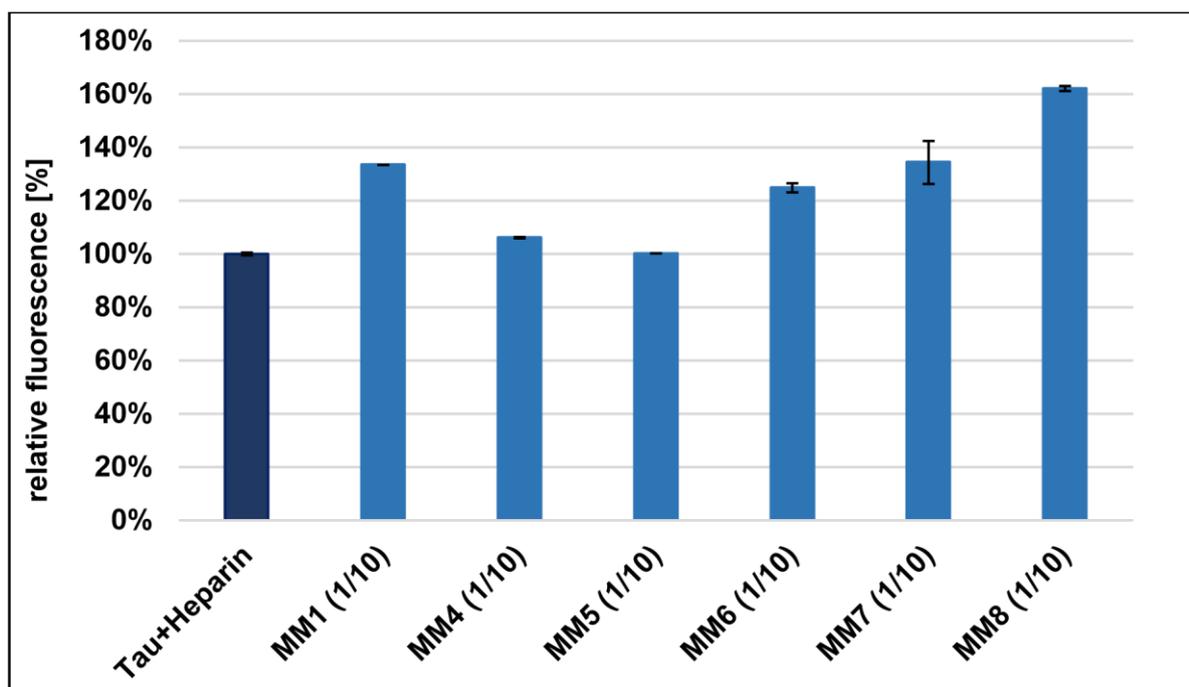
Figure 17: ThT assays indicate the ability of MM2 and MM3 to inhibit or reduce fibril formation of tau whereas MM1, MM4, MM5, MM6, MM7 and MM8 do not act as tau aggregation inhibitors. (A) Peptides MM2 and MM3 in molar ration 1:5 and 1:10 (tau:peptide) (B) peptides MM1, MM4, MM5, MM6, MM7 and MM8 in molar ratio 1:10 (tau:peptide). 24 µM tau and 6 µM heparin were incubated with and without the peptides in a molar ratio of 1:5 and/or 1:10 (tau:peptide), respectively. Upon addition of 10 µM ThT, 70 µL sample volume were pipetted into each well of a black 96-well µclear flat-bottom plate and incubated at 37°C for 72 h in photometer POLARstar Optima. The relative fluorescence intensity was read out at excitation and emission maxima of 450 and 482 nm, respectively (mean +/- standard deviations of results, three replicates per run). The relative fluorescence for the positive control (tau and heparin without peptides) after reaching the saturation level (36 hours of incubation) was set at 100%.

D-enantiomeric peptides are extremely protease stable and their suitability for *in vivo* applications has been demonstrated; consequently, the promising peptides MM2 and MM3 were ordered as D-enantiomer peptides and D-retro-inverso peptides to further investigate their ability to inhibit tau fibril formation. In addition, the promising peptides were obtained as FAM-labeled versions to assess their binding to tau monomers and tau fibrils. The newly synthesized peptides are listed in Table 10.

Table 10: MM2 and MM3 were selected for further characterization. The respective Dpeptide as well as the retro-inverso version were synthesized by JPT Peptide Technologies GmbH. The names and the sequences of newly synthesized peptides are listed below.

peptide name	sequence
MMD2	d-ltphkhhkhlha

MMD2rev	d-ahlhkhhkhptl
MMD3	d-dplkarhtsvwy
MMD3rev	d-ywvsthraklpd
MMD2-Lys(FAM)-NH2	d-ltphkhhkhlha-lys(FAM)-NH2
MMD3-Lys(FAM)-NH2	d-dplkarhtsvwy-lys(FAM)-NH2

4.3.3 The potential of the selected D-enantiomer peptides to inhibit the aggregation of full-length tau

To investigate the potential of the selected D-peptides MMD2, MMD2rev, MMD3 and MMD3rev to inhibit fibrillization of full-length tau, thioflavin fluorescence assays were performed. Tau aggregation was initiated by the addition of heparin to the tau protein at a concentration of 24 µM, the mixtures were incubated in the presence or absence of the respective peptide in a molar ratio of 1:10. After 36 hours of incubation, the positive control sample (tau with heparin) reached a saturation level, and the fluorescence intensity value was set to 100%. As can be seen in Figure 18, neither MMD2 nor MMD2rev inhibited the aggregation of tau significantly at molar ratio of 1:10 (tau:peptide). MMD2 reduced the aggregation of tau to about 90% and MMD2rev reduced the aggregation to approximately 70%. However, both peptides MMD3 and MMD3rev significantly inhibited formation of tau aggregates at a molar ratio of 1:10. MMD3 and MMD3rev proved to be equally efficient in significantly inhibiting the formation of tau fibrils.

Furthermore, the binding properties of MMD2 and MMD3 to tau monomers as well as to tau fibrils were investigated using ELISA. To enable the use of this method, FAM labeled versions of the peptides were ordered as displayed in Table 10. The retro inverso form of the D-peptides exhibits usually a very similar pattern of binding comparing with their D-peptides, therefore the binding properties of MMD2rev and MMD3rev were not tested.
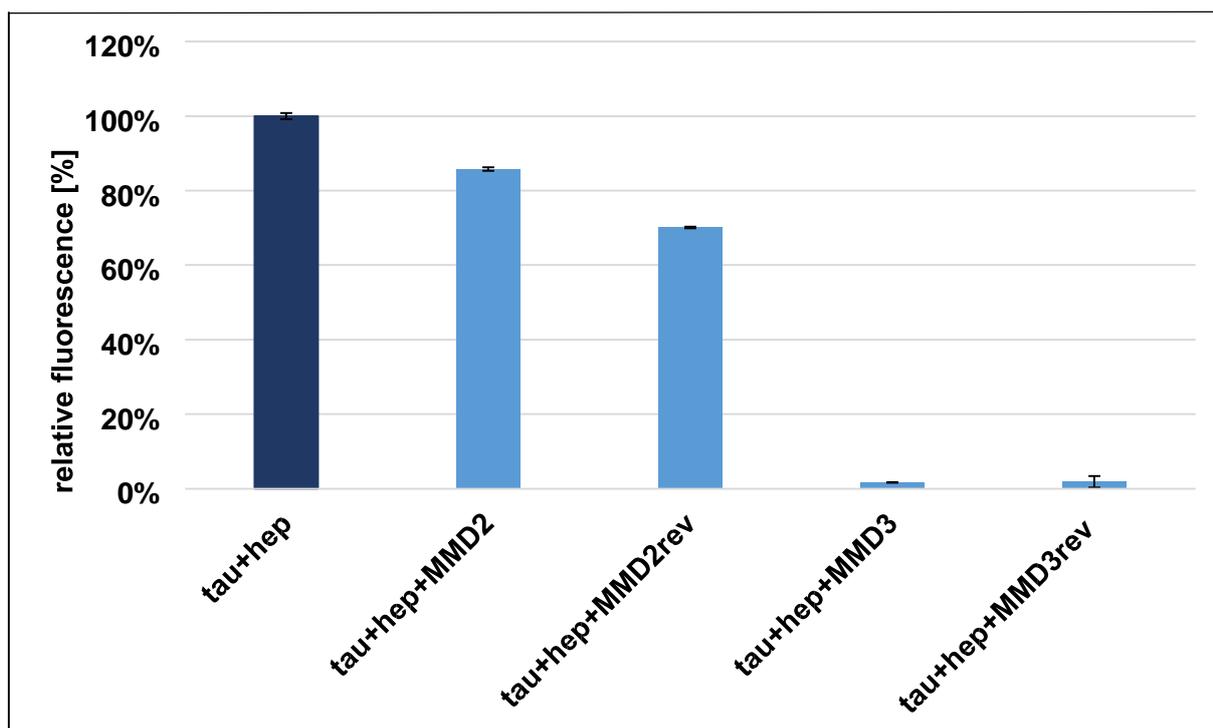
Figure 18: The ability of the selected peptides MMD2, MMD2rev, MMD3 and MMD3rev to reduce or inhibit formation of tau fibrils. 24 µM tau and 6 µM heparin were incubated with and without the peptides in a molar ratio of 1:10 (tau:peptide), respectively. Upon addition of 10 µM ThT, 70 µL sample volume were pipetted into each well of a black 96-well µclear flatbottom plate and incubated at 37°C for 72h in photometer POLARstar Optima. The relative fluorescence intensity was read out at excitation and emission maxima of 450 and 482 nm, respectively (mean +/- standard deviations of results, three replicates per run). The relative fluorescence for the positive control (tau and heparin without peptides) after reaching saturation level (36 hours of incubation) was set at 100%.

4.4 Demonstrating the binding properties of the selected peptides to tau monomers as well as to tau fibrils using ELISA

The binding properties of MMD2 and MMD3 to tau monomers and tau fibrils were tested using ELISA. After coating a 96-well plate with 10 µg/ml tau monomers as well as tau fibrils, the FAM-labeled peptides MMD2-FAM and MMD3-FAM were added in increasing concentrations. The detection was performed with anti-FAM HRP antibodies and absorbance was measured at 450 nm. As a negative control, coating buffer only was incubated in the wells.

The binding of MMD2 and MMD3 to tau monomers and tau fibrils could be demonstrated. Both peptides did not show any significant difference in their binding to the different conformers, though it appeared to be a minimal preference for tau

61

monomers. The binding of MMD2 to tau monomers and tau fibrils appeared to be generally stronger than MMD3 (Figure 19).
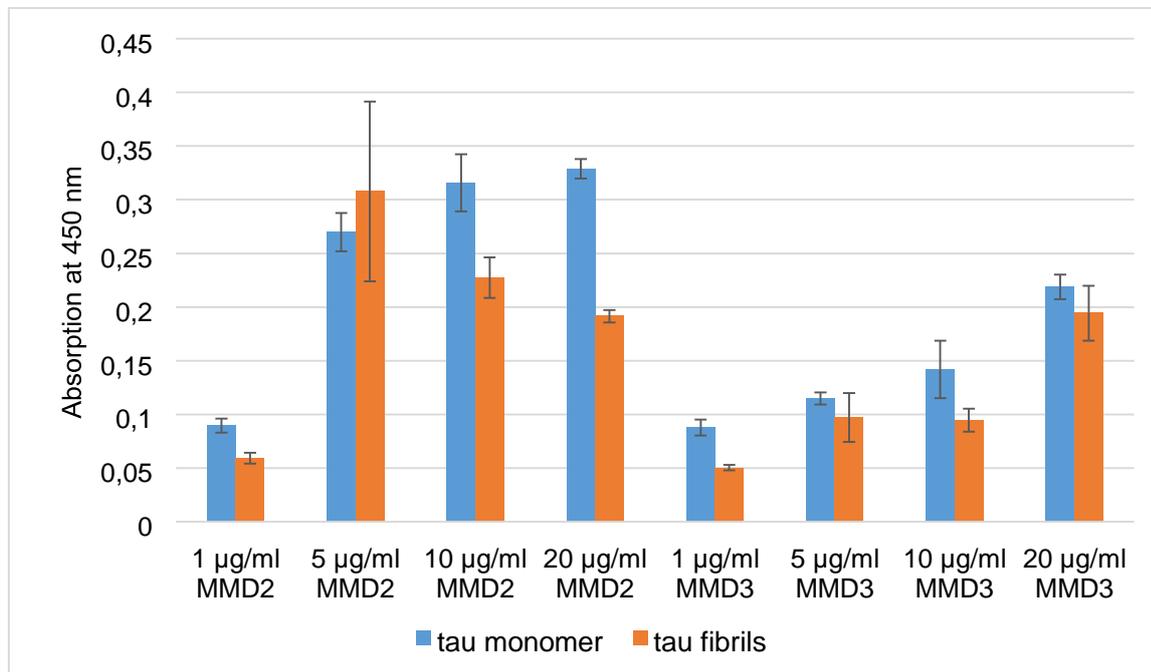
Figure 19: ELISA to demonstrate the binding properties of peptide MMD2 and MMD3 to tau monomers and tau fibrils. To enable the use of this method**,** a FAM-labeled version of the peptides was synthesized. The plate was coated with tau monomers and fibrils in a 10 µg/mL concentration. As a negative control, a NaHCO3 buffer was incubated in the wells in place of the tau protein solution. After blocking with 1% BSA in PBS, the peptides **MMD2-FAM** and **MMD3-FAM** were added in increasing concentrations (1µg/ml, 5 µg/ml, 10 µg/ml and 20 µg/ml), a horseradish peroxidase-conjugated sheep anti-FITC secondary antibody was used to detect the bound peptide. Subsequently, the TMB substrate solution was transferred to the relevant wells. Finally, the reaction was stopped with 20% H2SO4 and the plate was read at 450 nm. The absorption values were presented after subtraction of the negative controls. The mean of three absorption values (at 450 nm) is shown, as well as the standard deviation.

4.5 Mirror image phage display selection against D-PHF6* fibrils

In order to select more D-peptide inhibitors of tau aggregation, a second phage display selection was done using fibrils of the D-enantiomeric PHF6* as a target. The hexapeptide segment PHF6*, which represents residues 275 to 280 of the tau protein, was chosen as a target in our second selection as Seidler et al., 2018 reported that this segment has a powerful role in tau aggregation. We used the D-amino acid configuration of the target PHF6* in order to employ mirror phage display, an elegant and direct way to obtain peptide ligands in the D-conformation. In principle, the

selection was carried out exactly as in phage display but against the mirror image of the original target molecule.

4.5.1 Preparation of D-PHF6* fibrils for mirror image phage display selection

D-enantiomeric PHF6* fibrils were prepared for the selection, D-PHF6* was incubated in sodium phosphate buffer (Napi) in the presence of THT for at least 30 hours. Aggregation was detected by measuring ThT-fluorescence. The fibrillization was started after the incubation at 0 h. After 6 hours of incubation, PHF6* exhibited a greater rate of aggregation and the self-assembly into fibrils continued until ⌣28 h. After 28 hours of incubation, a plateau or the saturation point was attained. In contrast, the relative fluorescence intensity of the negative control was stable at a low value. The resulting fibrils were then immobilized in a microtiter plate and used as a target for mirror image phage display (Figure 20).
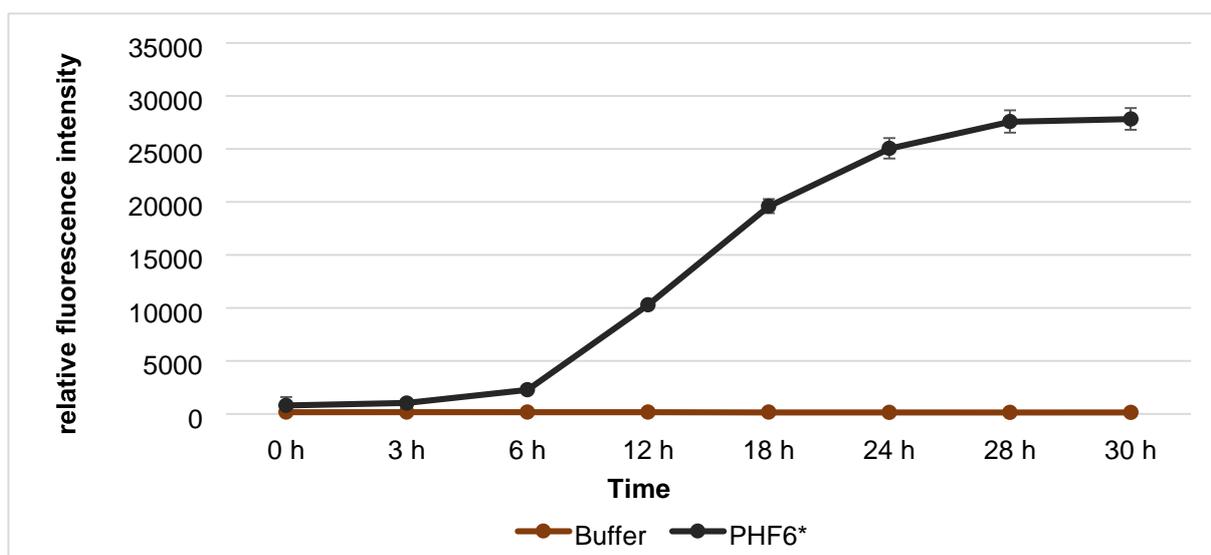
Figure 20: PHF6* fibrillizes spontaneously by incubation at room temperature. The assay was carried out using 100 µM PHF6* in NaPi buffer with 10 µM ThT (black line). As negative control, a solution containing 10 µM ThT in NaPi (without PHF6*) was used (brown line). Solutions were pipetted into a black 96-well half area µclear flat-bottom plate and incubated at RT for 30 hours. The relative fluorescence intensity was measured at excitation and emission maxima of 450 and 482 nm, respectively (mean +/- standard deviations of results, three replicates per run).

4.5.2 Enrichment ELISA after four panning rounds

After immobilization of D-PHF6* fibrils onto a microtiter plate, $1x\ 10^{11}$ phages from Ph.D.-12 Phage Display Peptide Library were added, the unbound phages were washed away and the bound phages were eluted. The eluted phages were amplified in *E.coli* and taken for another panning round. Four panning rounds were performed, after each panning round the input titer and the output titer were calculated. After counting the number of plaque forming units (pfu), the phages were diluted to a concentration of $1x\ 10^{11}$ phages and used for the subsequent panning round. The binding properties of the four eluted phages pools from each panning round were screened using enrichment ELISA. The four eluates were added to PHF6* coated wells. For non-specific binding, negative control wells were filled with coating buffer or coating buffer including 1% BSA.

As Figure 21 shows, the absorption value of the negative control wells in all panning rounds (which represent the binding) was relatively low in comparison to the absorption value of the wells coated with PHF6* fibrils. These results indicating specific binding of each eluted phage from different rounds of biopanning. We were unable to observe any increase in the absorption signal with increasing numbers of panning, which was unexpected. However, the first and second round of biopanning exhibited highest signal in the polyclonal phage ELISA. The binding ratio for all panning rounds was more than 2 (Table 11).

The binding properties of the individual phage clones from the third and fourth panning rounds to the target were tested using single phage ELISA.
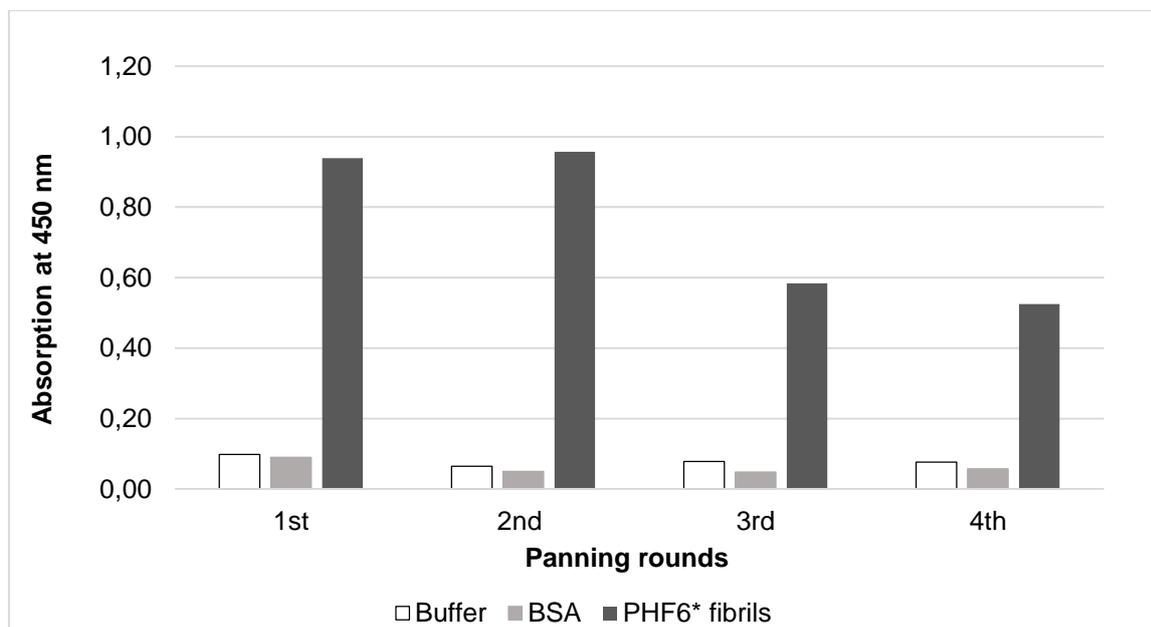
Figure 21: Enrichment ELISA showed a binding of the four panning rounds eluates to PHF6* fibrils. Wells were coated with 100 µg/ml D-PHF6* fibrils, wells containing only buffer or buffer with 1% BSA were used as negative controls. After blocking, amplified phages from rounds one to four were added to the respective wells and incubated for 1h. After washing, bound phages were detected with anti-M13 HRP monoclonal antibody. The unbound antibodies were washed away, the TMB substrate was added and the reaction was stopped with 20 %H2SO4. Finally, the absorption was measured at 450 nm.

Table 11: Binding ratio of D-PHF6* fibrils to the negative control (buffer) by enrichment ELISA

Round of panning	1	2	3	4
Enrichment ELISA (A450 nm ratio) tau monomer: buffer	10.3	15.8	7.4	6.8

4.5.3 Single phage ELISA

The eluates of the third and fourth panning rounds were plated on LB/IPTG/Xgal plates. Individual phage stock solutions were prepared by picking individual clones from LB/IPTG/Xgal plates and amplifying them in *E.coli*. After several steps of precipitation and centrifugation, individual phage stocks were produced and added to PHF6* fibrils coated wells to determine whether a selected phage clone would bind to the target.

Most of the phage clones exhibited a significantly high absorption value in comparison to the negative controls, indicating a binding to PHF6* fibrils. This included clone numbers (e. g. 1, 2, 3, 4, 6, 19 and 26). Other clones exhibited a relatively low binding to PHF6* fibrils in comparison, including phage numbers 13, 15, 17, 20, 23 and 28. Phages like No. 5, 7 and 8 exhibited an extremely low binding to PHF6* fibrils coated wells, potentially indicating a phage clones with nonspecific binding (Figure 22).

The DNA of the promising phage clones was extracted and sequenced to identify the sequences of the peptides displayed on the surface of phages. Over 60 clones were screened for specific binding to the immobilized PHF6* fibrils. Figure 22 represents an example of the binding properties of 28 phage clones.
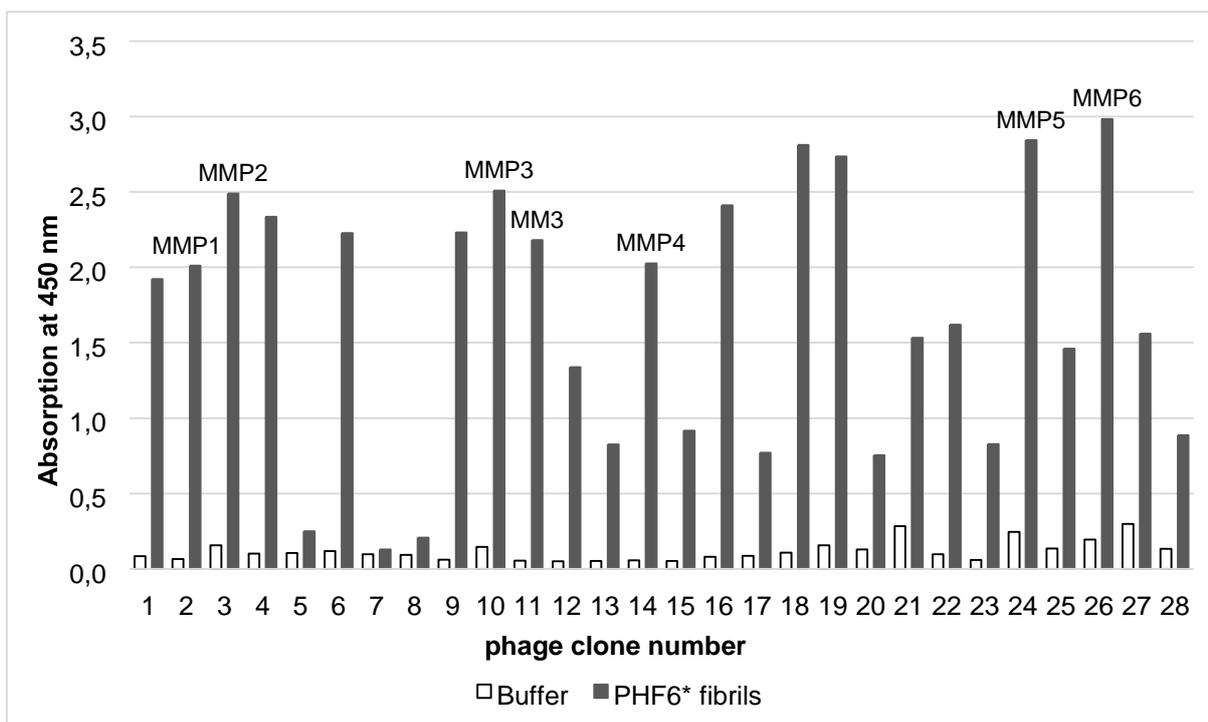
Figure 22: Identification of binding properties of individual randomly-selected phage clones to PHF6* fibrils by single clone ELISA. 100 µg/ml PHF6* fibrils were immobilized on the plate. As negative controls, wells were filled with the coating buffer. After blocking, individual phage stocks were added to the respective wells. After washing, bound phages were detected with anti-M13 HRP monoclonal antibody. Subsequently, the TMB substrate solution was transferred to the relevant wells. Finally, the reaction was stopped with 20% H2SO4 and the plate was read at 450 nm. The figure represents an example of 28 phage clones, approximately 60 phage clones were tested. Later, the synthesized peptides from the phage clones 2, 3, 10,11,14, 24 and 26 were named as MMP1, MMP2, MMP3, MM3, MMP4, MMP5 and MMP6 respectively.

4.5.4 DNA extraction for identification of peptides sequences

The DNA of the promising phage clones was extracted and sent for sequencing. The obtained DNA sequences were then translated into amino acid sequences. In total, 31 displayed peptides were identified and no one single dominating peptide sequence was evident in 31 sequences. The peptide sequences from the selection against PHF6* fibrils are listed in Table 12. Interestingly, the sequence of peptide MM3, which was obtained in the first selection against full-length tau and acted as a tau aggregation inhibitor, was also obtained in the selection against PHF6* fibrils.

Different characteristics of the peptides such as charge, hydrophobicity and molecular weight were analyzed using web tools like PepCalc (https://pepcalc.com/) and Peptide 2.0 Inc (https://www.peptide2.com/).

To exclude target-unrelated peptides from biopanning results, the peptide sequences were screened using the SAROTUP database ("Scanner And Reporter Of Target Unrelated Peptides". SAROTUP predicted one phage clone (No. 28, DHMPPYHWRPWD) to be a plastic binder and some phage clones were predicted to be rapidly growing phages (No. 3, 7, 14, 15, 19, 20, 25, 27 and 29) (Table 12). After excluding possible target-unrelated peptides, six peptides MMP1, MMP2, MMP3, MMP4, MMP5 and MMP6 were selected for further characterization. The peptides were synthesized as L-enantiomeric peptides to test their ability to inhibit the aggregation of PHF6*. Usually, the peptides obtained after mirror image phage display are synthesized directly as D-peptides and tested against the L-enantiomeric form of the target. However, due to the high cost of synthesizing six D-enantiomeric peptides, we decided to order them first in the L-enantiomeric form and test them against DPHF6* using THT assay. Subsequently, the promising L-peptides were synthesized as D-peptides.

Table 12: Selected peptides from mirror image phage display selection against D-PHF6* fibrils. The peptides' sequences were determined after DNA sequencing of the positive phage clones. The frequency of each sequence was listed in the table. Peptides' characteristics like charge, hydrophobicity and molecular weight in Dalton were also analyzed using the websites Peptide 2.0 Inc and PepCalc and listed below. Each sequence was given a number in the list.

No.	sequence	frequency	charge	hydrophobicity	MW (Da)	Name
1	YPVRAVPNQSGQ	1/31	+1	41.67%	1315.43	_
2	YVTHYNANYSNL	2/31	+0.1	25%	1458.53	_
3	YSLRLTSVTAPT	1/31	+1	41%	1308.48	
4	DPLKARHTSVWY	1/31	+1	41%	1472.65	MM3
5	MPHLHPSSANWS	1/31	+0.2	50%	1363.5	_
6	GRDMPMSALMRH	1/31	+1.1	50%	1401.69	MMP1
7	NHNHGYPITHRT	1/31	+1.3	16.67%	1446.53	_
8	GIALSEPVPNHH	1/31	-0.8	50%	1270.39	_
9	WPHDTKRYLFPA	1/31	+1.1	50%	1530.73	MMP2
10	YPMHPGYGTKLG	1/31	+1.1	33.33%	1320.52	_
11	YSGVSRGHSHGP	1/31	+1.2	16.67%	1240.29	_
12	YVPANNYHLHSP	1/31	+0.2	41.67%	1411.52	MMP3
13	SLSPIFIQNGTN	1/31	0	41.67%	1290.42	_
14	NLPPERGHLSWI	1/31	+0.1	50%	1418.6	_

15	SDASMQNKLPLW	1/31	+0.1	50%	1418.6	_
16	NLWKGLDGSGRT	1/31	+1	25%	1303.42	_
17	HSDLWRRSFELM	1/31	+0.1	25%	1576.78	MMP6
18	TPSYLMPLAPHT	1/31	+0.1	58.33%	1327.55	_
19	SLLHPNAIMPRT	1/31	+1.1	58.33%	1349.6	_
20	DEDQQVHYQIWR	1/31	-1.9	25%	1616.69	_
21	HPAPHRYHSNLH	2/31	+1.4	33.33%	1465.58	MMP4
22	TRTATLADNSWL	1/31	0	33.33%	1348.46	MMP5
23	HLTATELANSYH	1/31	-0.8	33.33%	1356.44	_
24	MKAHHSQLYPRH	1/31	+2.3	33.33%	1504.72	_
25	SYPSNALSLHKY	1/31	+1.1	33.33%	1379.52	_
26	NHSDKQMSSAFL	1/31	+0.1	33.33%	1364.49	_
27	SLSPAGYTRLSL	1/31	+1	41.67%	1264.43	_
28	DHMPPYHWRPWD	1/31	-0.8	50%	1636.79	_
29	KIHHSLTIRTAA	1/31	+2.2	41.67%	1347.57	_

4.6 *In vitro* aggregation assays for the characterization of peptides abilities to inhibit the aggregation of PHF6* as full-length tau

4.6.1 The potential of the selected L-enantiomer peptides to inhibit the aggregation of PHF6*

To investigate the potential of the synthesized peptides MMP1, MMP2, MMP3, MMP4, MMP5 and MMP6 to inhibit the fibrillization of D-enantiomeric PHF6*, thioflavin fluorescence assays were performed. The ability of MM3, obtained in both selections, to inhibit the aggregation of D-PHF6* was also tested. PHF6* fibril formation was detected in the presence and absence of tenfold more molar concentration of each peptide. The relative fluorescence value of the positive control (only PHF6*) after 30 hours (saturation level) was set to 100%. As can be seen in Figure 23, peptides MMP2 and MMP6 were the most potent PHF6* aggregation inhibitors; furthermore, MMP1 and MMP4 reduced the fibril formation of PHF6*. In contrast, MMP5 did not inhibit PHF6* fibrillization, while MMP3 seemed to increase the PHF6* aggregation. MM3,

which was previously confirmed by THT assay as full-length tau aggregation inhibitor, also acted as a potent PHF6* aggregation inhibitor (Figure 23).
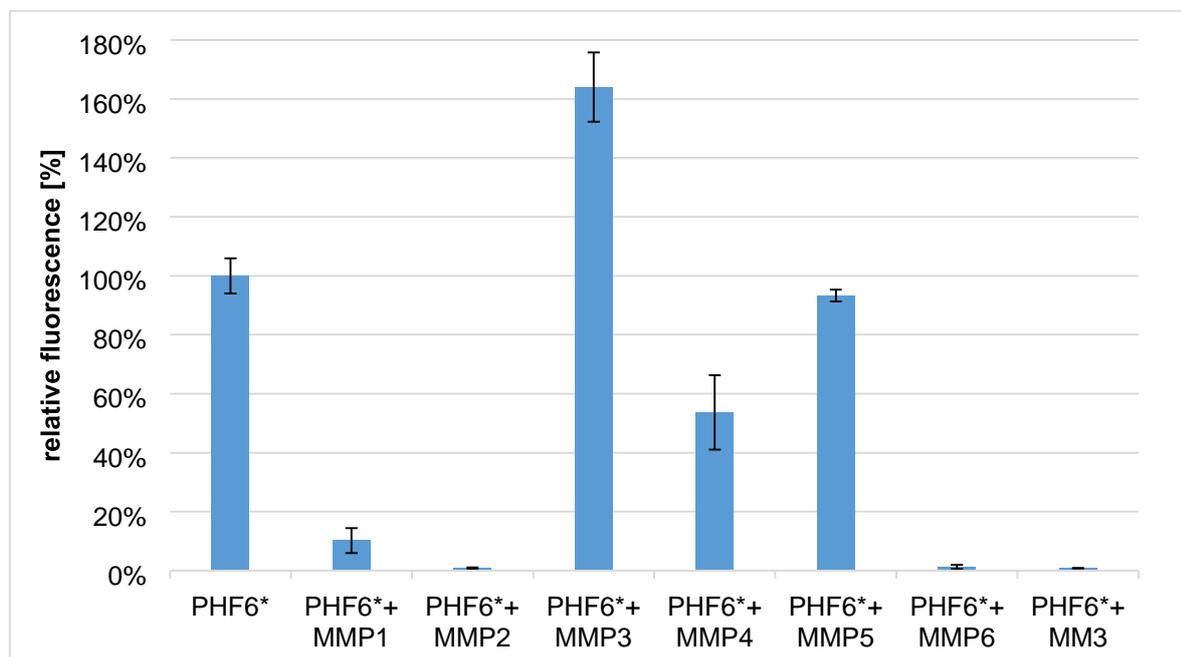
Figure 23: The ability of the selected peptides MMP1, MMP2, MMP3, MMP4, MMP5, MMP6 and MM3 to reduce or inhibit D-PHF6* fibrils formation. ThT assays were performed using 100 µM PHF6* in NaPi buffer with 10 µM ThT. The peptides were added in concentration of 1000 µM to PHF6* solution respectively. NaPi and 10 µM ThT without addition of PHF6* was used as a negative control. Solutions were pipetted into a black 96-well half area µclear flatbottom plate and incubated at RT for 42 hours. The relative fluorescence intensity was measured at excitation and emission maxima of 450 and 482 nm, respectively (mean +/- standard deviations of results, three replicates per run). The relative fluorescence for the positive control (only PHF6*) after reaching the saturation level (30 hours of incubation) was set at 100%.

Peptides MMP2 and MMP6 were selected for further characterization to test their ability to inhibit the aggregation of full-length tau. Both MMP2 and MMP6 were synthesized as D-enantiomeric peptides and named as MMPD2 and MMPD6 respectively.

4.6.2 The potential of the MMPD2 and MMPD6 to inhibit the aggregation of full-length tau

To test the ability of MMPD2 and MMPD6 to inhibit the fibrillization of full-length tau, similar thioflavin assays to those described above were carried out with full-length tau. Tau, heparin and MMPD2 or MMPD6 were incubated. As a control, MMD3, which was previously confirmed as full-length tau aggregation inhibitor, was tested. As a positive

control, tau was incubated with heparin and the relative fluorescence of the samples after reaching the saturation level were calculated in percent (Figure 24). Neither MMPD2 nor MMPD6 inhibited the aggregation of full-length tau. Indeed, MMPD6 even appeared to increase tau aggregation. MMD3, which was obtained in both the selection against full-length tau and the selection against D-PHF6* fibrils, showed again its ability to inhibit the aggregation of full-length tau.
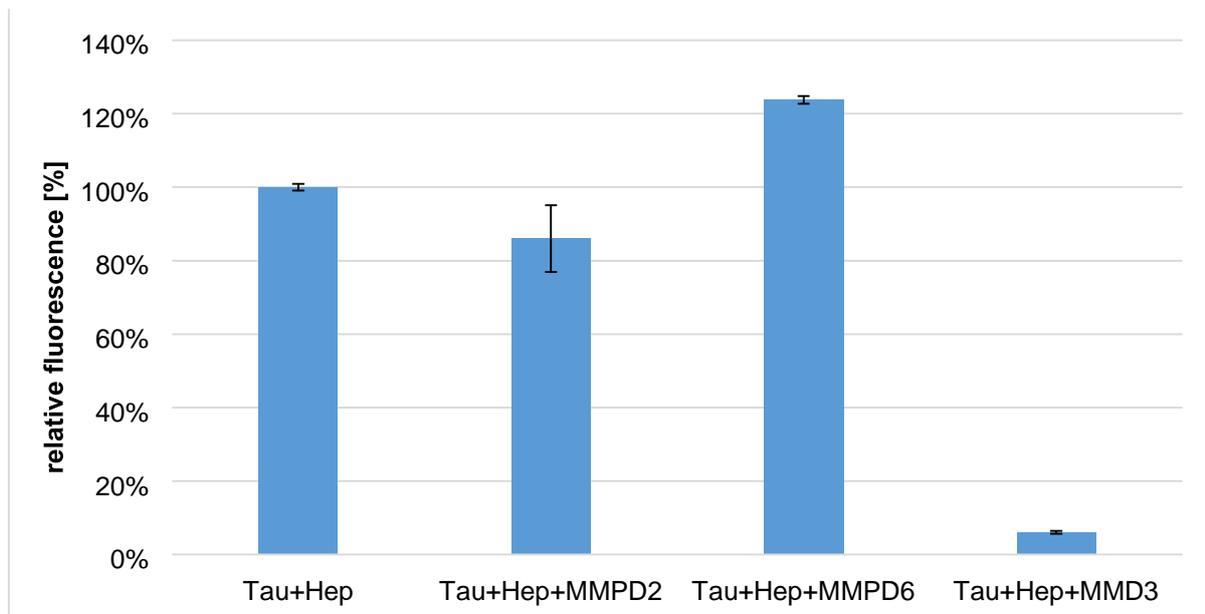
Figure 24: The ability of the selected peptides MMPD2, MMPD6 and MMD3 to reduce or inhibit tau fibril formation. 24 µM tau, 6 µM heparin and 10 µM ThT were incubated with and without the peptides in a molar ratio of 1:10 (tau:peptide), respectively. Samples were pipetted into each well of a black 96-well µclear flat-bottom plate and incubated at 37°C for 72h in photometer POLARstar Optima. The relative fluorescence intensity was read out at excitation and emission maxima of 450 and 482 nm, respectively (mean +/- standard deviations of results, three replicates per run). The relative fluorescence for the positive control (tau and heparin without peptides) after reaching the saturation level (36 hours of incubation) was set at 100%.

The peptides that were selected against the PHF6* motif were not used for further investigation, with the exception of peptide MMD3. Thus, further investigations on MMD3 and MMD3rev were performed.

4.6.3 The potential of the MMD2, MMD2rev, MMD3 and MMD3rev to inhibit the aggregation L-PHF6*, as well as the aggregation of PHF6

Given the observation that MM3 acted as a tau aggregation inhibitor as well as a PHF6* aggregation inhibitor, we hypothesized that MM3 is a specific inhibitor for PHF6* fibrillization. To test this possibility, the potential of MMD2, MMD2rev, MMD3 and MMD3rev to inhibit the aggregation of PHF6* segment as well as the aggregation of PHF6 segment were tested using thioflavin assays.

To test whether MMD3, MMD3rev, MMD2 and MMD2rev reduce PHF6* fibril formation, 1000 µM from the respective peptides were incubated with 100 µM PHF6* at RT. As a positive control, PHF6* was incubated alone. The relative fluorescence of THT was monitored over 30 h. As expected, MMD3 and MMD3rev, which were selected against PHF6* fibrils, inhibited the formation of PHF6* fibrils, while MMD2 and MMD2rev did not inhibit the fibrillization of PHF6* (Figure 25 A).

To evaluate the ability of MMD3, MMD3rev, MMD2 and MMD2rev to inhibit the aggregation of PHF6, 500 µM from the respective peptides were incubated with 50 µM PHF6 at RT. As a positive control, PHF6 was incubated alone. The relative fluorescence of THT was monitored over 30 h. As shown in Figure 25 B, PHF6* inhibitors MMD3 and MMD3rev did not affect the formation of PHF6 fibrils. In addition, MMD2 and MMD2rev, which were selected against full-length tau, did inhibit the fibrillization of PHF6.
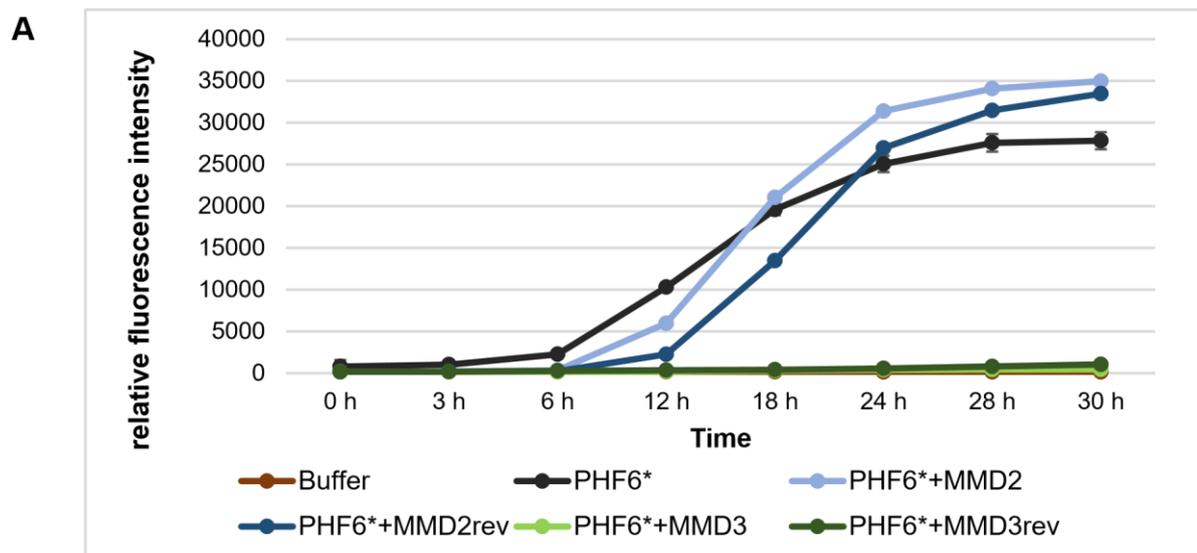
B
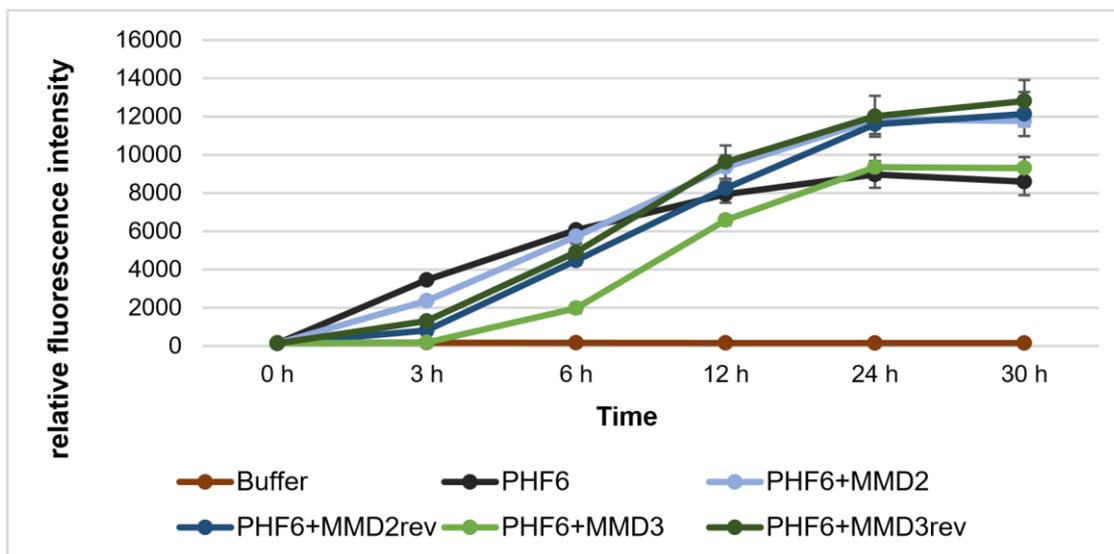
Figure 25: MMD3 and MMD3rev inhibit the aggregation of PHF6* but not of PHF6, while MMD2 and MMD2rev neither inhibit the aggregation of PHF6* nor of PHF6. (A) PHF6* fibrillization was performed by incubating 100 µM PHF6* in NaPi buffer with 10 µM ThT at room temperature (black line). NaPi and 10 µM ThT without addition of PHF6* was used as control (brown line). Peptides MMD2, MMD2rev, MMD3 or MMD3rev were added in concentrations of 1000 µM to 100 µM PHF6* samples (light blue line, blue line, light green line and green line respectively). Fluorescence was measured at 450/482 nm in relative units (mean +/- standard deviations of results, three replicates per run). Low ThT signals were observed in the samples treated with D-peptides MMD3 and MMD3rev, which indicates an inhibition of PHF6* aggregation. Samples treated with MMD2, MMD2rev do not exhibited a reduction in ThT signals, which indicates no inhibitory effect on PHF6* fibril formation **(B)** PHF6 fibrillizes spontaneously via incubation at room temperature. The assay was performed using 50 µM PHF6 in NaPi buffer with 10 µM ThT (black line). 10 µM ThT in NaPi without addition of PHF6 was used as negative control (brown line). Peptides MMD2, MMD2rev, MMD3 or MMD3rev were added in concentrations of 500 µM to 50 µM PHF6 samples (light blue line, blue line, light green line and green line respectively). Fluorescence was measured at 450/482 nm in relative units (mean +/- standard deviations of results, three replicates per run). Samples treated with all D-peptides do not exhibited a reduction in ThT signals, which indicates no inhibition of PHF6 fibril formation.

4.7   Demonstrating the binding properties of the MMD2 and MMD3 to PHF6* fibrils, as well as to PHF6 fibrils using ELISA

To evaluate the binding properties of MMD2 and MMD3 to both PHF6 fibrils and PHF6* fibrils, ELISA was performed with a FAM-labeled version of the peptides. The plate was coated with 50 µg/ml PHF6 fibrils as well as PHF6* fibrils and as a negative control, coating buffer only was added to the wells. The peptides were added at increasing

concentrations and the bound peptides were detected with anti-FAM antibodies. After adding the substrate, the absorption at 450 nm, representing the binding affinities, was measured.

As shown in Figure 26, both MMD2 and MMD3 bound to both PHF6 fibrils and PHF6* fibrils. Unexpectedly, MMD2, which did not inhibit the aggregation of tau, showed significantly higher binding signal to PHF6 fibrils. In contrast, MMD3, which inhibited both the aggregation of full-length tau as well as PHF6*, showed higher binding signal to PHF6 fibrils than PHF6* fibrils.
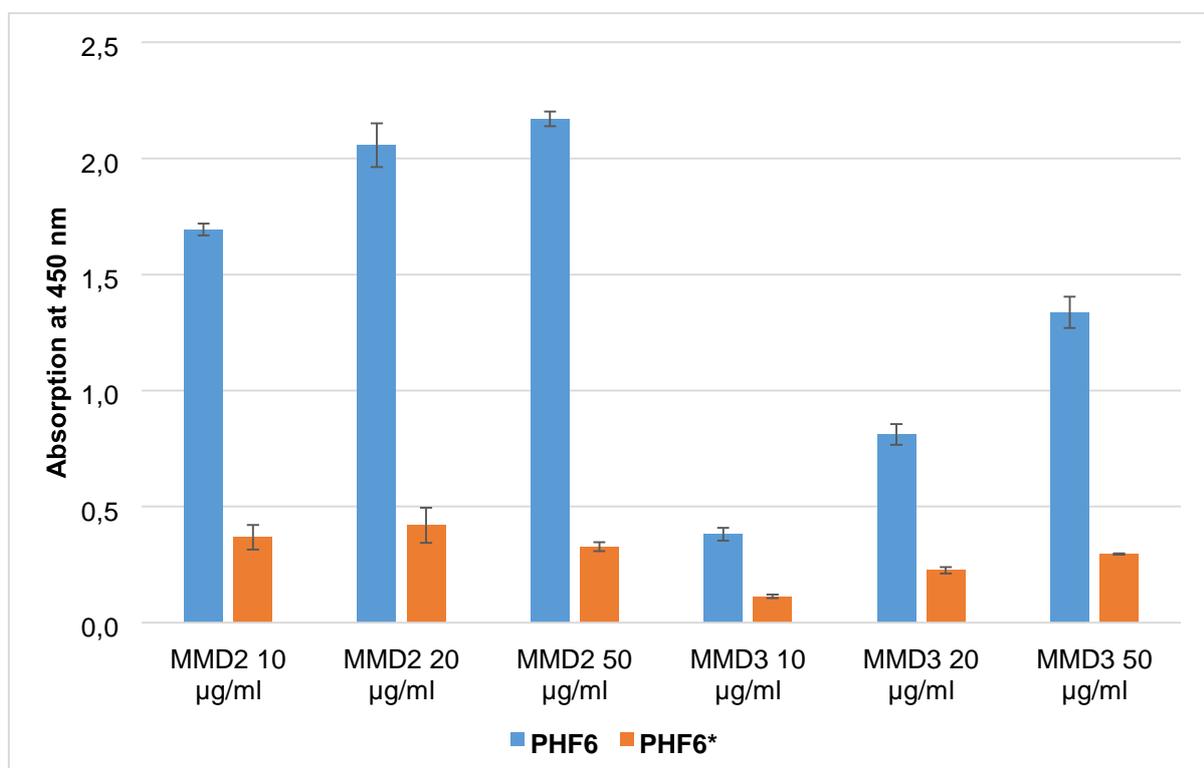
Figure 26: The binding properties of peptides MMD2 and MMD3 to PHF6 fibrils and PHF6* fibrils were tested using ELISA. To enable the use of this method, a FAM-labeled versions of the peptides were synthesized. The plate was coated with PHF6 fibrils and PHF6* fibrils in 50 µg/mL concentration. As a negative control, coating buffer only was incubated in the wells. After blocking with 1% BSA in PBS, the peptides **MMD2-FAM** and **MMD3-FAM** were added in increasing concentrations (10 µg/ml, 20 µg/ml and 50 µg/ml), a horseradish peroxidase-conjugated sheep anti-FITC secondary antibody was used to detect the bound peptide. Subsequently, the TMB substrate solution was transferred to the relevant wells. Finally, the enzymatic reaction was stopped with 20% H_2SO_4 and the plate was read at 450 nm. The absorption values were presented after subtraction of the negative controls. The mean of three absorption values (at 450 nm) is shown, as well as the standard deviation.

4.8 Thioflavin assays to test whether the PHF6*- based inhibitors are more potent in inhibiting the aggregation of full-length tau than PHF6-based inhibitors

To test whether inhibitors based on the structure of the PHF6* segment are more potent in inhibiting tau fibrillization than inhibitors based on the structure of the PHF6, we compared the tau aggregation inhibiting effects of PHF6* inhibitors MMD3 and MMD3rev with another peptide, designated APT, which was selected against PHF6 fibrils earlier by our group (Dammers et al, 2016). We further tested the performance of two peptides previously described in the literature, designated "Sievers" and "W.MINK", which bind to PHF6 and PHF6*, respectively.

Thioflavin assays were performed by incubating full length tau with heparin at 37 °C, the peptides were added at increasing concentrations (molar ratio 1:1, 1:5 and 1:10). The relative fluorescence of the positive control (tau with heparin) after reaching the saturation level was set at 100%. As shown in Figure 27, PHF6-based inhibitors ("Sievers" and APT) were able to hinder the aggregation of full-length tau with a similar potency to PHF6* based inhibitors (MMD3 and MMD3rev) at molar ratios of 1:5 and 1:10. At molar ratio 1:1, APT was the most effective peptide in blocking the seeding of tau protein. Conversely, W.MINK, a PHF6* binder, was in our hands less effective than the other peptides in reducing the aggregation of tau. In this assay, W.MINK even increased the aggregation of full-length tau at molar ratio 1:1.
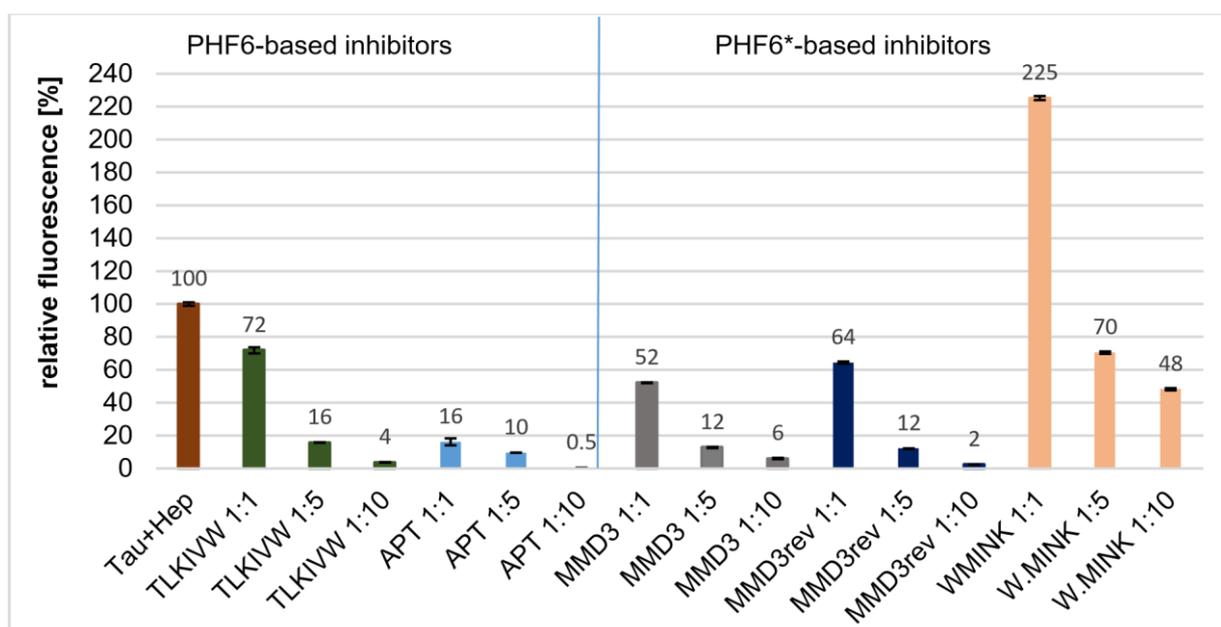
Figure 27: ThT assays to test whether the PHF6* based-inhibitors are more potent in inhibiting the aggregation of full-length tau than PHF6 based-inhibitors. The performance of the peptides selected in this project (MMD3 and MM3rev) were compared to the performance of already published peptides: APT, selected by our group against PHF6 fibrils (Dammers et al., 2016), TLKIVW (Sievers et al., 2011) and W.MINK (Seidler et al., 2018), which target PHF6 and PHF6*, respectively. 24 µM tau and 6 µM heparin were incubated at 37°C with and without the peptides at a molar ratio of 1:1, 1:5 and 1:10 (tau:peptide), respectively. After adding of ThT, fluorescence was measured at 450/482 nm in relative units (mean +/- standard deviations of results, three replicates per run). The relative fluorescence for the tau and heparin control without peptides after reaching the saturation level (36 hours incubation) was set at 100%. Numbers over the columns of the chart represent the value of the relative fluorescence of each sample.

5 Discussion

AD is characterized by the accumulation of Aß plaques and tau tangles in the brain. Tau aggregation is associated with more than 20 neurodegenerative disease, the most common of which is Alzheimer's disease (Terry et al., 1964; Kidd, 1963; Terry 1963; 1998; Ballatore et al., 2007). Since Aβ and tau were identified, AD therapeutic research has predominately focused on Aβ. However, tau-targeting strategies have gained more attention in recent years, in part because Aβ-targeting treatments have largely proven unsuccessful in clinical trials, in addition, studies have revealed that tau pathology (neurofibrillary tangles) correlates more closely with the severity of AD than Aß pathology (Arriagada et al., 1992).

Initially, one of the potential anti-tau therapy strategies was based on the inhibition of tau aggregation. Compounds that inhibit tau fibrillization may lead to prevent the spread of tau pathology (Congdon and Sigurdsson, 2018). Methylene blue is an effective tau aggregation inhibitor. This agent reduces tau pathology and improves cognitive phenotypes in transgenic mouse models of tauopathy (Panza et al., 2016). In addition, the methylene blue derivative (LMTX) reached the clinical trials phase III with AD patients and showed improvement in patients with mild or moderate AD who took LMTX alone without any other AD treatments. However, an additional phase III clinical trial was recently terminated to assess the effectiveness and the long-term safety of the drug (https://clinicaltrials.gov/show/NCT01689233 (2018)).

D-enantiomeric peptide-based drugs have become reasonable alternatives to chemical pharmaceuticals, and gained an extraordinary degree of scientific interest in their potential usage. D-enatiomeric peptides are highly resistant to proteases. In addition, they can be absorbed systemically after oral administration. Furthermore, Dpeptide immunogenicity has been demonstrated to be reduced in comparison to Lpeptides (Milton et al., 1992; Pappenheimer et al., 1994; Chalifour et al., 2003; Sadowski et al., 2004; Pujals et al., 2007). A variety of small peptides that target tau pathology and reduce its toxic effects have already been described and a fraction of them proved to be effective in AD animal models. Davunetide (DAP) is an eight amino acid peptide that targets tau pathology and promotes MT assembly. It has been shown to decrease tau phosphorylation and Aβ levels in tau transgenic mice. However, DAP dose not

considered as an inhibitor of tau fibrillization (Shiryaev et al., 2009; Matsuoka et al., 2008).

The formation of tau aggregates is triggered by two hexapeptide sequences within tau: 275-VQIINK-280 (PHF6*) und 306-VQIVYK-311 (PHF6). Both fragments are interesting targets for the development of tau aggregation inhibiting compounds, and some peptides were already described. The D-enantiomeric peptide, TLKIVW, was rationally designed by the Eisenberg group on PHF6 fibrils as templates and was shown to prevent the aggregation of PHF6, and of the truncated tau constructs (K12 and K19) (Sievers et al., 2011). In addition, our group selected D-enantiomeric peptides APT, KNT, APS, TD28 and TD28rev, which interact with PHF6 fibrils in a manner analogous to TLKIVW and inhibit the formation of PHF6 fibrils as well as fulllength tau fibrils (Dammers et al., 2016). Recently, in 2018, the Eisenberg group developed a new peptide, designated W.MINK, using the PHF6* fibrils as templates for a structure-based inhibitor design. W.MINK inhibits the aggregation of full-length tau in HEK293 biosensor cells (Seidler et al., 2018).

In this thesis, D-enantiomeric peptides were selected using phage display and mirror image phage display in order to inhibit the fibril formation of tau. For the phage display selection, tau monomer was used as a target in order to obtain peptides that inhibit the aggregation process at a very early stage, since tau pathological aggregation begins from tau monomers. For the mirror image phage display selection, the selection was performed against D-PHF6* fibrils, as in 2018 the Eisenberg group hypothesized that PHF6* is a more powerful driver for tau aggregation and that inhibitors of PHF6* aggregation are highly effective at preventing the aggregation of full-length tau (Seidler et al., 2018).

5.1   Expression and purification of recombinant tau protein

Efficient production of recombinant tau protein is required for the *in vitro* screening of tau aggregation inhibitors. *In vitro* tau fibrillization assays required significant quantities of tau and the presence of anionic inducer such as heparin.

Full-length tau protein with 441 amino acids (tau441 or tau 2N4R) was expressed and purified during this project according to two protocols, Margittai et al., 2004 and

KrishnaKumar et al., 2017, with minor modifications in each protocol. For purification, the heat stability of tau is an effective tool to remove host specific proteins. Therefore, cell lysate containing tau protein can be boiled and tau remains in the supernatant, maintaining its physiological function. The majority of other proteins, including proteases, become insoluble and precipitate under these conditions (Cleveland et al., 1977).

As described by Margittai and coworkers, tau-containing lysate was boiled and then purified using various purification methods, including ammonium sulfate precipitation, cation exchange chromatography and anion exchange chromatography. The overall yield of tau was about 3 mg from 1L culture. Most of tau protein expressed according to this method was used in the phage display selection against tau monomer.

In 2017, KrishnaKumar and his colleagues demonstrated a simplified method to obtain tau protein from *E.coli* with one-step purification. After boiling of the lysate, tau was purified using cation exchange chromatography. Here, some lower molecular additional bands were observed on the gel after performing the SDS-PAGE (Figure 11). Using Western blot analysis with the tau specific antibody anti-TAU5, we observed that all additional bands reacted with the tau specific antibody, indicating that all fragments are degradation products of tau and belong to the recombinant protein tau (Figure 12). All protein expressed according to this protocol was used in the subsequent thioflavin T aggregation assays. Thioflavin T aggregation assays with tau protein obtained from both protocols were performed under the same conditions, we observed that the kinetic courses of aggregation were the same, which indicated that these small amounts of degradation products did not alter the aggregation kinetics of tau. However, the method reported by KrishnaKumar et al. offers a fast and low cost method in comparison to currently existing methods. Our overall yield of tau from this protocol was about 3 mg from 1L culture, while the expressed yield achieved by KrishnaKumar et al. was 8-12 mg from 1 L culture.

5.2 Selection of full-length tau binding peptides using phage display

To select peptides that bind to full-length tau protein and inhibit the pathological aggregation of tau, a phage display selection against tau monomers was performed.

Tau monomer was used as a target, as studies suggest that targeting the early phase of the aggregation process is useful to reduce potential toxic oligomers and fibrils formation. In addition, small peptides that bind to the monomeric proteins could inhibit their aggregation and stabilize their functional native states (Pickhardt et al., 2015).

Four panning rounds were carried out and enrichment ELISA was performed to evaluate the binding properties of the amplified phage pools of each panning round, which contain a population of phages, to tau monomer. High binding signals of the phage pools from rounds 1-4 to tau monomer were observed compared to the very low signal of the phage pools in the negative control wells (Figure. 13). As expected, during successive rounds of the selection process, enrichment of phages that bind to the target protein was observed with an increasing number of panning rounds. The maximum enrichment was obtained in the fourth panning round.

In the literature, some phage display selections have been carried out with additional rounds of panning, such as the mirror image phage display selection described by Rudolph et al., 2016 against Aß. They performed six rounds of panning, while the mirror image phage display selection of Dammers et al. 2016 against PHF6 fibrils was performed with four panning rounds. However, we avoided the performing of more than four panning rounds as it could lead to an increase in the fast growing phages in the later rounds of panning, according to the recommendations of the manufacturer.

The enrichment in phage pools can be estimated after rounds of selection by calculating the binding ratio. A binding ratio >2 usually indicates a phage pool with specific binding phages. In contrast, a low ratio <2 may indicate a failure in the biopanning procedure. Furthermore, a ratio <2 with high negative control absorbance may indicate a presence of non-specific clones (such as plastic binders) in phage pool (Miersch et al., 2015).

In our selection, the binding ratio for all panning rounds was >2 (Table 8). An enrichment in phage pools was observed in rounds 3–4. Subsequently, the binding

79

properties of single clones from the third and fourth panning rounds were evaluated using single phage ELISA. Usually, individual clones are isolated from the last rounds of panning (usually the enriched rounds of panning) (Zadeh et al., 2019). In single phage ELISA, the amplified pool of phages after the panning round was plated on IPTG/Xgal plates and single clones were picked and prepared to obtain a solution conations only single phage clone. This method is useful to screen individual single phages from a population of phages. The binding properties of approximately 96 phage clones to full-length tau monomer were estimated using single phage ELISA. The single phage ELISA revealed several phages with a high signal in the wells coated with tau monomer, indicating the likely presence of binding phages to tau monomer.

The DNA of approximately 45 promising phage clones was extracted and sent for sequencing. Of these, 28 sequences could be identified after DNA sequencing. As some peptide sequences were identified more than once, the 28 identified sequences actually indicated 22 different peptides. These 22 sequences were then screened using screening web tools to exclude possible target-unrelated peptides.

In some phage display studies, the frequent occurrence of a peptide indicates that it is more likely to be a target-specific binding peptide (Agrawal et al., 2016). In the study by the Willbold group, Wiesehan et al. 2003, the most promising peptides D1 and D3, which were selected against D-Aß$_{1-24}$ by mirror image phage display, were dominated in the selections. D1 was obtained in 20 of 39 selected peptides and D3 was obtained in 9 of 23 selected peptides. However, in the study of Rudolph et al., 2015 from the same group, after performing mirror image phage against D-Aß$_{1-24}$ the DNA of 272 single phage clones was sent for sequencing. While several sequences obtained repeatedly and two sequences were found in 39 and 28 clones, the most promising peptide in his study occurred only once (Rudolph, 2015). In our study, the most promising peptide MMD3 also occurred only once in both performed selections (the selection against tau monomer and the selection against D-PHF6*). Hence, it seems reasonable to assume that the frequent occurrence of a peptide does not necessarily indicate that it is more likely to be a target-specific binding peptide.

After excluding possible target-unrelated peptides using SAROTUP, the remaining phages were further tested for their binding to tau monomers by single phage ELISA using the same concentration of each phage clone. Using this method, we can more

accurately compare the binding properties of different phage clones to the target tau. After amplifying each phage stock and titering the obtained phage solution, the same phage concentration from each individual phage solution was added to the tau-coated wells. Phages with relatively high absorption values comparing to the negative controls indicated a binding to the tau protein.

Finally, 8 peptides (MM1, MM2, MM3, MM4, MM5, MM6, MM7 and MM8) were selected to be synthesized as L-enantiomeric peptides to test their ability to inhibit the fibril formation of full-length tau protein.

The ability of the selected full-length tau binding peptides to inhibit the aggregation of full-length tau

After performing thioflavin T aggregation assays, two L-enantiomeric peptides, MM2 and MM3, showed their ability to inhibit the fibrillization of full-length tau (Figure 17). The D-enantiomeric form (MMD2, MMD3), as well as the D-enantiomeric-retro-inverso form (MMD2rev, MMD3rev), of both MM2 and MM3 were synthesized and tested for their ability to inhibit tau fibril formation. D-retro-inverso peptides are of particular interest. These have a reversed sequence of D-amino acids leads, and thus constitute molecules with almost the same structure and bioactivity as the original L-peptides, but with an increased resistance to proteolytic degradation (Chorev and Goodman, 1995; Fletcher et al., 1998).

THT aggregation assays indicated that while MMD2 and MMD2rev did not inhibit the aggregation of full-length tau protein, MMD3 and MMD3rev prevented significantly the formation of tau fibrils (Figure 18).

Other D-peptides were described in the literature and showed their ability to inhibit tau fibril formation. The D-peptides APT, KNT, LPS, TD28 and TD28rev which were developed against PHF6 fibrils by our group, inhibited the aggregation of full-length tau effectively when using the molar ratio (1:10) (tau:peptide) in THT assays (Dammers et al., 2016). Another D-peptide, TLKIVW, developed by computer-aided, structure-based design against PHF6 fibrils by Eisenberg group, also showed its ability to inhibit the formation of tau fibrils. The inhibitory effect of Sievers' peptide was also observed in a THT assay in molar ratio (1:10) (tau:peptide). However, this was observed not against

full-length tau, but against tau construct K12 (tau sequence 244-294) (Sievers et al., 2011).

After testing the inhibitory effect of MMD2 and MMD3, the peptides were further characterized. The binding of MMD2 and MMD3 to full-length tau was demonstrated using ELISA (Figure 19). Both MMD2 and MMD3 bound to tau monomers and fibrils, with a minimal preference for tau monomers. However, there was no significant difference between the absorption values of wells containing tau monomers and wells containing tau fibrils. In the study of Dammers et al., the binding of the selected peptides in her study to tau monomers and tau fibrils were also demonstrated using ELISA. These peptides also bound with minimal preference to tau monomers. In both, Dammers study and this study, the preference of the selected peptides to tau monomers was not significant; the light preference to tau monomers may be due to the fact that the binding sites of tau monomers are more accessible than tau fibrils.

The binding of MMD3 to tau monomers and tau fibrils was expected as MMD3 was obtained in the selection against tau monomers, and its binding site on tau monomers also available within tau fibrils. Also, MMD3 showed an effective inhibitory effect on tau fibril formation. Unexpectedly, MMD2 exhibited a stronger binding to both tau monomers and tau fibrils, while it did not prevent the formation of tau fibrils. It seems likely that the binding site for MMD2 on the tau does not involve inhibition of tau aggregation.

5.3 Selection of D-peptide against D-PHF6* fibrils using mirror image phage display

The two six-residue segments within tau, VQIVYK (PHF6) and VQIINK (PHF6*), promote the formation of amyloid aggregates of tau. PHF6 has been proposed to play a dominant role over PHF6* by initiating and stabilizing the tau fibrils (von Bergen et al., 2000; von Bergen et al., 2001; Barghorn et al., 2014). By targeting PHF6 fibrils, our group developed D-peptides that inhibit fibril formation of full-length tau *in vitro* (Dammers et al., 2016).

In 2018, the studies of Seidler and his coworkers suggested that the PHF6* segment is the more powerful driver of tau aggregation and a superior target for inhibitors of

fulllength tau fibrils formation. Therefore, we proposed that a comparative study to the previous research may be of interest and developing D-peptides that inhibit the aggregation of PHF6* could be a highly effective method for blocking the aggregation of full-length tau.

A mirror image phage display selection was performed using D-PHF6* fibrils. As short synthetic peptides such as PHF6* are difficult to adsorb on a plate, we prepared fibrils of D-enantiomeric PHF6* to be immobilized on the plastic surface of multi-well plates. The D-PHF6* fibrils were prepared by incubating D-PHF6* peptide, without adding of heparin, in RT for 30 h. Four panning rounds were performed and enrichment ELISA was carried out to estimate the success of the selection (Figure 21).

In this selection, no enrichment in phage pools was observed in rounds 3–4. Usually, an enrichment in the phages pool against the target protein is expected with an increasing number of panning rounds. However, the binding ratio for all panning rounds eluates was >2, which indicates the likely presence of specific binding phages (Table 11). The binding properties of single clones from the third and fourth panning rounds were evaluated by single phage ELISA. The eluates of the third and fourth panning rounds were used despite their lower binding ratio in comparison with the elutes of the first and second rounds. This was due to the common experience in phage display that later rounds are more likely to contain the promising phages. This can be explained by the fact that with increasing rounds of panning, the amplified elutes of the later rounds are more enriched with population of phages more likely to be specific binding phages. About 60 phage clones were screened for their binding to PHF6* fibrils by single phage ELISA. The outcome of the single phage ELISA revealed several clones with a high signal in the wells coated with PHF6* fibrils. Phage clones which exhibited a high signal to PHF6* fibrils are more likely to be target binding phages.

The DNA of about 40 promising phage clones was extracted and sent for sequencing. 31 sequences could be identified after DNA sequencing and as some peptide sequences were identified more than once, these 31 identified sequences indicated 29 different peptides. These 29 sequences were then screened using screening web tools to exclude possible target-unrelated peptides. Interestingly, peptide MM3, which was selected in the first selection against full-length tau and acted as a tau aggregation

inhibitor, was also among the selection against PHF6* fibrils. Finally, 6 peptides (MMP1, MMP2, MMP3, MMP4, MMP5 and MMP6) were selected to be synthesized as L-enantiomeric peptides to test their ability to inhibit the aggregation of D-PHF6*.

The inhibitory effects of the selected PHF6*-based inhibitor peptides

Usually, the peptides obtained after mirror image phage display are synthesized directly as D-peptides and tested against the L-enantiomeric form of the target. However, due to the high cost of synthesizing six D-enantiomeric peptides, we decided to order them first in the L-enantiomeric form and test them against already available D-PHF6* using THT. Two promising peptides (MMP2 and MMP6) were then synthesized in the D-enantiomeric form (named MMPD2 and MMPD6) and tested against full-length tau. However, Neither MMPD2 nor MMPD6 prevented the fibril formation of full-length tau.

As previously mentioned, MM3, which was selected against tau monomer, was also found in the selection against PHF6* fibrils. Therefore, it was of interest to test the ability of MMD3 and MMD3rev to inhibit the aggregation of PHF6*. After performing THT aggregation assays with PHF6*, both MMD3 and MMD3rev showed their ability to inhibit the fibril formation of PHF6*. In addition, we tested the ability of MMD3 and MMD3rev to inhibit the aggregation of PHF6. However, neither peptide was able to inhibit the PHF6 aggregation. These results were to be expected as MM3 was selected against PHF6* rather than PHF6.

In addition, the ability of MMD2 and MMD2rev, which were obtained in the selection against tau monomer, to inhibit the aggregation of PHF6* and PHF6 was tested using a THT assay. Neither of these peptides exhibited any inhibitory effect on PHF6* or PHF6 fibril formation (Figure 25). This was also expected as MM2 was found only in the selection against full-length tau and not against PHF6*. It seems likely that the binding site for MM2 on the tau is not located on PHF6 or on PHF6*.

Next, the binding behavior of MMD3 and MMD2 toward PHF6* and PHF6 fibrils was tested using ELISA. Both MMD2 and MMD3 exhibited high signals to PHF6* fibrils as well as to PHF6 fibrils, which demonstrated the binding of the selected peptide toward PHF6* and PHF6 fibrils. However, MMD2 exhibited stronger signals than MMD3 toward both PHF6* and PHF6 fibrils, which indicated a stronger binding of MMD2 to

both PHF6* and PHF6 fibrils (Figure 26). However, these findings could be considered somewhat controversial. While it was expected that MMD3 exhibited its binding to PHF6* fibrils, it was not expected that MMD3 exhibited any binding ability to PHF6 fibrils, as MMD3 was selected against PHF6* and not against PHF6. In addition, the strong binding of MMD2 toward PHF6* as well as PHF6 fibrils was somewhat unexpected as MMD2 was not selected against either PHF6 or PHF6*. Taking in consideration our findings that MMD2 was ineffective at inhibiting the aggregation of full-length tau, PHF6* and PHF6, despite its strong binding to each, it seems likely that MMD2 is a non-specific binding peptide resulting from a non-target specific phage.

Regarding MMD3, unexpectedly the peptide showed a stronger binding to PHF6 fibrils than PHF6* fibrils. This could be explained by the fact that the two segments PHF6 (VQIVYK) and PHF6* (VQIINK) have a very similar sequence with only two different amino acids. However, despite this similarity MMD3 did not exhibit any inhibiting effect on PHF6 fibrils formation while acted as an effective inhibitor for PHF6* aggregation (Table 13).

Table 13: Promising D-enantiomeric peptides selected during this project, and their potential to inhibit the full-length tau fibrillization, PHF6* fibrillization and PHF6 fibrillization according to THT assays.

Peptide name	Sequence	Selection	Inhibition of full-length tau fibrillization	Inhibition of PHF6* fibrillization	Inhibition of PHF6 fibrillization
MMD2	**d-ltphkhhkhlha**	Tau monomer	+/-	-	-
MMD2rev	**d-ahlhkhhkhptl**	Tau monomer	+/-	-	-
MMD3	**d-dplkarhtsvwy**	Tau monomer/ PHF6* fibrils	+	+	-
MMD3rev	**d-ywvsthraklpd**	Tau monomer/ PHF6* fibrils	+	+	-

 (+/-) indicates comparably low inhibition of tau fibril formation

Concerning the influence of charge and hydrophobicity of the D-peptides on the interaction with target protein, the group of Willbold addressed also this question in a recent publication by Ziehm et al. in 2018. They presented a detailed biophysical characterization of the interactions between the D-enantiomeric peptide D3 and optimized D-peptides ANK3 and ANK6 with their molecular target, the Aß monomer. D3 was selected previously by the same group using mirror image phage display against Aß. D3 showed its ability to inhibit the aggregation of Aß *in vitro* as well as *in vivo*. In order to increase drug efficacy, Ziehm et al. optimized the lead peptide, D3, by peptide microarrays resulting in D-peptides (named as ANK3 and ANK6) with increased hydrophobicity. The hydrophobicity of ANK3 and ANK6 was increased by exchanging some amino acids in D3 to hydrophobic amino acid residues. It was revealed that ANK3 was the most promising peptide, and its hydrophobic interactions significantly contribute to the driving force for binding, resulting in a more robust complex formation. They concluded that increased hydrophobicity resulted in an increased affinity binding mode. Later, ANK3 will be further studies *in vivo* to investigate whether increased hydrophobicity indeed leads to an optimized drug for the treatment of AD (Ziehm et al., 2018).

Comparing the physicochemical characteristics of MMD3 with MMD2, MMD3 was more hydrophobic than MMD2 (Table 14). Despite that MMD2 had a relatively high hydrophobicity, it was ineffective in inhibiting the aggregation of full-length tau. However, it is reported in the literature that the hydrophobic peptides are more likely to be polystyrene surface-binding peptides (Li et al., 2017).

In the future, optimizing our peptides MMD2 and MMD3 by exchanging some amino acid could lead also to optimized peptides for the inhibition of tau aggregation.

Table 14: Physicochemical characteristics of the D-peptides (MMD2 and MMD3) and the, the hydrophobicity was presented in two different scores; first, the hydrophobicity was calculated according to Kyte and Doolittle using the online tool ProtParam and expressed as GRAVY score. The higher the GRAVY score, the more hydrophobic the D-peptide. In addition, the Hydrophobicity was calculated in percentage using the online tool PEPTIDE2.0.

Peptide	Sequence	Net charge	Hydrophobicity in (GRAVY score)	Hydrophobicity in percentage
MMD2	ltphkhhkhlha	+2.5	-1.4	33%

| MMD3 | ywvsthraklpd | +1 | -0.88 | 41% |

5.4 The effectiveness of PHF6* and PHF6 aggregation inhibitors in preventing the fibrils formation of full-length tau

To date, it is not known which of the segments PHF6 and PHF6* is the more effective target for the therapy of Alzheimer 's disease. The study by Seidler and his colleagues suggested that PHF6* is likely an excellent target for the inhibitors of full-length tau fibril formation. Using THT, they compared the tau aggregation inhibition effect of the most promising PHF6*-inhibitor peptide developed in their study, named as W.MINK, with tau aggregation inhibition effect of a PHF6-inhibitor peptide, TLKIVW, developed by Sievers and his coworkers. According to data presented by Seidler et al., TLKIVW peptide was not able to significantly inhibit the aggregation of full-length tau *in vitro* (Sievers et al., 2011; Seidler et al., 2018). In the study of our group, Dammers et al. 2016, the performance of the TLKIVW peptide described by Sievers et al. was also compared with results of the peptides selected in Dammers study. However, the TLKIVW peptide demonstrated a weak effect while all peptides selected in the study of Dammers and her colleagues clearly inhibited fibril formation of the tau protein.

We performed preliminary experiments to investigate the hypothesis that PHF6* is the stronger driver of tau aggregation. THT assays were carried out to compare the tau aggregation inhibiting effects of the PHF6-based inhibitors, TLKIVW (Sievers et al., 2011) and the peptide APT (Dammers et al., 2016), with the PHF6*-based inhibitors, MMD3, MMD3rev and W.MINK (Seidler et al., 2018) (Figure 27). We used an increasing concentration of each peptide in a molar ratio 1:1, 1:5 and 1:10. We observed that ThT fluorescence decreased with increasing concentration of the peptides, indicating a dose-dependent inhibition of full-length tau aggregation for all peptides.

From our early preliminary data, it seems likely that PHF6* and PHF6 aggregation inhibitors are comparably effective in inhibiting the aggregation of full-length tau in THT test. Similar to the PHF6* aggregation inhibitors, MMD3 and MMD3rev, that inhibited the aggregation of full-length tau significantly, the PHF6 aggregation inhibitors TLKIVW

and APT showed a similar ability to inhibit the formation of tau fibrils. While, MMD3 and MMD3rev inhibitory effect was very similar to TLKIVW, APT showed the best inhibitory effect in our THT assays especially in a ratio of 1:1. In our hands, W.MINK, a PHF6* aggregation inhibitor, was less effective than the other peptides in reducing the aggregation of tau. In addition, all tested peptides inhibit seeding by tau fibrils in a concentration-dependent fashion (Figure 27).

It is notable to mention that all peptides tested above (TLKIVW, APT, MMD3, MMD3rev and W.MINK) were also tested in the Lab of Prof. Eckhard Madelkow in the German Center for Neurodegenerative Diseases (DZNE) for their ability to inhibit the aggregation of the tau construct TauRDΔK280 by ThS assay. Their results revealed that, except for the TLKIVW peptide, all other peptides (WINK, APT, MMD3 and MMD3rev) were effectively able to reduce the aggregation starting from ~1 µM concentrations. They used a concentration range of 1 nM to 200 µM from each peptide. Comparing with the concentrations used in our THT assays, we used higher concentrations of the peptides (24, 120 und 240 µM).

Future research is required to further characterize all these peptides using different biochemical and biophysical methods to determine which of the both sequences, PHF6 or PHF6*, is the more effective target for the development of tau aggregation inhibiting peptides.

6 Conclusion and outlook

Alzheimer's disease (AD) is characterized by extracellular deposition of Aβ peptide as amyloid plaques and intracellular accumulation of tau protein as neurofibrillary tangles. Development of compounds that inhibit tau protein aggregation is considered as a treatment strategy of AD, which can stop the disease progression.

In this project, we developed inhibitors that prevent the pathological aggregation of tau. Therefore, we performed phage display and mirror phage display selections to obtain D-peptides that bind to tau and block its fibril formation. The first phage display selection was performed against the monomer form of full-length tau protein. The second selection was a mirror image phage display selection using the D-enantiomeric form of PHF6* fibrils as a target.

The most interesting D-peptide MMD3 was found in both selections. MMD3 and its retro-inverso form MMD3rev were able to inhibit the aggregation of full-length tau as well as of PHF6* in THT aggregation assays. Furthermore, both MMD3 and MMD3rev bind to tau monomer, tau fibrils and PHF6* fibrils in ELISA experiments.

In addition, we performed preliminary experiments to investigate the hypothesis that PHF6* is the more powerful driver of tau aggregation. Our early preliminary data may suggest that PHF6 and PHF6* aggregation inhibitors have a similar ability to inhibit the aggregation of full-length tau.

Tau aggregation inhibiting effects of MMD3 and MMD3rev were also tested in the Lab of Prof. Eckhard Madelkow in the German Center for Neurodegenerative Diseases (DZNE) and they were able to able to prevent the aggregation in ThS assays at low concentrations (micromolar concentrations).

Recently, MMD3 and MMD3rev were designed as Alexa 647-labeled peptides and tested for their ability to enter N2a cells in the Lab of Prof. Eckhard Madelkow. The treatment of tau expressing N2a cells with ALEXA 647 labeled D-peptides revealed that MMD3 and MMD3rev are able to penetrate the cell membrane and are stable over the whole incubation time (4 days). As a next step, the ability of the peptides to inhibit the aggregation of tau in cells will be tested.

In addition, *in silico* modelling of the MMD3 and MMD3rev peptides complexes with PHF6* is also planned in order to gain a better understanding of the binding mode of the selected peptides to PHF6*. Furthermore, the binding kinetics of MMD3 and MMD3rev toward PHF6, PHF6* und Tau441 are proposed to be characterized using a BLItz™ system in the Lab of Prof. Eckhard Madelkow. The BLItz™ system provides a real time, label-free analysis of protein-protein interaction by employing Bio-Layer Interferometry (BLI) technology.

The aggregation inhibitory mechanism of MMD3 and MMD3rev is also proposed to be investigated to determine whether the selected peptide prevents the aggregation (e.g. by blocking the forming of the fibrils), dissolves the aggregates or transforms e.g. the oligomers to amorphous rather than toxic species. Additionally, to evaluate the diagnostic and therapeutic potentials of MMD3 and MMD3rev for the diagnosis and treatment of AD, the blood-brain barrier transport of these D-peptides should be quantitatively evaluated. To do that, an *in vitro* blood-brain barrier cell culture model, previously established, that mimics the blood-brain barrier can be used (Liu et al., 2010).

In the Lab of Prof. Eckhard Madelkow, it is also planned to investigate the influence of MMD3 and MMD3rev on the inducible hippocampal brain sections of transgenic mice. Using inducible hippocampal brain slices from transgenic mice expressing proaggregant tau repeat domain carrying ΔK280 mutation (termed Tau(RD)ΔK), the ability of tau aggregation inhibitors to prevent tau aggregation and neurotoxicity could be studied (Messing et al., 2013).

In the future, it is proposed to develop dimeric D-peptides which address PHF6 and/or PHF6* within one molecule. To do this, different peptides will be connected via linker molecules. It will be interesting to investigate the tau aggregation inhibitory effect of dimeric peptides against PHF6* (e.g. MMD3-MMD3) and dimeric peptides against PHF6 and PHF6* (e.g. APT-MMD3).

Finally, as MMD3 and MMD3rev have shown to be successful inhibitors of tau aggregation *in vitro*, they will be further investigated for their therapeutic potential. Ultimately, these peptides may present promising candidates for the treatment of AD.

7 References

Anand K and Sabbagh M. Early investigational drugs targeting tau protein for the treatment of Alzheimer's Disease (2015): *Expert Opin Investig Drugs.* 24(10): 1355–1360.

Anand R, Kaushal A, Wani WY and Gill KD (2012): Road to Alzheimer's disease:the pathomechanism underlying. *Pathobiology* 79(2): 55-71.

Arriagada PV, Growdon JH, Hedley-Whyte ET & Hyman BT (1992): Neurofibrillary tangles but not senile plaques parallel duration and severity of Alzheimer's disease. *Neurology* 42, 631–639 (1992).

Asuni AA, Boutajangout A, Quartermain D, Sigurdsson EM (2007): Immunotherapy targeting pathological tau conformers in a tangle mouse model reduces brain pathology with associated functional improvements. *J Neurosci.* 27(34):9115-29.

Ballatore C, Lee VM, Trojanowski JQ (2007): Tau-mediated neurodegeneration in Alzheimer's disease and related disorders. *Nat Rev Neurosci.* 8(9):663–672.

Barghorn S, Davies P, Mandelkow E (2004): Tau paired helical filaments from Alzheimer's disease brain and assembled in vitro are based on beta-structure in the core domain. *Biochem.* 43: 1694±1703.

Bateman RJ, Blennow K, Doody R, Hendrix S, Lovestone S, Salloway S, Schindler R, Weiner M, Zetterberg H, Aisen P, Vellas B (2019): Plasma Biomarkers of AD Emerging as Essential Tools for Drug Development: An EU/US CTAD Task Force Report. *Prev Alzheimers Dis.* 6(3):169-173.

Biagioni MC, Galvin JE (2011): Using biomarkers to improve detection of Alzheimer's disease. *Neurodegener Dis Manag.* 1(2):127–139.

Bickel H (1996): Need for nursing care by the elderly: results of a population based retrospective longitudinal study [Article in German]. *Gesundheitswesen*, 58(1), 56-62.

Binder LI; Frankfurter A; Rebhun LI (1985): The distribution of tau in the mammalian central nervous system. In: *The Journal of Cell Biology* 101 (4), S. 1371–1378.

Bird, T. D. (1993, last revision 2014): Alzheimer Disease Overview. *GeneReviews(R).* R.A. Pagon, M. P. Adam, H. H. Ardinger et al. Seattle (WA).

Bogdanovic N (2018). The Challenges of Diagnosis in Alzheimer's Disease. *US Neurology*. 4(1):15–16.

Boxer A.L., Lang A.E., Grossman M., Knopman D.S., Miller B.L., Schneider L.S., Doody R.S., Lees A., Golbe L.I., Williams D.R., et al. (2014): Davunetide in patients with progressive supranuclear palsy: A randomised, double-blind, placebo-controlled phase 2/3 trial. *Lancet Neurol*. 13:676–685.

Brunden KR, Trojanowski JQ, Lee VM (2009). Advances in tau-focused drug discovery for Alzheimer's disease and related tauopathies. *Nat Rev Drug Discov*. 8(10):783-93.

Buée L, Bussière T, Buée-Scherrer V, Delacourte A, Hof PR (2000). Tau protein isoforms, phosphorylation and role in neurodegenerative disorders. *Brain Res Brain Res Rev*. 33(1):95-130.

Buée L, Perez-Tur J, Leveugle B, Bue´e-Scherrer V, Mufson E.J., Loerzel A.J., Chartier-Harlin M.C., Perl D.P., Delacourte A., Hof P.R. (1996): Apolipoprotein E in Guamanian amyotrophic lateral sclerosis / parkinsonism–dementia complex: genotype analysis and relationships to neuropathological changes. *Acta Neuropathol*. 91:247–253.

Brunden KR, Trojanowski JQ, Lee VM (2009): Advances in tau-focused drug discovery for Alzheimer's disease and related tauopathies. *Nat Rev Drug Discov*. 8(10):783–793.

Chorev M, Goodman M (1995): Recent developments in retro peptides and proteins—an ongoing topochemical exploration. *Trends Biotechnol*. 13:438–445.

Cleveland, DW; Hwo, SY; Kirschner, MW (1977): Physical and chemical properties of purified tau factor and the role of tau in microtubule assembly. *In: Journal of molecular biology* 116 (2), S. 227–247.

Congdon, E. E., & Sigurdsson, E. M. (2018). Tau-targeting therapies for Alzheimer disease. *Nature reviews. Neurology* 14(7): 399–415.

Cowan CM, Quraishe S, Mudher A (2012): What is the pathological significance of tau oligomers?. *Biochem Soc Trans*. 40(4):693-7.

Crowe A, Huang W, Ballatore C, Johnson RL, Hogan AM, Huang R, Wichterman J, McCoy J, Huryn D, Auld DS, Smith AB 3rd, Inglese J, Trojanowski JQ, Austin CP, Brunden KR, Lee VM (2009): Identification of aminothienopyridazine inhibitors of tau assembly by quantitative high-throughput screening. *Biochemistry*. 48(32):7732-45.

Crowe A, Ballatore C, Hyde E, Trojanowski JQ, Lee VMY (2007). High throughput screening for small molecule inhibitors of heparin-induced tau fibril formation. *Biochemical and Biophysical Research Communications*.358:1–6.

Dammers C.: (2015) Structural analysis and aggregation of Alzheimer's disease related pyroglutamate- modified amyloid. Inaugural-Dissertation

Dammers C, Yolcu D, Kukuk L, et al. (2016): Selection and Characterization of Tau Binding ᴅ-Enantiomeric Peptides with Potential for Therapy of Alzheimer Disease. *PLoS One*;11(12):e0167432.

Dintzis, H.M., et al. (1993): A comparison of the immunogenicity of a pair of enantiomeric proteins. *Proteins*. 16(3): p. 306-8.

Elfgen, Anne; Hupert, Michelle; Bochinsky, Kevin; Tusche, Markus; González de San Román Martin, Estibaliz; Gering, Ian et al. (2019): Metabolic resistance of the D-peptide RD2 developed for direct elimination of amyloid-β oligomers. *In: Scientific Reports 9.*

Eschmann NA, Do TD, LaPointe NE, et al.(2015): Tau Aggregation Propensity Engrained in Its Solution State. *J Phys Chem B.* 119(45):14421–14432.

Farrer, L.A., Cupples, L.A. Haines, J.L., Hyman, B. Kukull, W.A., Mayeux R., Myers R.H., Pericak-Vance M.A., Risch N., van Duijn C.M. (1997): Effects of age, sex, and ethnicity on the association between apolipoprotein E genotype and Alzheimer disease. A meta-analysis. APOE and Alzheimer Disease Meta Analysis Consortium. *JAMA,* 278(16), 1349–56.

Fasulo L, Visintin M, Novak M and Cattaneo A (1998): Tau truncation in Alzheimer's disease: Expression of a fragment encompassing PHF core tau induces apoptosis in COS cells. *Alzheimer's Reports*. 1(1):25-32.

Fletcher, M. D., and Campbell, M. M. (1998): Partially Modified Retro-Inverso Peptides: Development, Synthesis, and Conformational Behavior. *Chem. Rev.* 98, 763−796.

Fotuhi M, Hachinski V, et al (2009): Changing perspectives regarding late-life dementia. *Nat Rev Neurol.* 5:649–658.

Fox NC, Cousens S, Scahill R, Harvey RJ, Rossor MN (2000). Using serial registered brain magnetic resonance imaging to measure disease progression in Alzheimer disease: Power calculations and estimates of sample size to detect treatment effects. *Arch Neurol* 57: 339–344.

Friedhoff, P; Schneider, A; Mandelkow, EM; Mandelkow, E (1998): Rapid assembly of Alzheimer-like paired helical filaments from microtubule-associated protein tau monitored by fluorescence in solution. In: *Biochemistry* 37 (28), S. 10223–10230.

Frost B, Götz J, Feany MB (2015): Connecting the dots between tau dysfunction and neurodegeneration. *Trends Cell Biol.* 25(1):46–53.

Funke SA, Willbold D. Peptides for therapy and diagnosis of Alzheimer's disease. Curr Pharm Des. 2012;18(6):755–767.

Funke SA, van Groen T, Kadish I, Bartnik D, Nagel-Steger L, Brener O, Sehl T, Batra-Safferling R, Moriscot C, Schoehn G, et al (2010): Oral treatment with the d-enantiomeric peptide D3 improves the pathology and behavior of Alzheimer's Disease transgenic mice. *ACS Chem Neurosci.* 1:639 – 48.

Galimberti, D. and E. Scarpini (2012): Progress in Alzheimer's disease. *J Neurol* 259(2):201-211.

Goedert M., Spillantini M.G., Potier M.C., Ulrich J., Crowther R.A. (1989): Cloning and sequencing of the cDNA encoding an isoform of microtubule-associated protein tau containing four tandem repeats: Differential expression of tau protein mRNAs in human brain*. The EMBO journal.* 8(2): 393–399.

Gómez-Isla T, Price JL, McKeel DW Jr, Morris JC, Growdon JH, Hyman BT (1996): Profound loss of layer II entorhinal cortex neurons occurs in very mild Alzheimer's disease. *J Neurosci.* 16(14):4491-500.

Götz J, Chen F, van Dorpe J, Nitsch RM (2001): Formation of neurofibrillary tangles in P301 l tau transgenic mice induced by Abeta 42 fibrils. *Science* 293:1491–1495.

Goux WJ, Kopplin L, Nguyen AD, Leak K, Rutkofsky M, Shanmuganandam VD, Sharma D, Inouye H, Kirschner DA (2004): The formation of straight and twisted filaments from short tau peptides. *J Biol Chem.* 279(26):26868-75.

Gura T. Hope in Alzheimer's fight emerges from unexpected places (2008): *Nat Med.* 14:894.

Guzmán-Martinez L, Farías GA, Maccioni RB (2013): Tau oligomers as potential targets for Alzheimer's diagnosis and novel drugs. *Front Neurol.* 4:167.

Hershko A., Ciechanover A. (1998): The ubiquitin system for protein degradation. *Annu. Rev. Biochem.* 67 425–479.

Hirokawa N, Shiomura Y, Okabe S (1988): Tau proteins: The molecular structure and mode of binding on microtubules. *J Cell Biol* 107: 1449–1459.

Huang, Y. and L. Mucke (2012): Alzheimer mechanisms and therapeutic strategies. *Cell* 148(6): 1204-1222.

Jadhav S, Avila J, Schöll M, Kovacs GG, Kövari E, Skrabana R, Evans LD, Kontsekova E, Malawska B, de Silva R, Buee L, Zilka N (2019): A walk through tau therapeutic strategies. *Acta Neuropathol Commun*. 15;7(1):22.

Kametani F, Hasegawa M (2018): Reconsideration of Amyloid Hypothesis and Tau Hypothesis in Alzheimer's Disease. *Front Neurosci*. 12:25.

Kutzsche J, Schemmert S, Tusche M, et al (2017): Large-Scale Oral Treatment Study with the Four Most Promising D3-Derivatives for the Treatment of Alzheimer's Disease. *Molecules*. 22(10):1693.

Lasagna-Reeves CA, Castillo-Carranza DL, Guerrero-Muoz MJ, Jackson GR, Kayed R (2010): Preparation and characterization of neurotoxic tau oligomers. *Biochemistry* 49:10039–10041.

Lasagna-Reeves, C.A., Castillo-Carranza, D.L., Sengupta, U., Clos, A.L., Jackson, G.R. and Kayed, R. (2011): Tau oligomers impair memory and induce synaptic and mitochondrial dysfunction in wild-type mice. *Mol. Neurodegener*. 6, 39.

Lee G., Neve R.L., Kosik K.S. (1989): The microtubule binding domain of tau protein. *Neuron* 2 1615–1624.

Leithold, Leonie H. E.; Jiang, Nan; Post, Julia; Ziehm, Tamar; Schartmann, Elena; Kutzsche, Janine et al. (2016): Pharmacokinetic Properties of a Novel D-Peptide Developed to be Therapeutically Active Against Toxic beta-Amyloid Oligomers. In: *Pharmaceutical research* 33 (2), S. 328–336.

Li N, Kang J, Jiang L, He B, Lin H, and Huang J (2017): PSBinder: A Web Service for Predicting Polystyrene Surface-Binding Peptides, *BioMed Research International*, vol. 2017, Article ID 5761517, 5 pages.

Lovestone S., Boada M., Dubois B., Hüll M., Rinne J.O., Huppertz H.J., Calero M., Andrés M.V., Gómez-Carrillo B., León T., et al (2015): A phase II trial of tideglusib in Alzheimer's disease. *J. Alzheimers Dis*. 45:75–88.

Lu Y, Jiang X, Liu S, Li M (2018). Changes in Cerebrospinal Fluid Tau and βAmyloid Levels in Diabetic and Prediabetic Patients: A Meta-Analysis. *Front Aging Neurosci*.10:271.

Mandelkow EM, Mandelkow E (2012): Biochemistry and cell biology of tau protein in neurofibrillary degeneration. *Cold Spring Harb Perspect Med.* 2(7):a006247.

Matsuoka, Y; Jouroukhin, Y; Gray, AJ; Ma, L; Hirata-Fukae, C; Li, HF et al. (2008): A neuronal microtubule-interacting agent, NAPVSIPQ, reduces tau pathology and enhances cognitive function in a mouse model of Alzheimer's disease. *The Journal of pharmacology and experimental therapeutics* 325 (1), S. 146–153.

McKhann G., Drachman D., Folstein M., Katzman R., Price D. and Stadlan E. M. (1984): Clinical diagnosis of Alzheimer's disease: report of the NINCDS-ADRDA Work Group under the auspices of Department of Health and Human Services Task Force on Alzheimer's Disease. *Neurology* 34(7): 939-944.

McKhann GM, Knopman DS, Chertkow H, Hyman BT, Jack Jr CR, Kawas CH, et al (2011): The diagnosis of dementia due to Alzheimer's disease: recommendations from the National Institute on Aging-Alzheimer's Association workgroups on diagnostic guidelines for Alzheimer's disease. *Alzheimers Dement.* 7:263–9.

Medina M. (2018): An Overview on the Clinical Development of Tau-Based Therapeutics. *Int J Mol Sci.* 19(4):1160.

Messing L, Decker JM, Joseph M, Mandelkow E, Mandelkow EM (2013): Cascade of tau toxicity in inducible hippocampal brain slices and prevention by aggregation inhibitors. *Neurobiol Aging.* 34(5):1343–1354.

Miersch, S., Li, Z., Hanna, R., McLaughlin, M. E., Hornsby, M., Matsuguchi, T., Paduch, M., Sääf, A., Wells, J., Koide, S, Kossiakoff, A, Sidhu, S. S. (2015): Scalable high throughput selection from phage-displayed synthetic antibody libraries. *Journal of visualized experiments : JoVE.* (95), 51492.

Morishima-Kawashima M., Hasegawa M., Takio K., Suzuki M., Titani K., Ihara Y. (1993): Ubiquitin is conjugated with amino-terminally processed tau in paired helical filaments. *Neuron.* 10: 1151–1160.

Neve RL, Harris P, Kosik KS, Kurnit DM, Donlon TA (1986): Identification of cDNA clones for the human microtubule-associated protein tau and chromosomal localization of the genes for tau and microtubule-associated protein 2. *Brain Res* 387: 271–280.

Novak M. (1994): Truncated tau protein as a new marker for Alzheimer's disease. *Acta Virol.* 38, 173–189.

Pappenheimer JR, Karnovsky ML, Maggio JE. Absorption and excretion of undegradable peptides (1997): role of lipid solubility and net charge. *J Pharmacol Exp Ther.* 280(1):292–300.

Parmley FS and Smith GP (1988): Antibody-selectable filamentous fd phage vectors: affinity purification of target genes. *Gene.* 73(2):305-318.

Parsons CG, Danysz W, Quack G (1999): Memantine is a clinically well tolerated N-methyl-D-aspartate (NMDA) receptor antagonist—a review of preclinical data. *Neuropharmacology.* 38:735-767.

Patterson KR. , Remmers C, Fu Y, Brooker S, Kanaan NM., Laurel Vana L, Ward S, Reyes JF., Philibert K, Glucksman MJ., Binder LI. (2011): Characterization of Prefibrillar Tau Oligomers in Vitro and in Alzheimer Disease. *J. Biol. Chem.* 286: 23063-23076.

Panza F et al. (2016): Tau-centric targets and drugs in clinical development for the treatment of Alzheimer's disease. *Biomed Res. Int*, 3245935.

Perl, D. P. (2010): Neuropathology of Alzheimer's disease. *Mt Sinai J Med.* 77(1): 32-42.

Perry G, Friedman R, Shaw G, Chau V (1987): Ubiquitin is detected in neurofibrillary tangles and senile plaque neurites of Alzheimer disease brains. *Proc Natl Acad Sci USA.* 84: 3033–3036.

Pickhardt M, Gazova Z, von Bergen M, Khlistunova I, Wang Y, Hascher A, Mandelkow EM, Biernat J, Mandelkow E (2005): Anthraquinones inhibit tau aggregation and dissolve Alzheimer's paired helical filaments in vitro and in cells. *J Biol Chem.* 280(5):3628-35.

Pickhardt M, Larbig G, Khlistunova I, Coksezen A, Meyer B, Mandelkow EM, Schmidt B, Mandelkow E (2007): Phenylthiazolyl-hydrazide and its derivatives are potent inhibitors of tau aggregation and toxicity in vitro and in cells. *Biochemistry.* 46:10016–10023.

Pickhardt M, Neumann T, Schwizer D, Callaway K, Vendruscolo M, Schenk D, St. George-Hyslop P, Mandelkow EM, Dobson CM, McConlogue L, Mandelkow E, Tóth G. (2015): Identification of Small Molecule Inhibitors of Tau Aggregation by Targeting Monomeric Tau As a Potential Therapeutic Approach for Tauopathies. *Current Medicinal Chemistry.* 12(9), 814–828.

Poirier J., Minnich A., Davignon J. (1995): Apolipoprotein E, synaptic plasticity and Alzheimer's disease. *Ann. Med.* 27 663–670.

Prince, M., R. Bryce, E. Albanese, A. Wimo, W. Ribeiro and C. P. Ferri (2013): The global prevalence of dementia: a systematic review and metaanalysis. *Alzheimers Dement* 9(1):63-75.

Qiang X, Sun K, Xing L, et al (2017): Discovery of a polystyrene binding peptide isolated from phage display library and its application in peptide immobilization. *Sci Rep.* 7(1):2673.

Rudolph S.: (2015) Selection and characterization of Amyloid-β1-42 binding D-enantiomeric peptides for potential therapeutic intervention of Alzheimer´s disease. Inaugural-Dissertation.

Rudolph, S., Klein, A. N., Tusche, M., Schlosser, C., Elfgen, A., Brener, O., Teunissen, C., Gremer, L., Funke, S. A., Kutzsche, J., & Willbold, D. (2016). Correction: Competitive Mirror Image Phage Display Derived Peptide Modulates Amyloid Beta Aggregation and Toxicity. *PloS one*, 11(7), e0159470. https://doi.org/10.1371/journal.pone.0159470

Rissman RA, Poon WW, Blurton-Jones M, Oddo S, Torp R, Vitek MP, et al (2004): Caspase-cleavage of tau is an early event in Alzheimer disease tangle pathology. *J Clin Invest.* 114:121-30.

Rogers SL, Doody RS, Mohs RC, Friedhoff LT (1998): and. Donepezil improves cognition and global function in Alzheimer disease: a 15-week, double-blind, placebo-controlled study. Arch Intern Med 158: 1021-31.

Saint-Aubert L, Lemoine L, Chiotis K, Leuzy A, Rodriguez-Vieitez E, Nordberg A (2017): Tau PET imaging: present and future directions. *Mol Neurodegener.* 12(1):19.

Seidler, P., Boyer, D. R., Rodriguez, J. A., Sawaya, M. R., Cascio, D., Murray, K., et al. (2018): Structure-based inhibitors of tau aggregation. *Nat. Chem.* 10, 170–176.

Schedin-Weiss S, Winblad B and Tjernberg LO (2014): The role of protein glycosylation in Alzheimer disease. *FEBS J.* 281(1):46-62.

Schweers O, Mandelkow EM, Biernat J, Mandelkow E (1995): Oxidation of cysteine-322 in the repeat domain of microtubule-associated protein tau controls the in vitro assembly of paired helical filaments. *Proc Natl Acad Sci.* 92: 8463–8467.

Schumacher T.N., Mayr L.M., Minor D.L., Jr., Milhollen M.A., Burgess M.W., Kim P.S. (1996): Identification of D-peptide ligands through mirror-image phage display. *Science.* 271:1854–1857.

Schweers O, Schonbrunn-Hanebeck E, Marx A, Mandelkow E (1994): Structural studies of tau protein and Alzheimer paired helical filaments show no evidence for β-structure. *J Biol Chem.* 269: 24290–24297.

Shiryaev, N; Jouroukhin, Y; Giladi, E; Polyzoidou, E; Grigoriadis, NC; Rosenmann, H; Gozes, I (2009): NAP protects memory, increases soluble tau and reduces tau hyperphosphor-ylation in a tauopathy model. *Neurobiology of disease* 34 (2), S. 381–388.

Sievers SA, Karanicolas J, Chang HW, et al. (2011): Structure-based design of non-natural amino-acid inhibitors of amyloid fibril formation. *Nature.* 475(7354):96–100.

Sigurdsson EM (2009): Tau-focused immunotherapy for Alzheimer's disease and related tauopathies. *Curr Alzheimer Res.* 6(5):446-50.

Smith, G.P. (1985): Filamentous fusion phage: novel expression vectors that display cloned antigens on the virion surface. *Science.* 228, 1315–1317.

Strittmatter W.J., Saunders A.M., Goedert M., Weisgraber K.H., Dong L.M., Jakes R., Huang D.Y., Pericak-Vance M., Schmechel D., Roses A.D. (1994): Isoformspecific interactions of apolipoprotein E with microtubule-associated protein tau: implications for Alzheimer disease. *Proc. Natl. Acad. Sci. USA.* 91(23): 11183– 11186.

Taniguchi S, Suzuki N, Masuda M, Hisanaga S, Iwatsubo T, Goedert M, Hasegawa M (2005): Inhibition of heparin-induced tau filament formation by phenothiazines, polyphenols, and porphyrins. *J Biol Chem.* 280(9):7614-23.

Tapiola T, Alafuzoff I, Herukka SK, Parkkinen L, Hartikainen P, Soininen H, Pirttilä T (2009): Cerebrospinal fluid β-amyloid 42 and Tau proteins as biomarkers of Alzheimer-type pathologic changes in the brain. *Arch Neurol.* 66:382–389.

Trojanowski J.Q., Lee V.M.Y. (1995): Phosphorylation of paired helical filament tau in Alzheimer's disease neurofibrillary lesions: focusing on phosphatases. *FASEB J.* 9(15):1570–1576.

van Groen T, Wiesehan K, Funke SA, Kadish I, Nagel-Steger L, Willbold D (2008): Reduction of Alzheimer's disease amyloid plaque load in transgenic mice by D3, A D-enantiomeric peptide identified by mirror image phage display. *ChemMedChem.* 3:1848 – 52.

van Groen T, Kadish I, Wiesehan K, Funke SA, Willbold D. 2009 In vitro and in vivo staining characteristics of small, fluorescent, Abeta42-binding Denantiomeric peptides in transgenic AD mouse models. ChemMedChem. 4:276 – 82.

Vodnik M, Zager U, Strukelj B, Lunder M. Phage display: selecting straws instead of a needle from a haystack. Molecules. 2011;16(1):790-817.

von Bergen, M. et al. (2000): Assembly of τ protein into Alzheimer paired helical filaments depends on a local sequence motif (306VQIVYK311) forming β structure. Proc. Natl Acad. Sci. USA 97, 5129–5134

von Bergen, M. et al. (2001): Mutations of tau protein in frontotemporal dementia promote aggregation of paired helical filaments by enhancing local beta-structure. *J. Biol. Chem.* 276, 48165–48174.

Wang JZ, Grundke-Iqbal I, Iqbal K (2007). Kinases and phosphatases and tau sites involved in Alzheimer neurofibrillary degeneration. *Eur J Neurosci.* 25(1):59-68.

Weingarten, MD; Lockwood, AH; Hwo, SY; Kirschner, MW (1975): A protein factor essential for microtubule assembly. In: *Proceedings of the National Academy of Sciences of the United States of America* 72 (5), S. 1858–1862.

Weinstock, M. T., Jacobsen, M. T., & Kay, M. S. (2014). Synthesis and folding of a mirror-image enzyme reveals ambidextrous chaperone activity. *Proceedings of the National Academy of Sciences of the United States of America*, 111(32), 11679–11684.

Wenk GL, Danysz W, Mobley SL. (1995): MK-801, memantine and amantadine show neuroprotective activity in the nucleus basalis magnocellularis. *Eur J Pharmacol.*; 293(3):267–270.

Weuve, J., L. E. Hebert, P. A. Scherr and D. A. Evans (2014): Deaths in the United States among persons with Alzheimer's disease (2010-2050). *Alzheimers Dement* 10(2):e40-46.

Willbold D, Kutzsche J. Do We Need Anti-Prion Compounds to Treat Alzheimer's Disease?. *Molecules*. 2019;24(12):2237.

Wischik CM, Edwards PC, Lai RYK, Roth M, Harrington CR. Selective inhibition of Alzheimer disease-like tau aggregation by phenothiazines. Proceedings of the National Academy of Sciences of the United States of America. 1996;93:11213–11218.

Wu XL, Piña-Crespo J, Zhang YW, Chen XC, Xu HX. Tau-mediated Neurodegeneration and Potential Implications in Diagnosis and Treatment of Alzheimer's Disease. *Chin Med J.* 2017;130(24):2978-2990.

Yang L.S., Ksiezak-Reding H., Calpain-induced proteolysis of normal human tau and tau associated with paired helical filaments. *Eur. J. Biochem.* 233 (1995) 9–17.

Zadeh AS, Grässer A, Dinter H, Hermes M and Schindowski K, Efficient (2019): Construction and Effective Screening of Synthetic Domain Antibody Libraries. *Methods Protoc.*, 2(1), 17.

Zhang X., Hernandez I., Rei D., Mair W., Laha J.K., Cornwell M.E., Cuny G.D., Tsai L.H., Steen J.A., Kosik K.S. Diaminothiazoles modify Tau phosphorylation and improve the tauopathy in mouse models. *J. Biol. Chem.* 2013;288:22042–22056.

Zhao LN, L. Lu, L. Y. Chew and Y. Mu (2014). "Alzheimer's disease--a panorama glimpse. *Int J Mol Sci* 15(7): 12631-12650.

Ziehm T, Buell AK, and Willbold D (2018): Role of Hydrophobicity and Charge of Amyloid-Beta Oligomer Eliminating d-Peptides in the Interaction with Amyloid-Beta Monomers. *ACS Chemical Neuroscience 9* (11), 2679-2688.

Publications, patents and poster presentations

Publications

Marwa Malhis[§], Senthilvelrajan Kaniyappan[§], Isabelle Aillaud, Ram Reddy Chandupatla, Lisa-Marie Ramirez, Markus Zweckstetter, Anselm H.C. Horn, Eckhard Mandelkow, Heinrich Sticht, Susanne Aileen Funke.
[§]Equal contribution
Potent Tau aggregation inhibitor D-peptides selected against Tau-repeat 2 using mirror image phage display. Manuscript was accepted for publishing in *ChemBioChem*. 03.August. 2021

Marwa Malhis und Susanne Aileen Funke
Spiegelbild-Phagen-Display zur Selektion von D-enantiomeren Peptiden
GIT Labor-Fachzeitschrift. Online auf Wiley Analytical Science. (8 April 2021)

Dammers C, Yolcu D, Kukuk L, Willbold D, Pickhardt M, Mandelkow E, Horn AH, Sticht H, **Malhis MN**, Will N, Schuster J and Funke SA.
Selection and Characterization of Tau Binding D-Enantiomeric Peptides with Potential for Therapy of Alzheimer Disease. PLoS ONE. (2016).

Patents

Tau protein-binding peptides for the potential treatment of Alzheimer's disease

Inventors: Susanne Aileen Funke 55%, **Marwa Malhis** 35% and Isabelle Aillaud 10%

Application filed by Coburg University of Applied Sciences.

Date of application: 02.08.2019 | Patentanmeldung Nr. 19 189 787.5

Poster presentations

Marwa Malhis and Susanne Aileen Funke

Selection and characterization of tau protein binding peptides for therapy of Alzheimer's disease

Jülich Symposium on Neurodegenerative Diseases, Düsseldorf, 2017

Marwa Malhis and Susanne Aileen Funke

Selection and characterization of tau protein binding peptides as a basis for future therapies of Alzheimer's disease

AD/PD[TM], the 14th International Conference on Alzheimer's and Parkinson's Diseases and related neurological disorders, Lisbon, 2019

(Eidesstattliche) Versicherungen und Erklärungen

(§ 8 Satz 2 Nr. 3 PromO Fakultät)

Hiermit versichere ich eidesstattlich, dass ich die Arbeit selbständig verfasst und keine anderen als die von mir angegebenen Quellen und Hilfsmittel benutzt habe (vgl. Art. 64 Abs. 1 Satz 6 BayHSchG).

(§ 8 Satz 2 Nr. 3 PromO Fakultät)

Hiermit erkläre ich, dass ich die Dissertation nicht bereits zur Erlangung eines akademischen Grades eingereicht habe und dass ich nicht bereits diese oder eine gleichartige Doktorprüfung endgültig nicht bestanden habe.

(§ 8 Satz 2 Nr. 4 PromO Fakultät)

Hiermit erkläre ich, dass ich Hilfe von gewerblichen Promotionsberatern bzw. – vermittlern oder ähnlichen Dienstleistern weder bisher in Anspruch genommen habe noch künftig in Anspruch nehmen werde.

(§ 8 Satz 2 Nr. 7 PromO Fakultät)

Hiermit erkläre ich mein Einverständnis, dass die elektronische Fassung der Dissertation unter Wahrung meiner Urheberrechte und des Datenschutzes einer gesonderten Überprüfung unterzogen werden kann.

(§ 8 Satz 2 Nr. 8 PromO Fakultät)

Hiermit erkläre ich mein Einverständnis, dass bei Verdacht wissenschaftlichen Fehlverhaltens Ermittlungen durch universitätsinterne Organe der wissenschaftlichen Selbstkontrolle stattfinden können.

……………………………………………………………………………….

Ort, Datum, Unterschrift